Molecular analysis of a *Tsc1*-deficient mouse

Submitted for the degree of Doctor of Philosophy at Cardiff University

Catherine Wilson

2006

ProQuest LLC
789 East Eisenhower Parkway
P.O. Box 1346
Ann Arbor, MI 48106-1346

Summary

Tuberous sclerosis complex (TSC) is an autosomal dominant disorder caused by mutation in either the *TSC1* or *TSC2* genes and characterised by the development of benign hamartomatous growths in multiple organ systems.

We have inactivated *Tsc1* in the mouse germ line by gene targeting in ES cells and confirmed that the mutant allele (*Tsc1*$^{-}$) has a recessive embryonic lethal phenotype. *Tsc1*$^{+/-}$ mice developed macroscopically visible renal lesions as early as 3-6 months. Renal lesions progressed from cysts through cystadenomas to solid carcinomas. Eighty percent of *Tsc1*$^{+/-}$ mice on a Balb/c background exhibited solid renal cell carcinomas (RCC) by 15-18 months and in 41%, RCCs were ≥5mm, resulting in grossly deformed kidneys. Some RCCs had a sarcomatoid morphology of spindle cells in whorled patterns and metastasised to the lungs. This new murine model of hamartin deficiency exhibits a more severe phenotype than existing models.

A Bloom's deficient mouse model (*Blm*$^{m3/m3}$) has been shown to induce colorectal tumourigenesis when crossed with *Apc*$^{+/Min}$ mice. Here, we investigate whether the *Blm*$^{m3/m3}$ genotype could induce tumourigenesis in extra-colonic tissues in *Tsc1*$^{+/-}$ mice that are predisposed to renal cystadenomas and carcinomas. *Tsc1*$^{+/-}$ *Blm*$^{m3/m3}$ mice had significantly more macroscopic and microscopic renal lesions at 3-6 months compared to *Tsc1*$^{+/-}$ *Blm*$^{+/m3}$ mice. *Tsc1*$^{+/-}$ *Blm*$^{m3/m3}$ mice tumours showed significantly increased levels of somatic LOH of the wild type *Tsc1* (*Tsc1*^{wt}) allele, as compared to those from *Tsc1*$^{+/-}$ *Blm*$^{+/+}$ mice. This work demonstrates the utility of the *Blm*$^{m3/m3}$ mice for inducing renal tumourigenesis and the high levels (~87%) of LOH in the resultant tumours will help facilitate mapping of loci involved in tumour progression.

TSC1 and *TSC2* are generally considered to act as tumour suppressors that fulfil Knudson's '2-hit hypothesis'. Here, we identified somatic *Tsc1* mutations (2nd hits) in ~80% of CAs and RCCs, but only 31.6% of cysts from *Tsc1*$^{+/-}$ mice, raising the possibility that haploinsufficiency for *Tsc1* plays a role in cyst formation. Consistent with this proposal, many cysts showed little or no staining for phosphorylated mTOR and phosphorylated S6 ribosomal protein, whereas >90% of CAs and RCCs showed strong staining for both markers. We also sought somatic mutations in renal lesions from *Tsc1*$^{+/-}$ *Blm*$^{-/-}$ mice that have a high frequency of somatic LOH, thereby facilitating the detection of 2nd hits. We also found significantly less somatic mutations in cysts, as compared to CAs and RCCs from these mice. Our data indicate that although activation of the mTOR pathway is an important step in Tsc-associated renal tumourigenesis, it may not be the key initiating event in this process.

Declaration

This work has not been previously been accepted in substance for any degree and is not being concurrently submitted in candidature for any degree.

Signed _____(candidate)

Date 14/10/06

Statement 1

This thesis is a result of my own investigations, except where otherwise stated. Other sources are acknowledged by footnotes giving explicit references. A bibliography is appended.

Signed _____(candidate)

Date 14/10/06

Statement 3

I hereby give consent for my thesis, if accepted, to be available for photocopying and for interlibrary loan, and for the title and summary to be made available to outside organisations

Signed _____(candidate)

Date 14/10/06

Acknowledgements

I would like to thank everyone who has been involved in this work.

In particular I would like to thank my supervisors Prof. Jeremy Cheadle and Prof. Julian Sampson for their continued guidance and support. Everyone in the lab Shelley, Cleo, Ant, James, Vikki, Nat, Julie, Carol, Duncan, Pete, Cassie, Sian and Alis. My mum and dad, family and friends for their unconditional support. A special thanks goes to Shelley Idziaszczyk for her technical support, assistance in genotyping, preparation of the knock-out construct and constant endeavour to make me a good scientist and teach me to spell.

I would like to thank Andrew Smith and Rosemary Bayne for performing the Gene Targeting and blastocyst manipulation. Lee Parry for the RT-PCR analysis. Carol Guy for assistance with tissue harvesting and genotyping of mice. The Wales Gene Park for assistance with sequencing. Cleo Bonnet for assistance with tissue sectioning and IHC. BMS for housing and husbandry of animals. The FMU for use of equipment

Finally, I would like to thank Tenovus, Wales Gene Park, Tuberous sclerosis alliance and Tuberous sclerosis association for their funding.

Abbreviations

A	Adenine
ABC	Avidin-biotin complex
aCGH	Array comparative genomic hybridisation
APC	Adenomatosis polyposis coli
AML	Angiomyolipomas
AMPK	AMP-dependant protein kinase
ATP	Adenosine 5'-triphosphate
BER	Base-excision repair
BHD	Birt Hogg Dube
BLAST	Basic Local Alignment Search Tool
BRRS	Bannayan-Riley-Ruvalcaba syndrone
BS	Bloom's syndrome
BSA	Bovine Serum Albumin
C	Cytosine
CA	Cystadenoma
CaM	Calmodulin
CD	Cowden's disease
CDK1	Cyclin-dependant kinase
CNC	Carney complex
CNS	Central nervous system
Cre	Cre recombinase protein from bacteriophage P1
CT	computed tomography
CTS	Contents a trade secret

DAB	3,3'-diaminobenzidine
DNA	Dioxiribonucleic acid
dNTPs	Deoxynucleotidetriphosphates
DPX	Dibutyl phthalate and xylene
E	Embryonic day
4e-BP1	Eukaryotic initiation factor 4E binding protein
EGFP	Enhanced green fluorescent protein
eIF4E	Eukaryotic initiation factor 4E
ENU	N-ethyl-N-nitrosourea
ER	Estrogen receptor
ERK	Extracellular signal-regulated kinase
ERM	Ezrin-radixin-moiesin
ES	Embryonic stem cells
FAP	Familial adenomatous polyposis
FISH	Fluorescence in situ hybridisation
FOXO	Forkhead family isoforms
G	Guanine
GAP	GTPase activating protein
GDP	Guanosine diphosphate
GFAP	Glial fibrillary acidic protein
GSK3	Glycogen synthase 3-kinase
GSK3ß	Glycogen synthase kinase-3ß
GTP	Guanosine triphosphate
H&E	Haematoxylin and eosin
HET	Heterozygous

HIF	Hypoxia-inducible factor
Hprt	Hypoxantine phosphoribsyltransferase
HRP	Horseradish peroxidase
IHC	Immunohistochemistry
IMS	Industrial methylated spirits
IPA	Intracisternal A particle
IRES	Internal ribosomal entry site
IRS	Insulin receptor
JP	Juvenile polyposis
LCM	Laser capture microdissected
LD	Long distance
LDD	Lhermitte-Duclos disease
LAM	Lymphangiomyomatosis
LOH	Loss of heterozygosity
MAPK	Mitogen-activated protein kinase
MEF	Mouse embryo fibroblast
MK2	MAPK-activated protein kinase 2
MMDBJ	Mouse microsatellite data base of Japan
MMR	Mismatch repair
MSH	MutS homolog
mTOR	mammalian target of rapamycin
mTORC1	mTOR complex 1
mTORC2	mTOR complex 2
neo	neomycin resistant gene
NF-L	Neurofilament-light chain

NF1	Neurofibromatosis
NER	Nucleotide-excision repair
NS	Not significant
OCT	Optimum cutting temperature
ORF	Open reading frame
PEN	Polyethylene napthalate
PCR	Polymerase chain reaction
PDGFR	Platelet derived growth factor receptor
PFGE	Pulsed-field gel eletrophoresis
PIKK	Phosphoinositides kinases-related kinase
PIP2	Phosphatidylinositol (4,5) bisphosphate
PIP3	Phosphatidylinositol (3,4,5) bisphosphate
PI3K	Phosphatidylinositol 3-kinase
PJS	Peutz-Jeghers syndrome
PKB	Protein kinase B
PKD	Polycystic kidney disease
PLS	Proteus like syndromes
PS	Proteus syndrome
PTEN	Phosphatase & tension homolog deleted on chrm 10
PTHs	PTEN hamartoma syndromes
RACE	Rapid amplification of cDNA ends
RCC	Renal cell carcinoma
Rheb	Ras-homolog enriched in brain
RNA	Ribonucleic acid
RSK1	p90 ribosomal S6 kinase 1

SCE	Sister-chromatid exchange
SEGA	Subependymal giant cell astrocytomas
SEN	Subependymal nodule
SMAD3	Mothers against DPP homolog 3
SMAD4	Mothers against DPP homolog 4
SSLP	Single-Sequence Length Polymorphism
S6	Ribosomal protein S6
S6K	ribosomal S6 kinase
S6K1	p70 ribosomal protein S6 kinase 1
T	Thymine
TGFβ	Transforming growth factors β
TOR	Target of rapamycin
TSC	Tuberous sclerosis complex
TSG	Tumour suppressor gene
UV	Ultra violet
VHL	von Hippel-Lindau disease
WT	Wild type

Contents

List of figures

List of tables

Chapter 1: Introduction

1.1 Cancer genetics

Cancer is a common genetic disease. Each year in the UK more than 275,000 people are diagnosed with cancer (Cancer research UK). Tumourigenesis in cancers is caused by alterations in three types of genes: Oncogenes, tumour-suppressor genes (TSGs) and stability genes (Vogelstein and Kinzler 2004). Oncogene and TSG mutations operate at a similar physiologic level; they drive the neoplastic process by increasing tumour cell number through the stimulation of cell division or through the inhibition of cell death or cell-cycle arrest (Vogelstein and Kinzler 2004). Stability genes are involved in DNA repair and when mutated, increase genetic instability. They keep genetic alterations to a minimum and, when they are inactivated, somatic mutations in other genes occur at a higher rate (Fodde and Smits 2002). Mutations in these three classes of genes can occur in the germline, resulting in hereditary predispositions to cancer, or in single somatic cells, resulting in sporadic tumours.

1.1.1 Oncogenes

Oncogenes are genes whose normal activity promotes cell proliferation (Strachan and Read 1996). They can be mutated in ways that render the gene constitutively active, or active under conditions in which the wild-type gene is not. Oncogene activation can result from chromosomal translocations, from gene amplifications or from subtle intragenic mutations

affecting crucial residues that regulate the activity of the gene product (Vogelstein and Kinzler 2004).

1.1.2 Tumour suppressor genes

TSGs are genes whose normal activity restricts cell proliferation. Mutations in TSGs generally reduce the activity of the gene product. Thus far, about thirty TSGs have been identified and definitively implicated in cancer development (Fearon and Vogelstein 2000). Inactivation of TSGs may arise from missense mutations at residues that are essential for product activity, from mutations that result in a truncated protein, from deletions or insertions of various sizes, or from epigenetic silencing (Vogelstein and Kinzler 2004). Tumourigenesis generally requires mutations in both the maternal and paternal alleles of TSGs as described by Knudson's 2-hit hypothesis (Fig. 1.1). Knudson's 2-hit hypothesis states that: Biallelic inactivation of a tumour suppressor gene is required for tumour formation and that both inherited and sporadic cancers can result from mutations of the same gene. Individuals carrying a germline mutation are predisposed to the disease because a single somatic event is sufficient to initiate tumour formation. In sporadic cases, the number of tumours is lower and cancer occurs at a later age because both alleles must be somatically inactivated (Knudson, 1971).

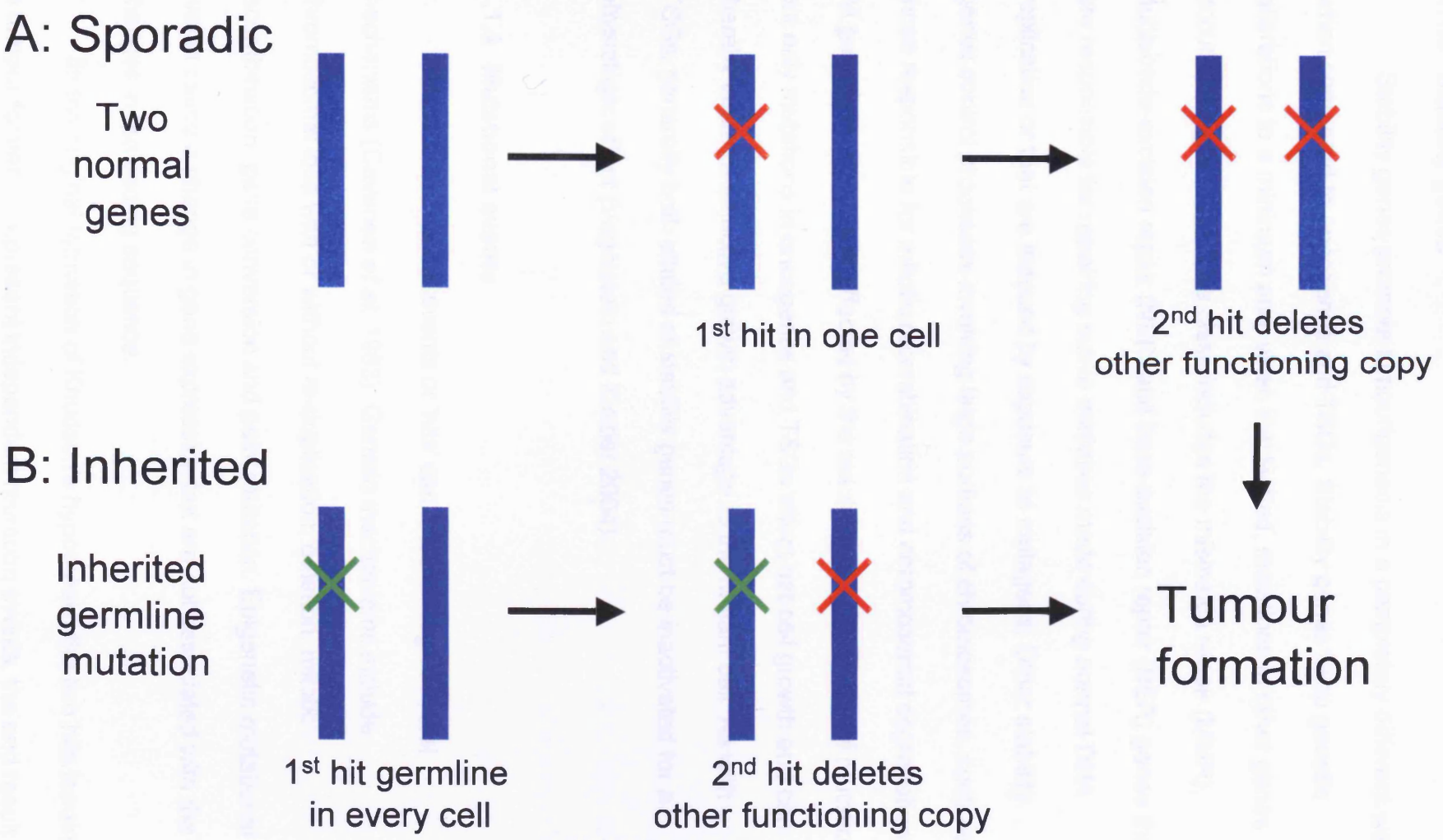

Figure 1.1: Knudson's 2-hit hypothesis of tumourigenesis in sporadic (A) and inherited (B) forms of cancer.

1.1.3 Stability genes

Stability genes promote tumourigenesis in a completely different way when compared to oncogenes and TSGs. Stability genes keep genetic alterations to a minimum and, when inactivated, mutations in other genes occur at a higher rate. This class includes the mismatch repair (MMR), nucleotide-excision repair (NER) and base-excision repair (BER) genes that are responsible for repairing subtle mistakes made during normal DNA replication or that are induced by exposure to mutagens. Other stability genes control processes involving large portions of chromosomes, such as those responsible for mitotic recombination and chromosomal segregation. All genes are potentially affected by the resultant increased rate of mutation, but only mutations in oncogenes and TSGs affect net cell growth and can thereby confer a selective growth advantage to the mutant cell. As with TSGs, generally both alleles of stability genes must be inactivated for a physiologic effect (Vogelstein and Kinzler 2004).

1.1.4 Mutational events

Somatic mutational events or 'hits' can arise through several mechanisms (Cavenee *et al.* 1983). Genetic mechanisms include chromosomal loss with or without re-duplication, deletion, mitotic recombination, gene conversion and point mutation. Epigenetic mutational events cause a change in gene expression but are not associated with the changes in the coding sequence.

In the original formation of Knudson's hypothesis, the two hits leading to tumour formation represent independent mutation events, the end result of

which is loss of tumour suppressor function (Knudson 1996). However, evidence from the adenomatosis polyposis coli (*APC*) gene suggests that the two hits may not always be independent and that the first hit may determine the nature of the second (Lamlum *et al.* 1999, Albuquerque *et al.* 2002).

1.1.5 Multistage evolution of cancer

Cancers represent one of the few disease types in which somatic mutations occurring after birth are pathogenic. Most of these alterations would be expected to be neutral but some produce a growth or survival advantage for the mutated cell. A somatic mutation in an oncogene or TSG, for example, can cause a clonal expansion and initiate the neoplastic process. Subsequent somatic mutations result in additional rounds of clonal expansion and thus in tumour progression. Consequently, during the course of cancer development, a normal cell progresses towards malignancy by acquiring a specific series of mutations. The theory that human cancers are the end result of several successive cellular changes was first suggested by Armitage and Doll (1954). Based on epidemiological data (Renan 1993) and *in vitro* data (Hahn *et al.* 1999), it is estimated that between four and eight rate-limiting mutations occur during the development of most human cancers (Quon and Berns 2001). In 1990, Fearon and Vogelstein presented a model for the genetic basis of colorectal neoplasia (Fig. 1.2). The colorectal tumours appear to arise first as a result of the mutational activation of oncogenes coupled with inactivation of TSGs. Mutations in at least 4 or 5 different genes are then required for the formation of a malignant tumour. Fewer changes are required for benign tumourigenesis. The total number of

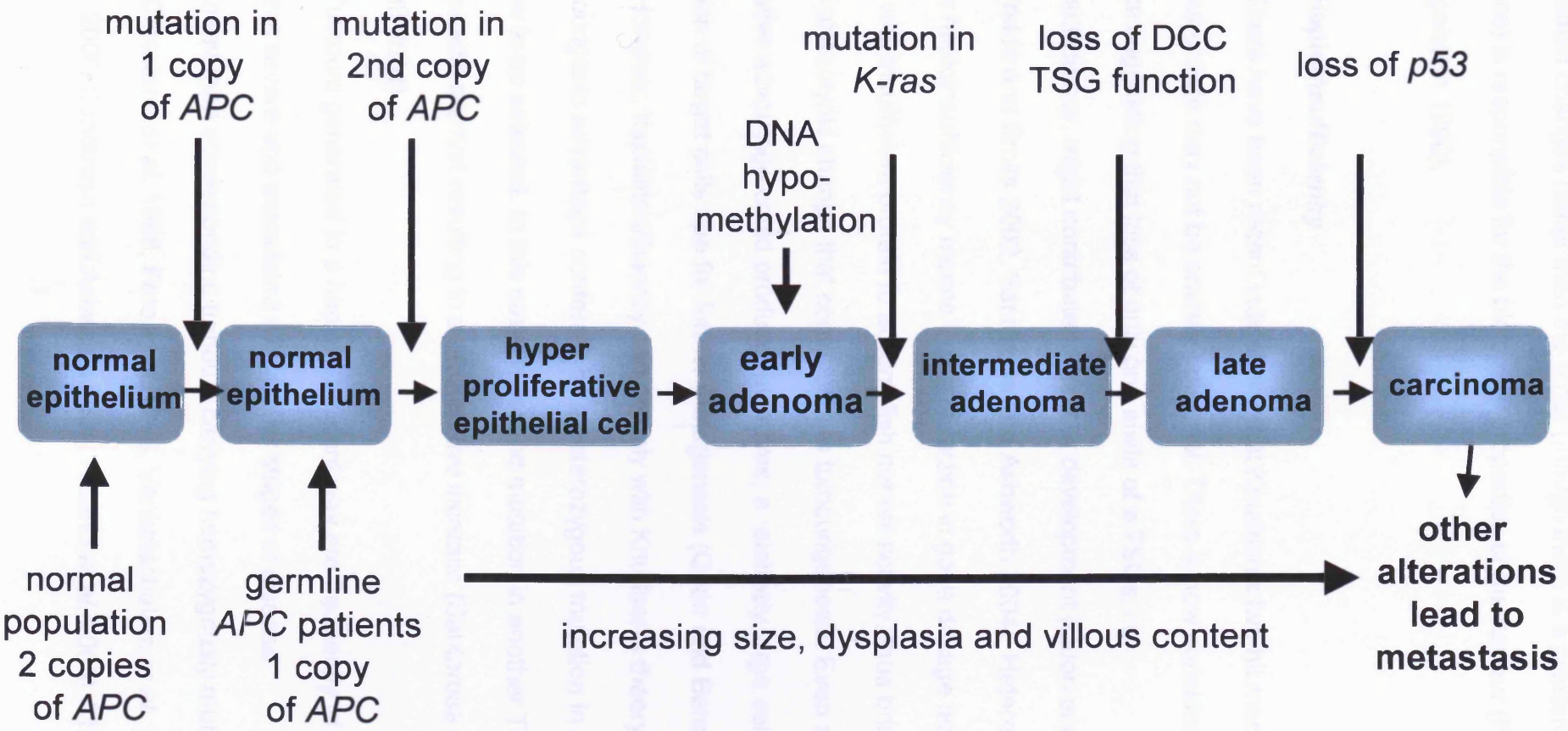

Figure 1.2: Multistage evolution of cancer for colorectal tumourigenesis: Tumourigenesis proceeds through a series of genetic changes involving oncogenes and TSGs (modified from Fearon and Vogelstein 1990).

accumulated changes rather than the order (though there is a preferred sequence) is responsible for the biological properties of the tumour (Fearon and Vogelstein 1990).

1.1.6 Haploinsufficiency

There have been recent indications that Knudson's two hit mechanism of tumour growth may not be entirely universal. There is now considerable evidence suggesting that loss of only one allele of a TSGs, i.e. haploinsufficiency, might contribute to tumour development (Quon and Berns 2001, Fodde and Smits 2002, Santarosa and Ashworth 2004). Heterozygous effect or haploinsufficiency means that a reduction in gene dosage leaves the cell with insufficient protein to accomplish normal activity, thus bringing about a phenotypic change that contributes to tumourigenesis. Even a small proliferative advantage could produce, over time, a relatively large sensitised population of target cells ripe for further mutagenesis (Quon and Berns 2001). However, haploinsufficiency can comply with Knudson's theory where the tumourigenic advantage conferred by a heterozygous mutation in a TSG is too low to be selected. In this case, a second mutation in another TSG can synergise with the first resulting in a proliferative increase (Santarosa and Ashworth 2004).

Tumours generated in a haploinsufficient way are frequently of later onset, less severe and associated with earlier stages of disease development than corresponding tumours carrying homozygously mutated genes (Cristofano *et al.* 1998, Fero *et al.* 1998, Venkatachalam *et al.* 1998, Xu *et al.* 2000, Santarosa and Ashworth 2004, Alberici *et al.* 2005). These

observations have lead to a model of strong or partial haploinsufficiency (Fig. 1.3). In partial haploinsufficiency, after a proliferative phase, the wild-type allele needs to be lost for tumour formation whereas in strong haploinsufficiency, a tumour can form in the absence of loss of the wild-type allele (Quon and Berns 2001).

1.2 Tuberous Sclerosis Complex

Tuberous sclerosis complex (TSC) is a genetically determined multi system disorder in which many organs are affected by unusual growths termed hamartomas.

1.2.1 Identification

The first report of TSC was in 1835 by Pierre Francois Olive Rayer who published an atlas illustrating skin disease with a plate closely resembling facial angiofibroma (Rayer 1835). Subsequently, TSC was named in 1880 by Desire-Magloire Bourneville. Bourneville used the term *tuberous sclerosis of the cerebral convolutions* for the unique cerebral nodular tumour pathology seen in the brain of a 15 year-old mentally handicapped female (Gomez *et al.* 1999). The umbrella term, tuberous sclerosis complex, was assigned to the syndrome by Moolten (1942).

1.2.2 Characterisation and early diagnosis

In 1908, Vogt described the association between the cerebral sclerosis reported by Bourneville and the facial adenoma sebaceum. Vogt established a classic clinical triad of features for the diagnosis of TSC consisting of

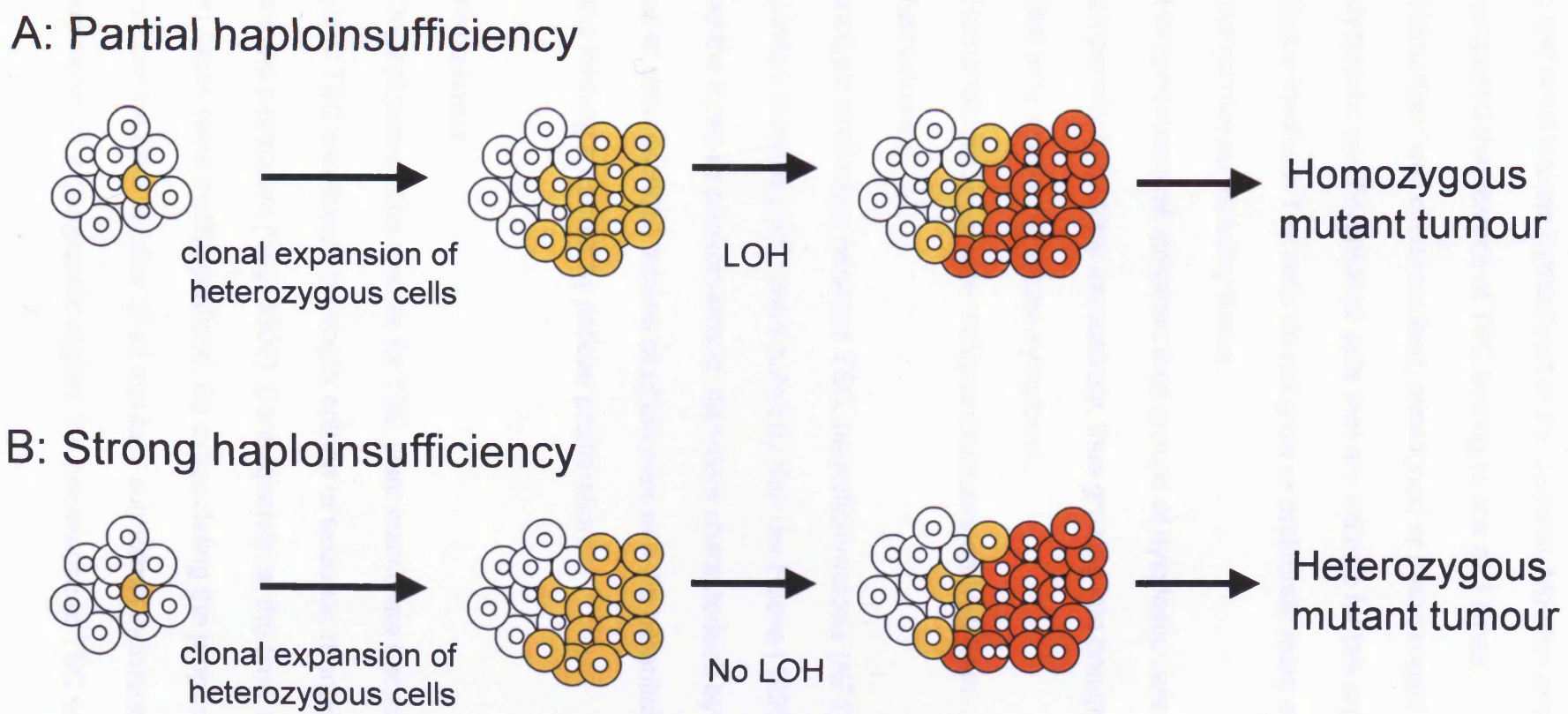

Figure 1.3: The effects of strong and partial haploinsufficiency with or without loss of heterozygosity (LOH). (A) Partial haploinsufficiency: after a proliferative phase, the wild type allele needs to be lost for tumour formation; (B) Strong haploinsufficiency: results in tumour formation in the absence of loss of the wild type allele. Wild type cells white, heterozygous 'normal' cells light orange, tumour cells dark orange. (modified from Quon and Berns 2001).

seizures, learning disability and adenoma sebaceum. He also noted that cardiac and renal lesions formed part of the disease. Moolten and colleagues (1942) proposed that lesions of TSC belong to one of 3 types:

1. Hamartias: well circumscribed, misaligned or misarranged groups of dysplastic undifferentiated cells that are intrinsic for the organ or tissue involved. The cells do not grow or proliferate more rapidly than the normal surrounding tissue.
2. Hamartomas: well circumscribed groups of dysplastic cells that have a propensity to multiply excessively, thus growing into benign tumours that may or may not cause symptoms.
3. Hamartoblastomas: rare malignant tumours derived from hamartomas.

Phenotypic similarities between TSC, neurofibromatosis (NF1) and von Hippel-Lindau disease (VHL) were noted by Van der Hoeve (1920). He classified the three as phakomatoses; disorders characterised by the presence of circumscribed lesions or phakomas with the potential of getting larger and forming a tumour by cellular proliferation.

1.2.3 Prevalence

Original prevalence studies for TSC were inaccurate because the diagnosis of TSC was based on Vogt's criteria of seizures, mental handicap and adenoma sebaceum (Vogt 1908). Consequently, at the time, the majority of known cases were institutionalised. By extrapolating the proportion of TSC sufferers from the total number of all mentally subnormal individuals in an entire population of a geographic region, the prevalence of TSC was

estimated between 1:20,000 to1:150,000 (Gunther and Penrose 1935, Ross and Dickerson 1943, Dawson 1954, Paulson and Lyle 1966, Zaremba 1968). In the early 20th century, abundant reports of small groups of patients with TSC indicated that TSC was not as rare as earlier believed. More recently, appreciation of the differing phenotypes and advancement of technologies has meant the prevalence estimates of TSC have increased. Population based studies in Olmsted County have estimated prevalence as 1:9704 to 1:14,492 (Wiederholt et al. 1985, Shepherd *et al.* 1991)

1.2.4 Manifestations

Pathologically, tuberous sclerosis is a disorder of cellular migration, proliferation and differentiation. Manifestations may be systemic and variable. The skin, brain, kidney and heart are most commonly involved. However the eyes, lungs, bones and many other organs may also be affected (Gomez 1988). Approximately 96% of patients with TSC have one or more type of skin lesion, 90% have symptoms or signs of cerebral pathology, 84% have or had seizures, an estimated 60% have renal pathology, and nearly 50% have retinal harmartomas (Gomez *et al.*1999). The phenotype of TSC patients varies according to organ or organs involved, number and size of lesion, and sometimes the exact location of lesion. The age of the patient is another factor to be considered. Rhabdomyomas appear in foetal life and may disappear in infancy, while angiomyolipomas do not appear untill later in life. Phenotypic severity, both inter- and intra-familial is also highly variable making the assignment of disease status difficult.

1.2.4.1 Manifestations of the central nervous system

1.2.4.1.1 CNS lesions

Central nervous system lesions in patients with TSC include cortical tubers, focal cortical dysplasia, subependymal nodules (SENs) and subependymal giant cell astrocytomas (SEGAs). Spinal cord involvement is rare (Lee-Jones *et al.* 2004).

Cortical tubers (Fig. 1.4a) constitute the hallmark of TSC. Cortical and subcortical tubers are hypomyelinated hamartias involving mainly the cerebral cortex and underlying white matter. Tubers are often multiple, vary in size and in cortical location (Gomez *et al.* 1999). Cortical tuber count is a biomarker of cerebral dysfuntion (Roach *et al.* 1987, Curatolo *et al.* 1991, Shepherd *et al.* 1995, Goodman *et al.* 1996), and there is some correlation with neurological outcome. Histologically, cortical tubers are characterised by architectural disarray. They vary considerably in cellularity and feature both neurons and large cells (Gomez *et al.* 1999).

SENs (Fig. 1.4a) are found in 80% of TSC patients. They are hamartomatous growths that are typically located along the outer walls of the lateral ventricles. They are often multiple and small in size, ranging from 2 to 10mm, and are often partially or completely calcified (Hosoya *et al.* 1999). SENs develop during foetal life and are usually asymptomatic. Histologically, SENs are smooth surfaced, consisting of spindle and epithelioid, astrocyte-like cells (Gomez *et al.* 1999).

SEGAs are histologically identical to SENs but are classified on the basis of their larger size. It is generally accepted that SEGAs evolve from SENs (Scheithauer 1992).

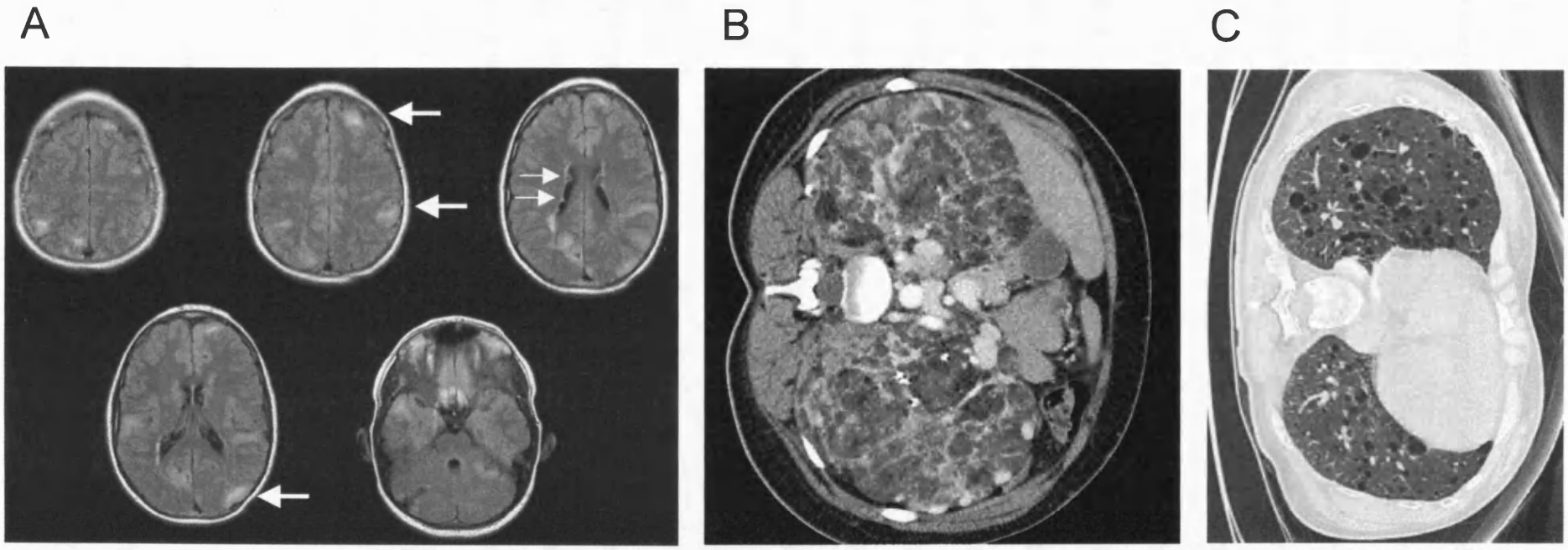

Figure 1.4: TSC manifestations. (A) Magnetic Resononance Imaging study of the brain of a patient with Tuberous Sclerosis. With cortical and subcortical tubers (the peripheral, bright spots, large arrows) and subependymal nodules (the darker lumps along the outer walls of the lateral ventricles, small arrows). (B) Appearance of severe renal angiomyolipomas by contrast enhanced computed tomography (CT) examination of the abdomen; both kidneys are enlarged and essentially replaced by large masses of fat, blood vessels and soft tissue. (C) High-resolution CT imaging of the chest shows multiple cysts within the lung parenchyma which is the typical appearance of lymphangioleiomyomatosis (LAM). Images from http://commons.wikimedia.org/

1.2.4.1.2 Neurological manifestations

Abnormalities in neuronal migration, cellular proliferation and the formation of various brain lesions lead to neurological manifestations. These include seizures, learning disability and autism. Seizures are the most common neurological symptom of TSC and occurred in 92% of patients referred to the Mayo clinic (Gomez 1988). Patients with TSC range from intellectually normal to severely impaired. Children with infantile spasms and hypsarrhythmia are reported to be more severely impaired than those with any other form of epilepsy (Gomez 1988). In addition to learning disability, multiple behavioural problems including sleep disorders, hyperactivity, attention deficit, aggressiveness and autism have been found in children with TSC (Curatolo *et al.* 1991, Gillberg *et al.* 1994). Overall, the degree of intellectual deficit and behavioural disturbance varies greatly.

1.2.4.1.3 Ophthalmic manifestations

Approximately 50% of patients with TSC demonstrate ocular pathology. Retinal hamartomas, retinal pigmentation, retinal vascular changes, optic nerve atrophy, glaucoma, and coloboma of the iris, lens, choroids and retina are among the most frequent ophthalmologic manifestations (Curatolo 2003).

1.2.4.2 Renal manifestations

Eventually, more than 80% of patients with TSC develop morphologic abnormalities in their kidneys. These lesions include angiomyolipomas (AMLs), renal cysts and, rarely, renal cell carcinomas (RCCs).

AMLs (Fig. 1.4b) are nonencapsulated localised proliferations of blood vessels, smooth muscle and fat, and are the most common renal lesions in patients with TSC. Because of their histological characteristics, they have been regarded histologically as tumourous malformations rather than true neoplasms (Bjornsson *et al.* 1999). AMLs are usually multiple and bilateral, with prevalence related to patient age (Stillwell *et al.* 1987, Cook *et al.* 1996). There is a slight preponderance to higher occurance in females than in males (1.2:1) (Ewalt *et al.* 1998).

The incidence of renal cysts in TSC patients varies between sexes being 9% in females to 20% in males (Torres *et al.* 1995). The true prevalence of renal cysts may be higher as, in autopsy studies, 53% of TSC patients had renal cysts (Stillwell *et al.* 1987). The cysts have a unique epithelial lining of hypertrophic, hyperplastic eosinophilic cells (Stapleton *et al.* 1980, Bernstein 1993). Renal cysts can cause impairment to renal function and hypertension (Gomez *et al.* 1999). Severe renal cystic disease, similar to advanced autosomal dominant Polycystic kidney disease (PKD), is seen in patients where deletions disrupt both *TSC2* and the neighbouring *PKD1* gene (Sampson *et al.* 1997).

An association appears to exist between TSC and RCC. The carcinomas are usually found at a younger age than would be expected typically in the general population and are thought to evolve from the lining of hyperplastic cysts (Bjornsson *et al.* 1996). RCCs in TSC patients include clear cell, papillary and chromophobe types, and have been shown to be metastatic (Bjornsson *et al.* 1996, Al-Saleem *et al.* 1998). The incidence of RCC in TSC has been estimated at 4.4% in the Mayo Clinic cohort (Stillwell

et al. 1987) and 2.2% in the UK (Cook *et al.* 1996). These could be under estimates reflecting the younger patients who are typically followed by TSC clinics and the under recognition that TSC is a genetic syndrome predisposing to RCCs that are heterogeneous (Henske 2004). TSC associated RCCs may be rare, but they have clinical, pathologic and genetic features distinguishing them from sporadic RCCs (Weiner *et al.* 1998).

1.2.4.3 Dermatological manifestations

Dermatological manifestations are common in TSC. According to Gomez (1988), 96% of patients with TSC have one or more skin lesions (facial angiofibromas, ungula fibromas, shagreen patch and/or hypomelanotic macules).

Facial angiofibromas are pink to red nodules with a smooth glistening surface that are distributed bilaterally over the centrofacial areas. They usually present between the 2nd and 5th year of age (Curatolo 2003) and are composed of vascular fibrous and dermal tissue elements (Kwiatkowski and Short 1994). Ungual fibromas are fleshy lesions arising from beneath the nails, which histologically resemble facial angiofibromas. Shagreen patches are firm yellow-brown or pink hamartomatous lesions of the connective tissue. They occur mainly on the lower back and are generally multiple and small, but can become large lesions more than 10cm in diameter (Curatolo 2003). Hypomelanotic macules are patches of abnormal whiteness, which can be seen from the time of birth, and so are regarded as the first visible sign of TSC. Miscellaneous nevoid lesions also associated with TSC include

forehead fibrous plaque, confetti like macules, café-au-lait macules and soft fibromas such as molluscum fibrosum pendulum.

1.2.4.4 Cardiac manifestations

Cardiac rhabdomyomas are very common and often multiple in neonates with TSC. Approximately 50% of infants with TSC have been reported to have rhabdomyomas (Bass *et al.* 1985, Smith *et al.* 1989), although, in most patients, these cardiac tumours have little or no clinical significance (Smith *et al.*1989). Cardiac rhabdomyomas represent the earliest detectable hamartoma in TSC and, interestingly, appear to be the only lesions in TSC that may regress with age (Curatolo 2003). The lesions may be detected in any of the cardiac chambers but occur more commonly in the ventricles than in the atria (Fenoglio *et al.* 1976, Jozwiak *et al.* 1994). On gross examination, cardiac rhabdomyomas have a grey or yellowish-white appearance and vary in size. The tumour cells are typically characterised by a chicken wire appearance and by so called spider cells (Mair *et al.* 1999).

1.2.4.5 Pulmonary manifestations

Symptomatic pulmonary involvement in TSC is rare. It is estimated to occur in 1% to 6% of cases (Uzzo *et al.* 1994, Kwiatkowski and Short 1994). It develops predominantly in women between 20 and 40 years of age (Taylor *et al.* 1990, Uzzo *et al.* 1994) and thus has led to the hypothesis that estrogen regulates TSC signalling (Astrinidis and Henske 2005). The TSC lung lesions are morphologically undistinguishable from sporadic lymphangiomyomatosis (LAM) (Fig. 1.4c). Histologically, LAM is

characterized by the diffuse, bilateral proliferation of abnormal smooth muscle cells and cystic degeneration of the lung parenchyma (Henske 2003). Patients with both sporadic LAM and TSC-LAM often have benign renal AMLs. The smooth muscle cells within the angiomyolipomas can be morphologically very similar to the smooth muscle cells in pulmonary LAM. Recent studies suggest that pulmonary LAM may be the result of a highly unusual disease mechanism: the metastasis of 'benign cells' (Karbowniczek *et al.* 2003, Henske 2003). The prognosis of LAM is often poor (Shepherd *et al.* 1991), though lung transplantation can be useful (Boehler *et al.* 1996).

1.2.4.6 Additional manifestations of TSC

An association of arterial aneurysms and TSC has been reported in a number of patients (Curatolo 2003). Hepatic hamartomas or hepatic AMLs have been reported in patients with TSC (Jozwiak *et al.* 1992). Dental enamel pitting is seen in 90% of patients with TSC (Flannagan *et al.* 1995). Other rare manifestations of TSC can been seen in the endocrine system (thyroid, pancreas, gonads, hypothalamus and pituitary) as well as the digestive tract, and spleen (Gomez *et al.* 1999).

1.2.5 Clinical diagnosis of TSC

After Vogt (1908) pointed out the early diagnostic triad of TSC, it was not until 1979 that Gomez succeeded in greatly improving the diagnostic method. Gomez observed that only 29% of patients presented all three of Vogt's triad characteristics (Gomez 1979, Gomez 1988). Gomez believed there were two different criteria for the primary and secondary diagnosis of

TSC. For primary diagnosis, patients must have one of the following three groups of clinical signs; (1) a characteristic skin lesion; (2) cortical tubers or subependymal hamartomas; (3) multiple retinal hamartomas. If a primary characteristic was not present, two secondary features were acceptable for diagnosis. Secondary features included; infantile spasms, hypomelanotic macules, shagreen patch, single retinal hamartoma, subependymal or cortical calcifications, multiple renal tumours, cardiac rhabdomyoma or an immediate relative with TSC. In 1998 at the Tuberous Sclerosis Complex Consensus Conference, the diagnostic criteria were reassessed. The new criteria were divided into two groups, major and minor (Table 1.1); the diagnosis of TSC is established when two major features or one major plus two minor features can be demonstrated.

1.2.6 Identification of the TSC genes

TSC was first recognised as a genetic condition by Kirpicznik in 1910. He described the condition in fraternal twins and in a family with affected individuals in 3 generations. The hereditary nature of TSC was first reported by Berg in 1913 and, in 1914, Schuster confirmed it. Since then, studies by Gunther and Penrose (1935) and Nevin and Pearce (1968) demonstrated the dominant inheritance of TSC and its high mutation rate. Linkage between the ABO blood group on chromosome 9q34 and TSC was reported in 1987 (Fryer *et al.* 1987). Analysis by Connor *et al.* (1987) supported this view but other early reports contradicted these findings (Northrup *et al.* 1987, Povey *et al.* 1988, Kandt *et al.* 1989). An international collaboration was established in an attempt to resolve the apparently contradicting data. Subsequent

results confirmed linkage at 9q34 in approximately half the families studied (Sampson *et al.* 1992). This locus was denoted *TSC1*. Evidence for locus heterogeneity was presented (Northrup *et al.* 1987, Sampson *et al.* 1989, Janssen et al 1990, Northrup *et al.* 1992, Sampson *et al.* 1992) and further studies of five large families not linked to 9q34 led to the identification of a second locus at chromosome 16p13.3, denoted *TSC2* (Kandt *et al.* 1992). Among families large enough to permit linkage analysis, half show linkage to 9q34 and half to 16p13. There is no linkage evidence for a third TSC locus (Janssen *et al.* 1994, Povey *et al.* 1994).

Table 1.1: Clinical diagnostic criteria for TSC (modified from Roach *et al.* 1998)

Major features	**Minor features**
Facial angiofibromas or forehead plaques	Multiple pits in dental enamel
Non-traumatic ungual or periungual fibroma	Hamartomatous rectal polyps
Hypomelanotic macules (3 or more)	Bone cysts
Shagreen patch (connective tissue nevus)	Cerebral white matter
Multiple retinal nodular hamartomas	radial migration lines
Cortical tuber	Gingival fibromas
Subependymal nodule	Non-renal hamartoma
Subependymal giant cell astrocytoma	Retinal achromic patch
Cardiac rhabdomyoma	'Confetti' skin lesions
Lymphangiomyomatosis	Multiple renal cysts
Renal angiomyolipoma	

1.2.6.1 *TSC1*

The identification of *TSC1* was a lengthy process that proved difficult for a number of reasons. First, the 9q34 region is gene rich with numerous *TSC1* potential candidates. Secondly, several parts of the region were unstable in multiple cloning vectors (Zhou *et al.* 1995, Hornigold *et al.* 1997). Thirdly, unlike the *TSC2* locus where the characterisation of large deletions in several families significantly reduced the candidate region (The European Chromosome 16 Tuberous Sclerosis Consortium 1993), no large rearrangements were identified at the *TSC1* locus. Finally, conflicting linkage and haplotype studies pointed to both the distal and proximal parts of the candidate region (Nellist *et al.* 1993, Pitiot *et al.* 1994, Janssen *et al.* 1994). Initial definition of the 1.5Mb *TSC1* candidate region on chromosome 9q34 was achieved by identification of key meiotic recombination events in large *TSC1* linked families (Haines *et al.* 1991, Nellist *et al.* 1993). Microsatellite markers from this region were identified and a contig assembled (Povey *et al.* 1994, van Slegtenhorst *et al.* 1995, Au *et al.* 1996, Hornigold *et al.* 1997). The region was further narrowed to 900kb between the markers D9S2127 and *DBH* by two additional recombination events in unaffected individuals. In all, 30 genes were identified or mapped to the 900kb critical region and several genes identified appeared to be good candidates based on probable roles in signal transduction pathways. However, no mutations in these genes were identified in patients with TSC (van Slegtenhorst *et al.* 1997). A strategy to sequence the 900kb region was implemented. Predicted and confirmed exons in the initial 208kb of sequence were screened for mutations using heteroduplex analysis in a cohort of twenty unrelated TSC families with

linkage to 9q34 and in 40 sporadic TSC cases. Mobility shifts in ten samples were revealed in the 62nd exon screened and sequencing confirmed truncating mutations in eight samples (7 frameshift and 1 nonsense mutations). A combination of 5'RACE, RT-PCR and isolation of other cDNA clones defined the remainder of the open reading frame of *TSC1*. The complete genomic structure of *TSC1* was determined by comparison of the genomic and cDNA sequences (van Slegtenhorst *et al.* 1997). *TSC1* spans approximately 43kb of genomic DNA and consists of 23 exons encoding a 1164 amino acid, 130kDa protein named hamartin (Fig. 1.5). The translation initiation and termination codons are at nucleotides 222 in exon 3 and 3738 in exon 23, respectively. Northern blot analysis revealed a widely expressed 8.6kb transcript (van Slegtenhorst *et al.* 1997).

1.2.6.2 *TSC2*

The identification *TSC2* was rapid compared to *TSC1*. Two factors in particular aided in its swift discovery. First, mapping at the 16p13.3 locus was already advanced and, secondly, chromosomal rearrangements were identified that defined a small region in which the gene could be sought. Initially, linkage studies identified *TSC2* to be located in a 1.5Mb region of chromosome 16p (Kandt *et al.* 1992). At the same time, a family with both TSC and autosomal dominant *PKD* was found to have a translocation between chromosomes 16p and 22q. The mother and daughter each carried a balanced translocation involving 16p13.3 (46,XX,t(16;22)(p13.3;q11.21) and had typical signs of PKD but no TSC. The son, on the other hand, had inherited an unbalanced karyotype (45,XY,-16,-

22,+der(16)(16qter→16p13.3::22q11.21→22qter) and had CNS and skin phenotypes typical of TSC as well as renal cysts (European Polycystic Kidney Disease Consortium 1994). It was reasoned that the son manifested TSC because of a deletion of one copy of the *TSC2* gene, the implied location of which was telomeric to the translocation breakpoint on 16p13.3. The breakpoint of the translocation was mapped by a combination of fluorescence in situ hybridisation (FISH) and pulsed-field gel eletrophoresis (PFGE) and was defined as lying 150kb telomeric to 16AC2.5. A previously reported patient had a *de novo* truncation of 16p but had no clinical manifestations of TSC (Wilkie *et al.* 1990), thus excluding approximately 1.1Mb of the1.4Mb *TSC2* candidate region. A cosmid contig of the remaining 300kb was generated and a cohort of 255 patients with TSC was screened for rearrangements in the region using PFGE and Southern blotting. Deletions ranging from 30kb to 100kb were observed in five patients all involving the same 120kb region. Four genes were isolated from this region by screening cDNA libraries, and it was shown only one of these genes was disrupted by all five deletions. Further analysis of this gene revealed 4 smaller intragenic deletions thus confirming the identity of the *TSC2* gene. *TSC2* spans approximately 44kb of genomic DNA and consists of 41 exons encoding a 1807 amino acid, 198kDa protein that was named tuberin (Fig. 1.6). The translation initiation and termination codons are at nucleotides 19 in exon 1 and 5440 in exon 41, respectively. A non-coding leader exon (exon 1a) has been identified (Kobayashi *et al.* 1997) and exons 25, 31 and the first codon of exon 26 are alternately spliced (Xu *et al.* 1995). Northern blot analysis reveals a widely expressed 5.5kb transcript.

1.2.7 Mutation analysis of *TSC1* and *TSC2*

More that 300 germline mutations have been reported for *TSC2*, including missense, nonsense, frameshift deletions/insertions and splice site mutations (Jones *et al.* 1999, Dabora *et al.* 2001, Sancak *et al.* 2005). Interestingly, exons 35–39 which encode the essential GTPase activating protein domain contained 46% of missense mutations and 93% of all in-frame deletions (Sancak *et al.* 2005). In contrast, nearly all (>90%) reported in *TSC1* mutations are either nonsense or frameshift variants that cause premature protein truncation (Sancak *et al.* 2005). Both somatic and germline mosaicism for causative mutations in *TSC1* and *TSC2* has been documented in many patients (Cheadle *et al.* 2000a).

In agreement with Knudson's two hit hypothesis, inactivation of both alleles of either *TSC1* or *TSC2* is necessary for some of the clinical manifestations, suggesting that *TSC1* and *TSC2* function as tumour suppressor genes. Loss of heterozygosity (LOH) at *TSC1* and *TSC2* has been observed in 56% of renal AMLs and rhabdomyomas, but in only 4% of TSC-associated brain lesions. This suggests that brain lesions can result from different pathogenic mechanisms as compared to kidney and heart lesions (Henske *et al.* 1996). A novel mechanism specific to TSC-associate brain lesions has been proposed whereby tuberin can be inactivated by physiologically inappropriate phosphorylation (Han *et al.* 2004).

1.2.8 Genotype/phenotype correlations

TSC2 mutations are approximately five times more common than *TSC1* mutations in sporadic patients with TSC. This may be attributed to the smaller size and less complex structure of hamartin. However, the two genes appear to account for an equal proportion of mutations in large TSC families (Povey *et al.* 1994, Jones *et al.* 1997). Therefore, the rate of germline *TSC1* mutation appear to be lower than for *TSC2* but each new sporadic *TSC1* patient has a better chance of founding a family than a *TSC2* patient. These observations suggest that, on average, patients with *TSC1* mutations may be less severely affected than those with *TSC2* mutations (Cheadle *et al.* 2000a, Kwiatkowski 2005). Studies of large cohorts indicate that patients with a *TSC1* mutation are less likely to be mentally retarded (Jones *et al.* 1999, Sancak *et al.* 2005), whilst patients with *TSC2* mutations have a higher number or severity of clinical features including renal AMLs and renal cysts (Dabora et al 2001, Sancak *et al.* 2005). Sex differences have also been noted. Males with TSC have been reported to have a higher risk of learning disorders, autism (Smalley *et al.* 1992) renal cysts, retinal lesions and fibromas (Sancak *et al.* 2005) when compared to females.

1.2.9 Biochemistry of the TSC proteins

1.2.9.1 Hamartin

Hamartin and tuberin expression analysis has been difficult due to antibody limitations but generally it is considered that hamartin is expressed in most cell types including those of the nervous system (Gutmann *et al.* 2000), endocrine tissues and in many organs such as the kidney, uterus,

intestine and liver (Fukuda *et al.* 2000, Johnson *et al.* 2001). Most reports place hamartin in the cytoplasm, localised to cytoplasmic vesicles (Plank *et al.* 1998, Nellist *et al.* 1999).

Hamartin is hydrophilic and forms homomeric complexes. It has a weakly predicted transmembrane domain at amino acids 127-144 (Fig. 1.5) and a predicted coiled-coil region at residues 719-998 (Nellist *et al.* 1999). It has a tuberin interaction domain that spans residues 302-430 (Hodges et al. 2001, Nellist *et al.* 2001) and forms a tumour suppressor complex with tuberin (discussed below). Hamartin also has an ezrin-radixin-moesin (ERM) interaction domain that spans residues 881-1084 and a Rho-activating domain at amino acids 127-144; it has been suggested that hamartin regulates actin dynamics and cellular adhesion through these interacting domains (Lamb *et al.* 2000). Hamartin has also been found to bind to neurofilament-light chain (NF-L) and possibly functions as a novel integrator of the neuronal cytoskeleton (Haddad *et al.* 2002). Taken together, these data suggest that hamartin may act as a scaffolding protein for proper localisation of tuberin (Astrinidis and Henske 2005).

Reversible protein phosphorylation is a key mechanism controlling the activity of numerous proteins within the cell. Phosphorylation of hamartin by cyclin-dependant kinase CDK1 has been reported, late in the cell cycle, at three residues T417, S584 and T1047 (Astrinidis *et al.* 2003). Hamartin with alanine mutations in the three CDK1 phosphorylation sites increased the inhibition of p70 ribosomal protein S6 kinase 1 (S6K1) by the hamartin-tuberin complex, suggesting phosphorylation of hamartin regulates the function of the hamartin-tuberin complex during cell cycle progression

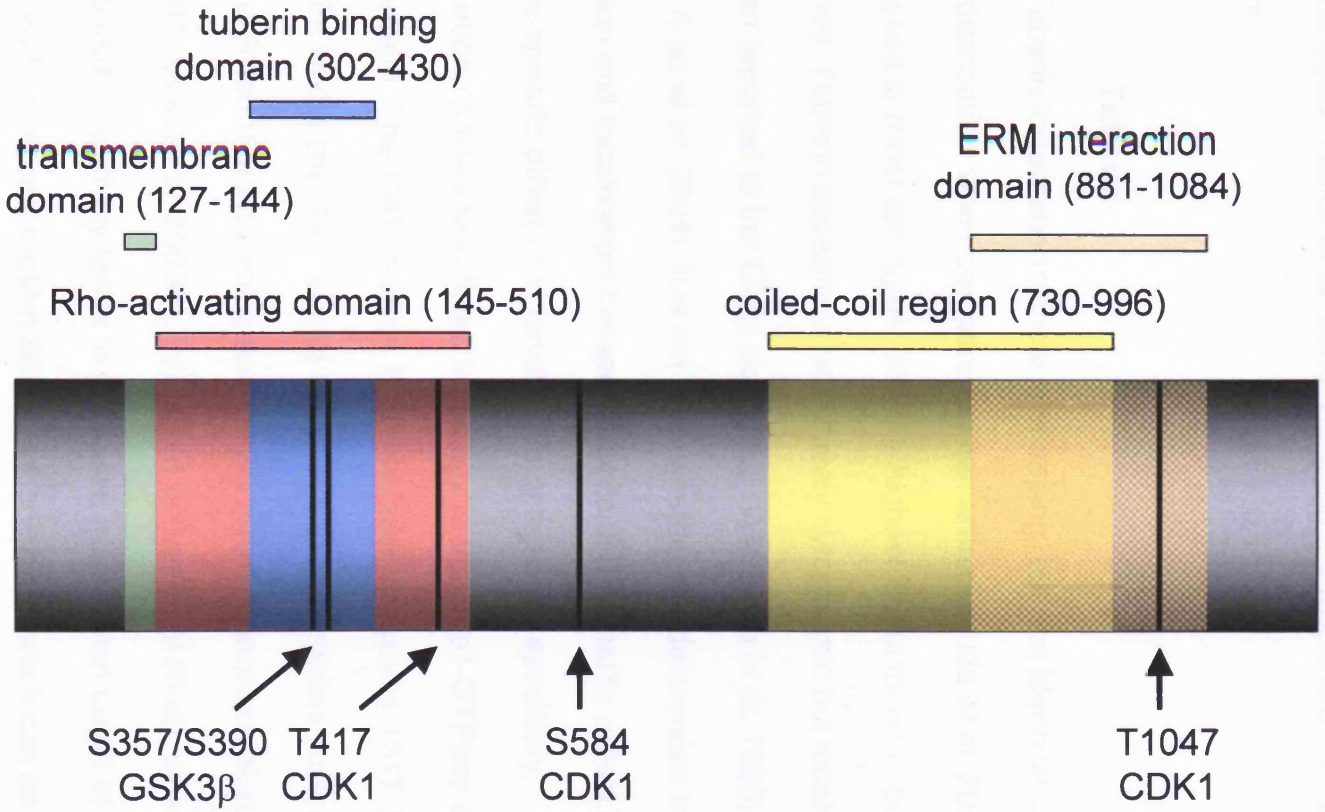

Figure 1.5: Two-dimensional representation of Hamartin. Harmartin is a 1164 amino acid protein with a molecular mass of 130kDa. It interacts with tuberin through amino acids 302-430. It has a potential transmembrane domain, Rho-activating domain and an ezrin-radixin-moesin (ERM) interaction domain as well as a coiled-coil region from amino acids 730- 996. It is phosphorylated by cyclin-dependant kinase (CDK1) (residues T417, S584, T1047) and by Glycogen synthase kinase-3ß (GSK3β) (S357, S390).

(Astrinidis *et al.* 2003). In addition to phosphorylation by CDK1, hamartin is phosphorylated by Glycogen synthase kinase-3ß (GSK3ß) at residues T357 and T390 (Mak *et al.* 2005). This increases the stability of the TSC complex causing reduction of ß-catenin signalling. Finally, hamartin is phosphorylated at residue S505 (Nellist *et al.* 2005) although the responsible kinase is as yet unknown.

1.2.9.2 Tuberin

Tuberin localisations show overlapping, but non identical organ and cellular distribution when compared to hamartin (Fukuda *et al.* 2000). Tuberin is expressed in most cell types, with the highest levels found in brain, heart and kidney. Tuberin appears to be diffusely cytoplasmic but localisation has also been reported to the Golgi apparatus (Wienecke *et al.* 1996) and the nucleus (Lou *et al.* 2001). It is not clear whether the differences in cell type expression and localisation between tuberin and hamartin reflect cell type- or cell cycle-specific differential localisation or antibody specificity.

Tuberin shows significant homology to the Rap1-GTPase activating (GAP) protein. The GAP domain in tuberin spans residues 1517-1674 (Fig. 1.6) GAPs inhibit the Ras-related family of small G proteins such as Rap1, Rab5 and Rheb (Ras-homolog enriched in brain) (Wienecke *et al.* 1995, Xiao *et al.* 1997, Inoki *et al.* 2003a). Increased activation of Rheb, when tuberin is dysfunctional, effectively leads to increased mammalian target of rapamycin (mTOR) and ribosomal protein S6 phosphorylation, which can be blocked by the immunosuppressant drug rapamycin (Tee *et al.* 2003).

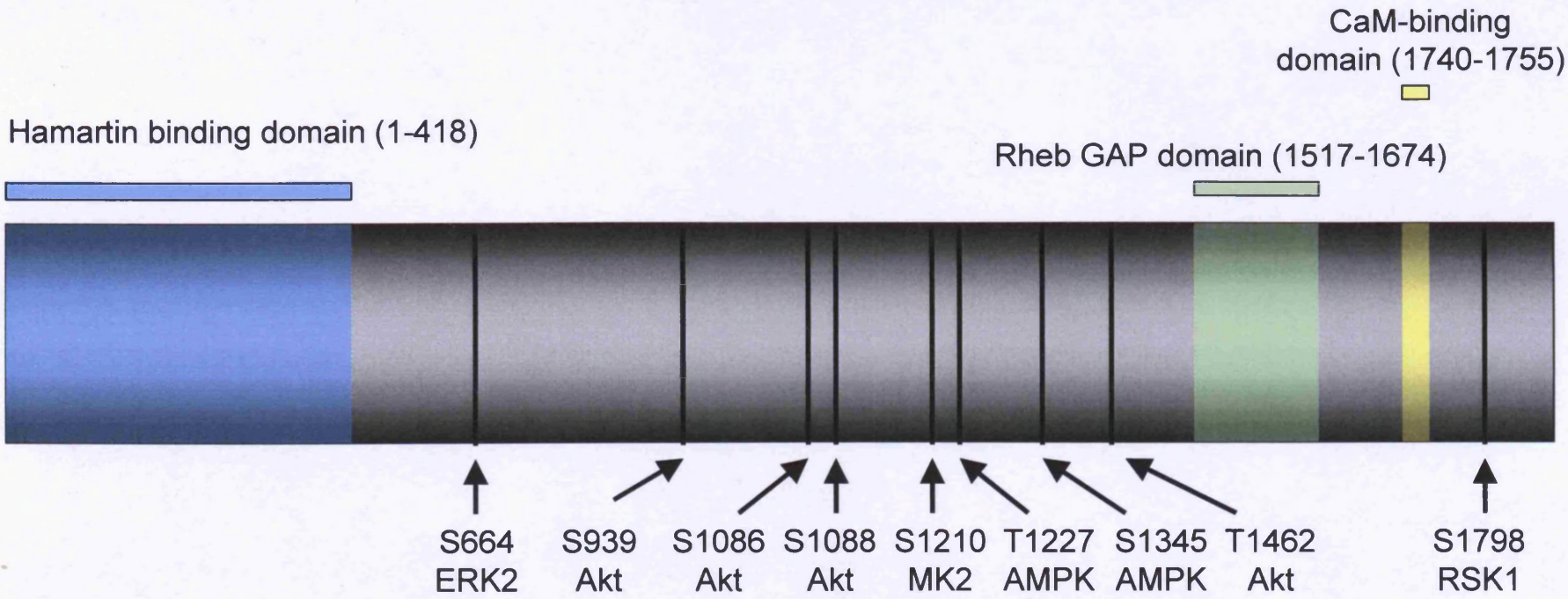

Figure 1.6: Two-dimensional representation of tuberin. Tuberin is 1807 amino acid protein with a molecular mass of 200kDa. It interacts with hamartin through amino acids 1- 418. It has a GTPase activating protein (GAP) domain with specificity for Rheb. It has a calmodulin (CaM) binding domain at amino acids 1750-1755. It is phosphorylated by the serine/threonine kinase Akt (residues S939, S1086, S1088, T1462), MAPK-activated protein kinase 2 (S1210), ribosomal S6 kinase 1 (RSK1) (1798), AMP-dependant protein kinase (AMPK) (T1227, S1345) and extracellular signal-regulated kinase 2 (ERK2) (S664).

Tuberin has a sequence (amino acids 1740-1755) that is capable of forming a basic amphipathic helix indicative of a calmodulin (CaM) binding domain (Noonan *et al.* 2002). Deletion mutagenesis studies suggested that this CaM binding domain is required for tuberin modulation of steroid receptor function. Competition binding studies identified a competitive relationship for binding of tuberin by estrogen receptor (ER) α and CaM, that is modulated by the presence of hamartin, supporting the hypothesis that interactions between the TSC complex, ER alpha, and CaM may play a critical role in the pathology of TSC and LAM disease (York *et al.* 2005).

The serine/threonine kinase Akt phosphorylates tuberin at S939, S1086, S1088 and T1462, which negatively regulates the TSC complex (Dan *et al.* 2002). A similar negative effect is also produced by phosphorylation of tuberin at residue S1798 by p90 ribosomal S6 kinase 1 (RSK1) (Roux *et al.* 2004). RSK1 is activated in the Raf/MAPK pathway. The phosphorylation of tuberin at residue S1210 by p38 MAPK-activated protein kinase 2 (MK2) (Li *et al.* 2003b) promotes binding of tuberin with 14-3-3 proteins, which may sequester tuberin from its physiological substrates (Astrinidis and Henske 2005). extracellular signal-regulated kinase 2 (ERK2) inactivates tuberin by phosphorylation at residue S664 (Ma *et al.* 2005) that disrupts the hamartin/tuberin complex. These four kinases cause inactivating phosphorylation of tuberin and positively regulate the mTOR signalling pathway, thus allowing protein translation and cell proliferation in response to growth factors. In contrast, under energy deprivation, tuberin undergoes activating phosphorylation at T1227 and S1345 by AMP-dependant protein kinase (AMPK) leading to enhanced inhibition of S6 ribosomal protein (Inoki

et al 2003b). Another positive effect on tuberin is triggered in response to hypoxia; the TSC complex is required for mTOR inhibition during hypoxic conditions. Disruption of the complex through loss of TSC1 or TSC2 blocks the effects of hypoxia on mTOR and results in abnormal accumulation of hypoxia-inducible factor (HIF) (Brugarolas *et al.* 2004). Additional tuberin phosphorylation sites at S1395/1397 and S1775 have been identified (Nellist *et al.* 2005a) but the kinase(s) are as yet unknown.

1.2.9.3 Interaction of the TSC proteins

The similarities in phenotypes produced by mutations in *TSC1* or *TSC2* suggest shared functions. However, there is no homology between the primary amino acid sequence of tuberin and hamartin, suggesting that they do not belong to the same family of proteins. An alternative explanation is that tuberin and hamartin work together in the same biological pathway (Au *et al.* 2004). Direct interaction between tuberin and hamartin was demonstrated by van Slegtenhorst *et al.* (1998) using the yeast two-hybrid system and is further supported by co-immunoprecipitation experiments (Plank *et al.* 1998, van Slegtenhorst *et al.* 1998, Nellist *et al.* 1999, Hodges et al. 2001). Gel filtration studies indicate that tuberin (200kDa) and hamartin (130kDa) are found in a TSC complex of approximately 450kDa, though the other components of this complex, if any, are yet to be defined (Nellist *et al.*1999). It has been proposed that tuberin acts as a chaperone in the TSC complex, preventing hamartin from self-aggregation (Nellist *et al.*1999). Thus, the stability of tuberin and hamartin appear to be interdependent (Benvenuto *et al.* 2000).

Immunohistochemical studies have demonstrated absent or diminished amounts of both proteins in TSC-related tumour cells (Mizuguchi *et al.* 2000). Furthermore, patient-derived TSC2 mutations that disrupt the association of tuberin with hamartin have decreased GAP activity, indicating that the interaction with hamartin is important for tuberin's function as a GAP (Nellist *et al.* 2005b). In addition, it has been shown that TSC1-TSC2 interaction is regulated by tuberin phosphorylation, and defective phosphorylation of tuberin is associated with loss of tumour suppressor activity (Aicher *et al.* 2001). Taken together, these data explain why complete deficiency of either protein has the same biochemical consequence, and produces a similar disease phenotype.

1.2.9.4 The mTOR signalling network

The *Tor* genes were originally identified in yeast as the targets of the immunosuppressant drug rapamycin (Heitman *et al.* 1991). TOR is a member of the phosphoinositide kinases-related kinase (PIKK) family and is structurally and functionally conserved between yeast and mammals (mTOR) (Inoki *et al.* 2005). TOR has been shown to have a central role in controlling cell growth, proliferation and metabolism by regulating translation, transcription, mRNA turnover, protein stability, actin cytoskeletal organisation and autophagy (Inoki *et al.* 2005). mTOR functions in two separate pathways in two distinct protein complexes (Fig. 1.7). mTOR complex 1 (mTORC1) consists of mTOR, raptor and gephyrin and is inhibited by the action of rapamycin. mTOR complex 2 (mTORC2) requires binding of rictor, and gephyrin and is rapamycin insensitive (Jozwiak *et al.* 2005). mTORC2

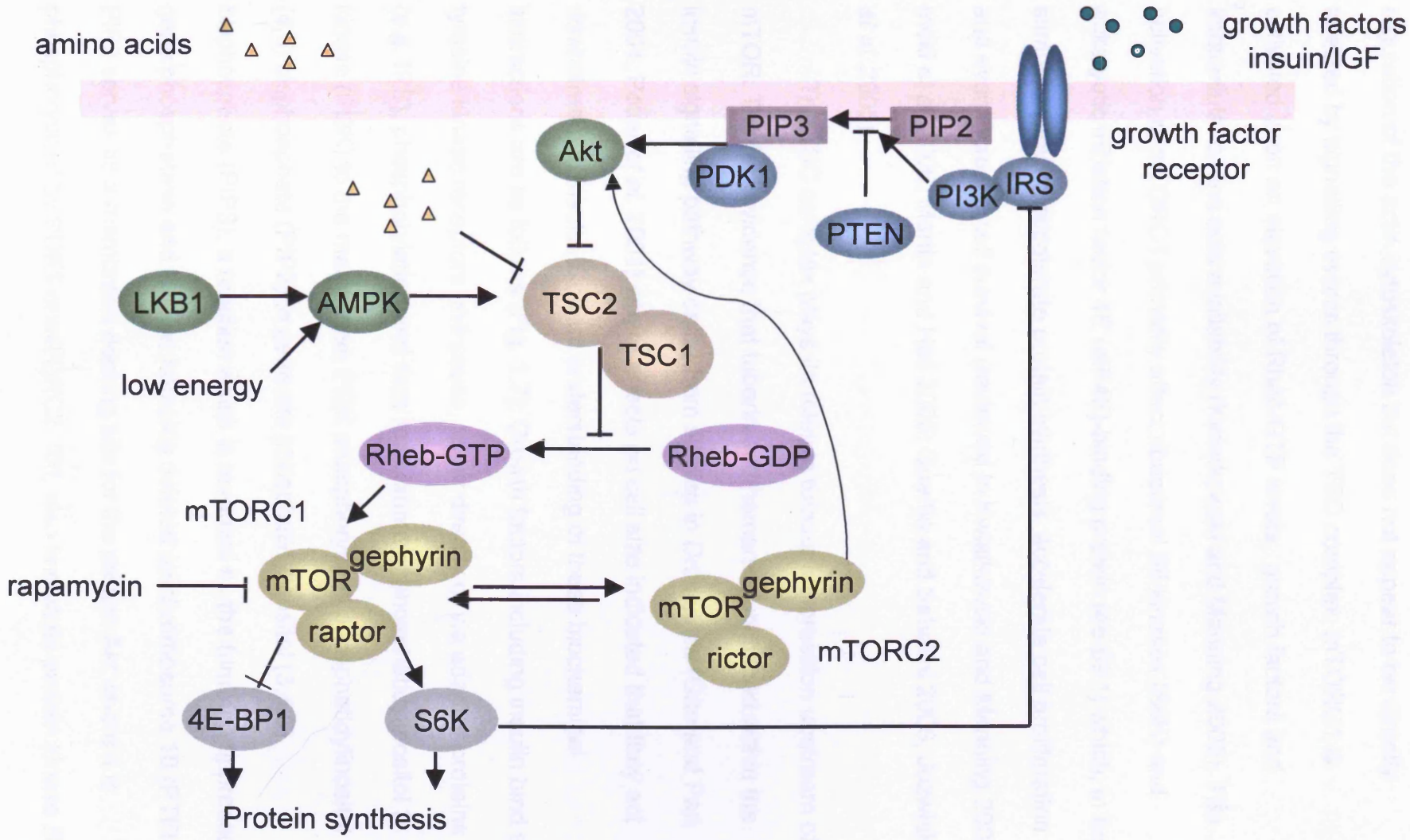

Figure 1.7: The mTOR signalling network. The mTOR pathway integrates the three inputs of nutrients (amino acids), growth factors (insulin) and cellular energy status to control cell growth (adapted from Martin and Hall 2005). See text for explanation of abbreviations.

phosphorylates Akt at serine 473 (Sarbassov *et al.* 2005) and has a role in regulation of the actin cytoskeleton but does not appear to be directly affected by signalling events through the TSC complex. mTORC1 is activated upon an elevation of Rheb-GTP levels, growth factors and intracellular amino acid availability (Kwiatkowski and Manning 2005). The activation of mTORC1 primarily affect ribosomal S6 kinases (S6K) and eukaryotic initiation factor 4E (eIF4E)-binding protein (4e-BP1) which, in turn, stimulate growth, accelerate protein synthesis, accelerate cell proliferation and even increase cell survival (reviewed in Kwiatkowski and Manning 2005, Inoki *et al.* 2005, Martin and Hall 2005, Guertin and Sabatini 2005, Jozwiak *et al.* 2005).

The TSC complex plays its roles in tumour suppression upstream of mTOR. The first evidence that tuberin and hamartin functioned within the insulin signalling pathway came from studies in *Drosophila* (Gao and Pan 2001, Potter *et al.* 2001) where effects on cell size indicated that they act downstream of insulin. Current understanding of these biochemical interactions are as follows (Fig. 1.7): Growth factors including insulin bind to tyrosine kinase receptors and cause, either directly or via adapter proteins (e.g. IRS), phosphorylation and thus recruitment of phosphatidylinositol 3-kinase (PI3K) to the membrane. PI3K phosphorylates phosphatidylinositol (4,5) bisphosphate (PIP2) to generate phosphatidylinositol (3,4,5) bisphosphate (PIP3), a reaction which is reversed by the tumour suppressor gene phosphatase and tension homolog deleted on chromosome 10 (PTEN). PIP3 serves as a membrane docking site for the protein Akt where it is phosphorylated by PDK1 or mTORC2. Akt, also known as protein kinase B

(PKB), is one of the most frequently activated protein kinases in human cancer. Akt hyperactivation is associated with resistance to apoptosis, increased cell growth, cell proliferation and cellular energy metabolism. Akt phosphorylates several proteins including Forkhead family (FOXO) isoforms, BCL-2 family member BAD, Glycogen synthase 3-kinase (GSK3) as well as tuberin. Tuberin is a key within the pathway responding to phosphorylation from ERK1/2, RSK1 and AMPK as well as Akt. The TSC1/2 complex acts as a GAP for Rheb-GTP enhancing conversion to Rheb-GDP. When the TSC tumour suppressor complex is phosphorylated and inhibited by Akt, Rheb-GTP is able to accumulate. Rheb-GTP strongly enhances the kinase activity of mTOR and thus enhances protein translation and cell growth (reviewed in Kwiatkowski and Manning 2005, Inoki et al 2005, Martin and Hall 2005, Guertin and Sabatini 2005, Jozwiak *et al.* 2005). When no growth stimulus is present, Rheb-GDP is in abundance and consequently there is no mTOR activation. When growth stimuli are available or TSC1/2 are not functioning (biallelic inactivation) Rheb-GTP formation from its inactive substrate cannot be inhibited, thus leading to activation of mTOR.

1.2.9.5 The role of hamartin/tuberin in energy sensing

In addition to its control by nutrients and growth factors, the TSC complex is also targeted by the energy sensitive AMP-activated protein kinases (AMPK) (Fig. 1.7). AMPK is activated upon energy deprivation, and phosphorylation of tuberin enhances the stability of the TSC complex. Herein lies a link between two signalling pathways responsible for the formation of hamartomatous syndromes. Loss of both TSC1/2 or the serine/threonine

kinase LKB1 TSG responsible for Peutz-Jeghers syndrome (PJS) result in the formation of multiple benign hamartomas. Interestingly, the LKB1 tumour suppressor gene controls AMPK by direct phosphorylation upon ATP depletion, and loss of LKB1 results in down regulation of the TSC complex thus stimulating mTOR activity. These finding suggest that hamartomas develop as a consequence of constitutively high mTOR activity (reviewed in Martin and Hall 2005, Inoki *et al.* 2005, Kwiatkowski and Manning 2005, Hardie 2005).

1.2.9.6 mTOR associated hamartoma syndromes

In addition to TSC and PJS, other hamartoma syndromes have also been linked to the mTOR pathway (Fig. 1.8). These include Cowden's disease, Bannayan-Riley-Ruvalcaba syndrone (BRRS), Lhermitte-Duclos disease and Proteus syndrome that are grouped together as PTEN hamartoma syndromes (PTHs). All are caused by germline mutations in *PTEN* (Inoki *et al.* 2005). PTEN lies upstream of Akt. It reduces intracellular levels of PI3K lipid products thereby inhibiting Akt activation. Thus, in cells lacking PTEN, Akt is constitutively active, and there is a corresponding increase in TSC2 phosphorylation and mTOR signalling (Manning *et al.* 2005). In addition to these syndromes with a well established molecular link to dysregulation of mTOR, further neoplastic syndromes are associated with dysregulation of mTOR related pathways. Neurofibromatosis type 1 (NF1) is caused by a mutation in the NF1 gene that is a GTPase-activating protein that can activate PI3K (Inoki *et al.* 2005). Some cases of juvenile polyposis (JP) are caused by mutations in mothers against DPP homolog 4 (*SMAD4*)

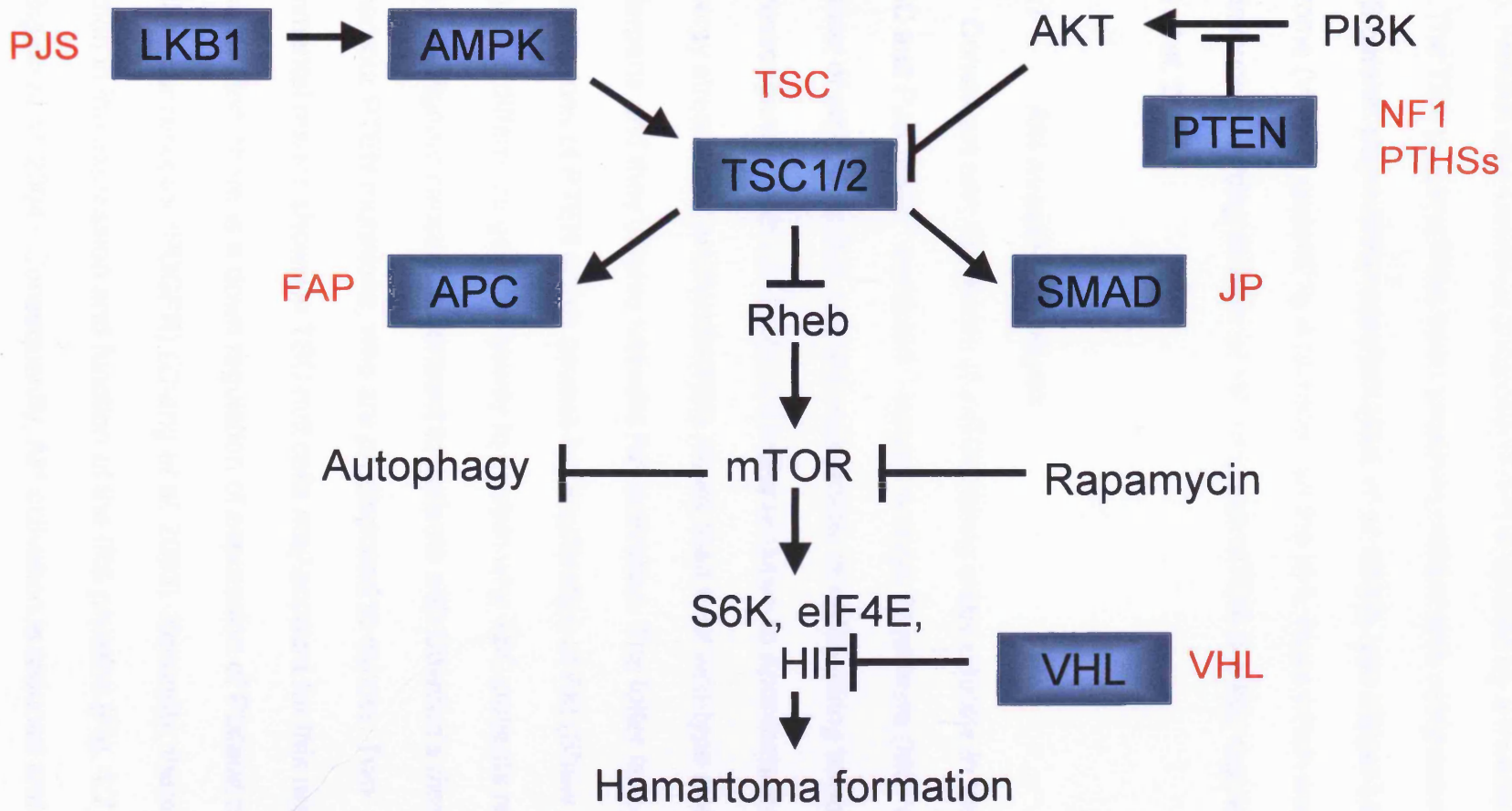

Figure 1. 8: The molecular link between several inherited hamartoma syndromes (adapted from Inoki *et al.* 2005). Dysregulation of the mTOR pathway has been implicated in PTEN hamartoma syndromes (PTHs), Neurofibromatosis type 1 (NF1), Juvenile polyposis (JP), von Hippel-Lindau syndrome (VHL) and TSC1/TSC2 have been linked to Familial adenomatous polyposis (FAP), Peutz-Jeghers syndrome (PJS)

which interacts with mothers against DPP homolog 3 (*SMAD3*) which in turn has been shown to interact with Akt and *TSC2* (Birchenall-Roberts *et al.* 2004). Familial adenomatous polyposis (FAP) is caused by a mutation in *APC*. The TSC proteins have been shown to interact with components of the APC/β-catenin degradation complex (Mak *et al.* 2003). von Hippel-Lindau syndrome (VHL) is caused by a mutation an the VHL locus which encodes a protein involved in degradation of HIF of which mTOR is a key regulator (Inoki *et al.* 2005).

1.2.9.7 Akt negative feedback

Consistent with the theory of mTOR being a key effector in the biology of TSC and PJS, *Tsc2*$^{-/-}$ and *Lkb1*$^{-/-}$ mouse embryo fibroblasts (MEFs) share a number of properties that are uncharacteristic of cells lacking tumour suppressor genes. Both cell types are hypersensitive to apoptosis induced by energy stress, they proliferate more slowly than their wild-type derived counterparts and they display reduced Akt activation. The latter is in stark contrast to loss of PTEN which causes hyperactivation of Akt (Shaw *et al.* 2004). This difference goes someway to explain why TSC patients rarely develop malignant cancers in contrast to patients with Cowden's disease, that harbour PTEN mutations, who are predisposed to cancer. Two experimental results shown in TSC null cells may account for this negative feedback. First, there is a down regulation of expression of Platelet derived growth factor receptor (PDGFR) (Zhang *et al.* 2003). Secondly, there is a reduction in the expression and function of the IRS proteins (Fig. 1.7) (Harrington *et al.* 2004). Consequently, Akt activation is reduced and its

multiple targets that promote cell growth and survival do not become active. This model is supported by recent observations in *Tsc2*$^{+/-}$*Pten*$^{+/-}$ mice. In *Tsc2*$^{+/-}$ mice, TSC related lesions are slow growing with no Akt activation but, in *Tsc2*$^{+/-}$ *Pten*$^{+/-}$ mice, lesions are more severe and display Akt activation (Manning *et al.* 2005, Ma *et al.* 2005).

1.2.10 Treatments

Since mTOR is directly activated upon loss of *TSC1* or *TSC2*, rapamycin, the mTOR inhibitor, has been identified as a potential therapeutic agent for TSC. Rapamycin (or Sirolimus, Wyeth, Madison, NJ) is a peptide that was isolated in 1975 from the bacteria strain *Streptomyces hygroscopicus* found in a soil sample from Easter Island (Sehgal *et al.* 1975). It is an antibiotic, which demonstrates anti-fungal, anti-inflammatory, anti-tumour and immunosuppressive properties. Rapamycin is used as an immunosuppressant during renal transplant. It possesses high specificity against mTOR through binding with the receptor protein FKBP12. Treatment of *TSC1* or *TSC2* null cells with rapamycin results in apoptosis and decreased proliferation. Furthermore, rapamycin induced a reduction of tumour size in both the Eker rat and *Tsc2*$^{+/-}$ mice (Kenderson *et al.* 2005, Lee *et al.* 2005). However, small precursor lesions were unresponsive to rapamycin treatment suggesting mTOR activation may be critical to tumour progression but that it is not necessary for tumour initiation (Kenerson *et al.* 2005). Clinical trials of rapamycin are ongoing but results so far look encouraging with regression of astrocytomas (Franz *et al.* 2006) and renal AMLs (Julian Sampson, unpublished data). The identification of the Akt

feedback loop (Manning 2004) has led to concerns about rapamycin treatment. Rapamycin treatment restores insulin signalling towards Akt, and may increase the risk of malignant tumours in patients with TSC by reactivating Akt and is plethora of downstream biochemical signalling pathways.

Both *Tsc1*$^{+/-}$ and *Tsc2*$^{+/-}$ mice develop liver hemangiomas consisting of proliferating smooth muscle cells, endothelial cells and vascular channels similar to LAM and renal AMLs. They occur at a higher frequency in female mice as compared to males (Onda *et al.* 1999, Kwiatkowski *et al.* 2002), suggesting that oestrogen may contribute to their development. El-Hashemite at al. (2005) treated *Tsc1*$^{+/-}$ mice with both oestrogen and tamoxifen. Tamoxifen is an anti-oestrogen drug that was developed over 30 years ago and is used widely to treat breast cancer. Oestrogen treatment increased the severity and frequency of live hemangiomas. In contrast, tamoxifen reduced symptoms, thus, suggesting a benefit in the treatment of renal AMLs and LAM.

1.2.11 TSC models

The ability to create specific gene modifications to produce animal models of inherited disease has allowed for *in vivo* analysis of gene function and greater understanding of pathogenic mechanisms of human disease. Interestingly, the first genetic model for TSC dates to the era before molecular biology. First described in 1954 by Reidar Eker, the Eker rat strain contains a germline inactivation of one allele of TSC2. Following the identification of the *TSC1* and *TSC2* genes, murine and *Drosophila* models

were quickly established. Extensive homology searches have failed to identify TSC1 and TSC2 homologs in *Caenorhabditis elegans* or *Saccharomyces Cerevisiae*, however, *Schizosaccharomyces pombe* does contains these homologs.

1.2.11.1 *Schizosaccharomyces pombe*

Comparison of human and *Drosophila TSC1* and *TSC2* genes with the fission yeast genome lead to the identification of fission yeast homologs of the genes that encode Tsc1 and Tsc2 proteins with calculated molecular weights of 103kD and 156kD, respectively (Matsumoto *et al.* 2002). The GAP related domain of tuberin is particularly well conserved with 39% identity. The fission yeast TSC1 and TSC2 physically interact with each other and hence appear to be similar to their mammalian counterparts in structure but also in biochemical properties. However, introduced TSC1 does not rescue yeast lacking Tsc1, indicating the functions have diverged significantly (Matsumoto *et al.* 2002). Disruption of either *Tsc1* or *Tsc2* in *S. pombe* results in amino acid uptake defects and partial sterility (Matsumoto *et al.* 2002, van Slegtenhorst *et al.* 2004).

1.2.11.2 *Drosophila*

In 1999, Ito and Rubin identified the *Drosophila* homologs of TSC1 (dTsc1) and TSC2 (dTsc2 or *gigas*). Loss of dTsc2 was reported to result in dramatic increase in cell size and cells appeared to repeat S phase without entering M phase (Ito and Rubin 1999). dTsc1 mutants were shown to have a similar increased cell-size phenotype (Goa and Pan 2001, Potter *et al.*

2001, Tapon *et al.* 2001) Over expression experiments indicate that the dTsc1 protein binds to the dTsc2 protein *in vitro* (Potter *et al.* 2001) in a similar way to their mammalian counterparts. Genetic analysis identified the *Tsc* genes as novel negative regulators of insulin signalling, placing the dTsc1-dTsc2 complex genetically downstream of Akt but upstream of S6K (Goa and Pan 2001, Potter *et al.* 2001). The dTsc1-dTsc2 complex has been shown to physically associate with TOR, and negatively regulate TOR activity during the control of cell growth in *Drosophila* (Gao *et al.* 2002). More recently, several groups have identified the small GTPase Rheb in *Drosophila* (Saucedo *et al.* 2003, Stocker *et al.* 2003, Patel *et al.* 2003) and placed Rheb downstream of the Tsc complex, suggesting that Rheb is the target of the GAP activity of dTsc2 (Saucedo *et al.* 2003, Stocker *et al.* 2003).

1.2.11.3 Eker Rat

Hereditary cancer was first described in the rat by Eker and Mossige in 1954. The Eker rat model of hereditary RCC was the first example of a Mendelian dominantly-inherited predisposition to a specific cancer in an experimental animal (Eker and Mossige 1961, Hino *et al.* 2001). The Eker renal carcinoma locus was mapped to rat chromosome 10q12 by linkage analysis (Yeung *et al.* 1993, Hino et al 1993a). After the human TSC2 gene was identified by positional cloning, the Eker phenotype was shown to be tightly linked to its rat homologue (Hino *et al.* 1994). In addition, TSC2 expression was not seen in Eker rat RCCs compared to normal renal tissue that expressed TSC2 (Hino *et al.* 1994). Detailed analysis confirmed that the

Eker rat phenotype is caused by a mutation in *Tsc2* that results from the insertion of a 6.3kb intracisternal A particle (IPA) on one allele which produces aberrant RNA expression (Yeung *et al.* 1994, Kobayashi *et al.* 1995). No stable protein product has been demonstrated from the mutant allele, indicating that the Eker mutation is functionally null (Kobayashi *et al.* 1995).

Phenotypically homozygous mutants are embryonicly lethal at 13 days and appear to be two days behind in development with brains showing grossly abnormal development (Hino *et al.* 1993b). In heterozygotes, renal carcinomas develop mainly in the outer cortex from early phenotypically altered renal tubules that begin to appear at 2 months of age, and have ~100% penetrance by 1 year (Hino *et al.* 2003). Kidney lesions vary in morphology and include pure cysts, cysts with papillary projections and solid adenomas (Eker *et al.* 1981). Histological studies suggest that cystic adenomas arise from the distal nephron, principally the collecting duct, whereas the solid atypical tubules, hyperplasias, and adenomas arise from the proximal nephron, principally the proximal tubule (Wolf *et al.* 1995). A small minority of these tumours become malignant with nuclear atypica. They expand to include the entire kidney and metastasize to the lungs, pancreas and liver (Eker at al. 1981). Investigations of extra renal lesions reveal hemangiomas/ hemangiosarcomas of the spleen, leiomyomas/ leiomyosarcomas of the uterus (Everitt *et al.* 1992), pituitary adenomas (Kubo *et al.* 1995) and brain lesions such as subependymal hamartomas, subcortical hamartomas, cortical tubers and anaplastic gangliogliomas (Yeung *et al.* 1997, Mizuguchi *et al.* 2000).

1.2.11.4 Mouse models

Spontaneous mutations in rodent models like the Eker rat are relatively infrequent events and the occurrence of specific mutations of biomedical interest are extremely rare. However, mice are invaluable tools for studying disease due extensive chromosome homology between mouse and man (Yu and Bradley 2001), the availability of inbred strains and the ease of controlled breeding. Chromosomal deletions, duplications, inversions and translocations can be induced in mice by using radiation or chemical mutagens. However, the usefulness of the rearrangements is limited by the fact that they cannot be predetermined (Yu and Bradley 2001). Consequently, chromosomal engineering and embryonic stem (ES) cell technology has been used to produce specific murine models of disease. Typically, murine models are produced in 2 ways. First, DNA can be integrated in a random fashion by microinjection into the pronucleus of a fertilized ovum. Secondly, site specific gene targeting can be performed by introducing DNA into ES cells and selecting for cells in which the DNA has undergone homologous recombination.

1.2.11.4.1 Microinjection

The first report describing transgenic mice that developed from microinjected eggs was published in 1980 (Gordon *et al.* 1980). It quickly became apparent that the foreign genes could be expresseds, incorporated into the germline, and these expressions and integrations could be passed onto offspring causing a physiological effect (Palmiter and Brinster 1986).

Microinjection involves introducing genes in a random fashion into the germline by injection of purified, cloned DNA into the pronucleus of fertilised mouse eggs. The eggs are then transferred into the oviduct of pseudopregnant foster mothers for gestation. The DNA integrates randomly, and usually in multiple copies, causing a fraction of the mice born to be transgenic (Klysik 2002).

1.2.11.4.2 Embryonic stem cell technology and gene targeting

Embryonic stem cell technology was initiated at the beginning of the 1980s when ES cells were derived from the inner mass of the blastocyst (Evans and Kaufman 1981). ES cells allow site-specific genetic alterations to be efficiently transmitted into the germline, thus enabling manipulation of any locus within the mouse genome (Klysik 2002).

Production of transgenic mice by embryonic stem cell technology and gene targeting involves first targeting the ES cells at defined loci via homologous recombination. Alterations may be a single nucleotide change, gene knockouts or chromosomal rearrangements. The genetically modified cells are then injected into blastocysts (from mice with a different coat colour) and the modified blastocyst introduced into a pseudopregnant foster mother (Fig. 1.9). ES cells are pluripotent and have the ability to contribute to several tissues of the foetus, including the germ cells. The resultant chimeras with the most transgenic cells, predicted by coat colour, are likely to transmit the modified allele to some of the F1 progeny. A further intercross of F1s will produce F2 homozygous animals (Klysik 2002).

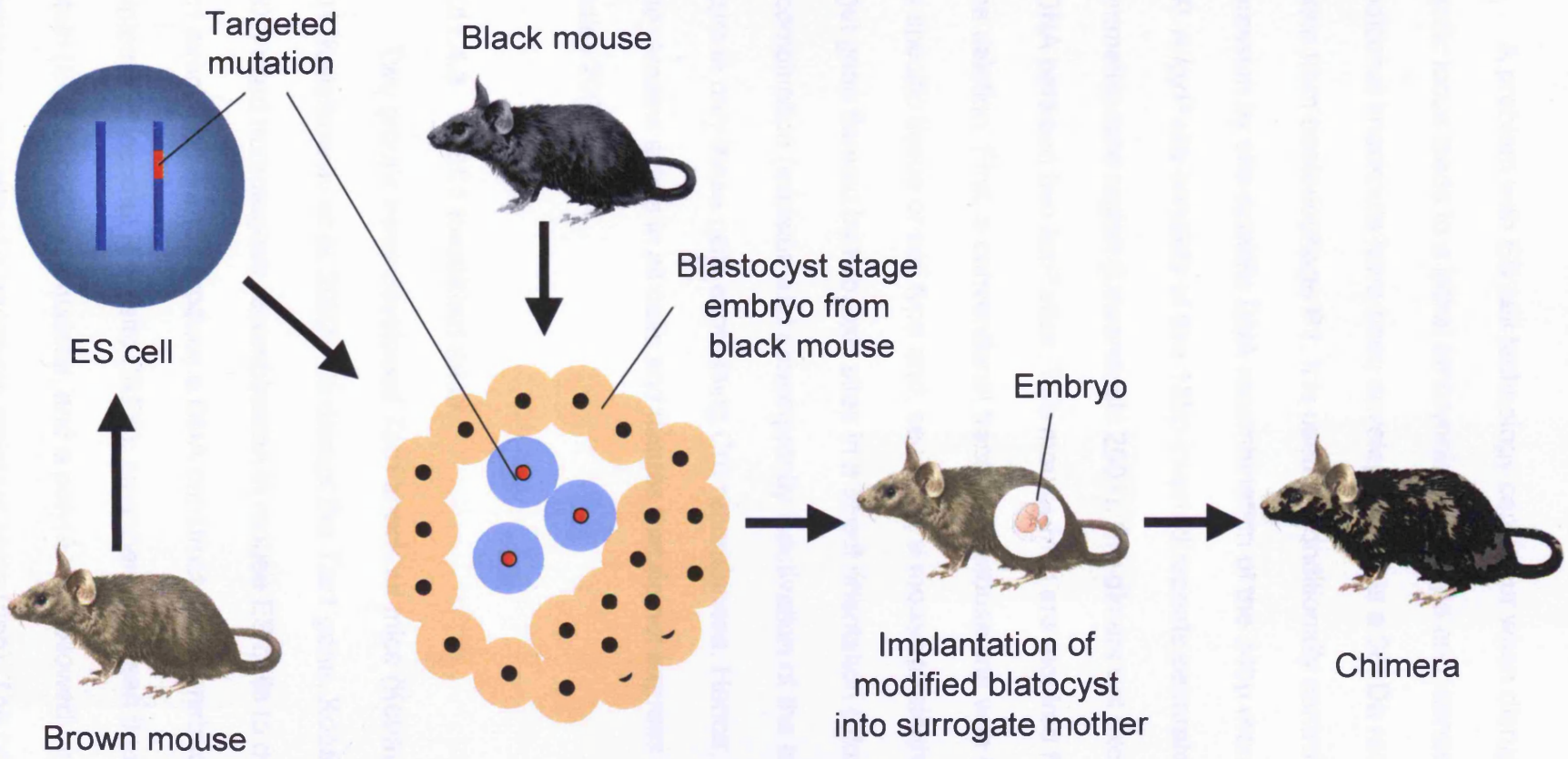

Figure 1.9: Generation of transgenic mice by embryonic stem cell technology and gene targeting. Targeted ES stem cells from a brown mouse are injected into a blastocyst from a black mouse and introduced into a pseudopregnant foster mother. The chimera that is produced will be partly transgenic (brown areas) and partly normal (black areas). Subsequent F1 and F2 generations will be heterozygous and homozygous mutants, respectively.

A problem with ES cell technology can occur when disruption of a specific locus leads to a lethal embryonic phenotype and, consequently, conditional knockouts have been developed. Cre is a 38kDa recombinase protein from bacteriophage P1. It is used to conditionally control gene expression by site-specific DNA recombination of the 34bp recognition site *loxP*. A *loxP* site consists of two 13bp-inverted repeats separated by an 8bp asymmetric core region (Lewandoski 2001). Cre dimers will excise the region of DNA between two *loxP* sites. Two mouse lines are required for conditional gene deletion. First, a conventional transgenic mouse line with Cre targeted to a specific tissue or cell type and, secondly, a mouse strain that has a target gene flanked by two loxP sites in a direct orientation ("floxed gene"). Recombination (excision and consequently inactivation of the target gene) occurs in only those cells expressing Cre recombinase. Hence, the target gene remains active in all cells and tissues that do not express Cre (Yu and Bradley 2001).

1.2.11.4.3 TSC1 knockout mice

Two groups have developed *Tsc1* knockout mice (Kobayashi *et al.* 2001, Kwiatkowski *et al.* 2002). To disrupt the *Tsc1* gene, Kobayashi *et al.* (2001) used homologous recombination in mouse ES cells to delete mouse *Tsc1* exons 6 to 8 and introduce a DNA construct. The construct contained an internal ribosomal entry site (IRES), an enhanced green fluorescent protein (EGFP) coding sequence, and a poly(A) tail followed by an expression cassette of a neomycin resistant gene (neo). The consequence of

this targeting event was predicted to cause splicing from exon 5 to exon 9 resulting in a frameshift (Kobayashi *et al.* 2001). Northern blot analysis of homozygous lethal (*Tsc1*$^{-/-}$) embryos revealed that the 8kb mRNA transcript of *Tsc1* had disappeared. Kwiatkowski *et al.* (2002) used a two-step process to disrupt the *Tsc1* allele. First, homologous recombination in mouse ES cells was used to insert a DNA fragment containing 2 *LoxP* sites that flanked exons 17 and 18. Next, Cre recombinase expression was employed to yield a *Tsc1* allele where exons 17 and 18 were deleted (Kwiatkowski *et al.* 2002). Deletion of exons 17 and 18 from *Tsc1* was predicted to result in premature termination of translation as the message goes out of the reading frame. Immunoblot analysis indicated that no hamartin was produced from the mutant allele (Kwiatkowski *et al.* 2002). Both *Tsc1* mouse models display a homozygous lethal embryonic phenotype between embryonic day E9.5 and E13.5 of gestation (Kobayashi *et al.* 2001, Kwiatkowski *et al.* 2002). Null embryos were smaller, approximately a day behind normal development, and some exhibited failed neural tube closure, abnormal morphology of myocardial cells, liver hypoplasia and poor development of other abdominal organs (Kobayashi *et al.* 2001, Kwiatkowski *et al.* 2002).

The phenotype of *Tsc1*$^{+/-}$ mice is similar to that of the Eker rat in that they develop macroscopically visible multiple bilateral renal cystadenomas by 15 to 18 months (Kwiatkowski *et al.* 2002). Microscopically, phenotypically altered tubules (cysts) were also seen at 9 to 12 months (Kobayashi *et al.* 2001). Histologically, the lesions varied from pure cysts, cysts with papillary projections and solid adenomas. There was no evidence of metastasis. Strain dependant differences were observed whereby BALB/c-129/Sv hybrid

mice had more cystadenomas than C57BL6-129/Sv hybrid or 129/Sv mice (Kwiatkowski *et al.* 2002). Molecular analysis of renal lesions demonstrated that 33% (2/6) of lesions showed LOH of the wild type *Tsc1* allele, suggesting that a second hit may be a critical event for the development of renal tumours in $Tsc1^{+/-}$ mice (Kobayashi *et al.* 2001). Extra-renal lesions included hepatic hemangiomas, tail or paw hemangiomas and leiomyoma or leiomyosarcomas in the uterus (Kobayashi *et al.* 2001, Kwiatkowski *et al.* 2002). Hepatic hemangiomas caused early mortality and consisted of aberrant vascular channels of highly variable size that often had cuboidal-columnar endothelial cells and proliferation of smooth muscle cells. The lesions were more frequent, of larger size, and caused death more commonly in females as compared to male $Tsc1^{+/-}$ mice (Kwiatkowski *et al.* 2002).

1.2.11.4.4 TSC2 knockout mice

Two groups have developed *Tsc2* knockout mice (Kobayashi *et al.* 1999, Onda *et al.* 1999). To disrupt the *Tsc2* gene, Kobayashi *et al.* (1999) used homologous recombination to insert a targeting vector containing a LacZ reporter gene and a neomycin selection marker. This caused a deletion of codon 74 in exon 2 through to codon 164 in exon 5. Inactivation of the *Tsc2* gene was confirmed by a lack of signal to an anti-tuberin antibody in Western blot analysis (Kobayashi *et al.* 1999). Onda *et al.* (1999) used a similar approach to disrupt the *Tsc2* gene. The targeting vector contained a neomycin selection marker that disrupted exon 2 of the *Tsc2* gene. Inactivation of the *Tsc2* gene was confirmed by lack of expression of tuberin

by immunoblot analysis (Onda *et al.* 1999). Both *Tsc2* mouse models exhibited a lethal embryonic phenotype. Most *Tsc2*$^{-/-}$ embryos died at E10.5 and none were seen past E12.5 (Kobayashi *et al.* 1999, Onda *et al.* 1999). Lethality was thus seen at a similar stage to *Tsc1*$^{-/-}$ embryos and they displayed a similar phenotype. However, survival of *Tsc1*$^{-/-}$ embryos was significantly improved over that of *Tsc2* null embryos as *Tsc1*$^{-/-}$ embryos are viable up to E13.5 (Onda *et al.* 1999).

Tsc2$^{+/-}$ mice develop multiple bilateral renal cystadenomas by 6 months of age, with complete penetrance by 15 months of age. Renal lesions display a similar histology to that of *Tsc1*$^{+/-}$ mice. Rarely, lesions progressed to RCC and metastasis to the lung was observed in one mouse (Kobayashi *et al.* 1999, Onda *et al.* 1999). Molecular analysis of renal lesions demonstrated that 24% (9/37) of lesions showed LOH of the wild type *Tsc2* allele (Onda *et al.* 1999). In addition to renal lesions, *Tsc2*$^{+/-}$ mice displayed liver hemangiomas, angiosarcomas on extremities, and alveolar adenomas (Kobayashi *et al.* 1999, Onda *et al.* 1999).

1.2.11.4.5 Cre-*LoxP* mouse models of TSC

In an attempt to model TSC associated central nervous system abnormalities in mice, Uhlmann *et al.* (2002) have produced astrocyte-specific *Tsc1* conditional knockout mice using the Cre-*Lox*P system. Mice with two copies of the conditional *Tsc1* allele (*Tsc1*$^{c/c}$) were generated by insertion of *LoxP* sites flanking exons 17 and 18 (Kwiatkowski *et al.* 2002). These were crossed with transgenic mice that express nuclear targeted Cre recombinase under the control of the human glial fibrillary acidic protein

(GFAP) promotor. The *Tsc1*$^{c/c}$GFAP-Cre conditional knockout mutants demonstrate increased astrocyte proliferation, abnormal neuronal organisation, seizures by two months of age and death by four months (Uhlmann *et al.* 2002). A second conditional knockout has been produced where the *Cre* recombinase allele was expressed in ventricular myocytes (Meikle *et al.* 2005). *Tsc1*$^{c/c}$ mice with LoxP sites flanking exons 17 and 18 (Kwiatkowski *et al.* 2002) were crossed with mice having a modified myosin light chain 2*v* allele expressing *Cre* recombinase (MLC2*vcre*KI). The *Tsc1*$^{c/c}$ MLC2*vcre*KI mice developed dilated cardiomyopathy with scattered foci of enlarged ventricular myocytes containing excess glycogen. Mice survived only 8 months.

1.3 Aims

The aims of the project were:

- To develop and characterise a Tsc1 deficient mouse model to help determine the mechanisms by which hamartin deficiency leads to TSC-associated disease.
- To attempt induction of tumourigenesis with increased somatic deletions in *Tsc1*$^{+/-}$ mice by crossing onto a Bloom's-deficient background (*Blm*).
- Investigate the potential role of *Tsc1* haploinsufficiency in Tsc-associated renal tumourigenesis by molecular and immunohistochemical examination of cysts, cystadenomas and renal cell carcinomas from *Tsc1*$^{+/-}$ and *Tsc1*$^{+/-}$ *Blm*$^{-/-}$ mice.

Chapter 2: Materials and Methods

2.1 Suppliers

Names and locations of all suppliers whose products were used in this study are listed below:

Abcam Ltd (Cambridgeshire, UK)

ABGene (Surrey, UK)

GE Healthcare (Buckinghamshire, UK)

Applied Biosystems (Cheshire, UK)

Bethesda Research Laboratories (Frederick, MD, USA)

Bibby Sterling (Staffordshire, UK)

Bioquote (Yorkshire, UK)

Bio Rad Laboratories Ltd (Hertfordshire, UK)

Cell Signalling Technologies (Danvers, MA, USA)

Corning Inc. (Surrey, UK)

DAKO (Cambridgeshire, UK)

Eurogentec (Hampshire, UK)

Fisher Scientific (Leicestershire, UK)

Flowgen (Leicestershire, UK)

Genetic Research Instrumentation (GRI) (Essex, UK)

Genta Medical (West Yorkshire, UK)

Invitrogen Life Technologies (Strathclyde, UK)

Invivogen (Toulouse, France)

Millipore (Hertfordshire, UK)

Motic (Suffolk, UK)

MWG-Biotech (Buckinghamshire, UK)

New England Biolabs (Hertfordshire, UK)

Nikon (Surrey, UK)

Olympus (London, UK)

PALM (Bernried, Germany)

QBiogene (Cambridgeshire, UK)

Qiagen (West Sussex, UK)

Raymond A Lamb Ltd (East Sussex, UK)

Roche Biochemicals (East Sussex, UK)

Santa Cruz Biotechnologies (Santa Cruz, CA, USA)

Sigma-Aldrich (Dorset, UK)

Starlabs (Buckinghamshire, UK)

Thermo Electron Corporation (Middlesex, UK)

Upstate cell signalling solutions (Buckinghamshire, UK)

Vector Laboratories (Peterborough, UK)

VWR International Ltd (Dorset, UK)

Carl Zeiss Limited (Hertfordshire, UK)

2.2 Materials

2.2.1 Chemicals

Chemicals of analytical grade were supplied by Sigma-Aldrich or Fisher Scientific unless otherwise stated.

2.2.2 Histology

Microtome blades, processing cassettes, paraffin wax and cork disks were purchased from Raymond A Lamb Ltd. Slides, cover slips, dibutyl phthalate and xylene (DPX) mountant, xylene, formaldehyde, optimum cutting temperature (OCT) embedding compound, haematoxylin and eosin (H&E), toluidine blue, hydrogen peroxide and isopentane were purchased from VWR International. Poly-L-lysine and mineral oil were obtained from Sigma-Aldrich. LacZ Reporter Assay Kit was purchased from Invivogen. PEN (polyethylene napthalate) membrane slides were purchased from PALM. Industrial methylated spirits (IMS) was purchased from Genta medical, and ethanol from VWR International.

2.2.3 Nucleic acid extraction and purification

QIAamp DNA mini kits, QIAamp DNA micro kits and proteinase K were supplied by Qiagen. Aquaphenol was purchased from QBiogene, chloroform from Sigma-Aldrich, and isopropanol from VWR international.

2.2.4 Oligonucleotides

Oligonucleotides were purchased from either MWG or Eurogentec and diluted to 100pM in sterile water for stock solutions.

2.2.5 PCR

AmpliTaq Gold DNA polymerase and GeneAmp PCR buffers were purchased from Applied Biosystems. Deoxynucleotidetriphosphates (dNTPs) were from GE Healthcare.

2.2.6 PCR purification

Exonuclease I was purchased from New England Biolabs and shrimp alkaline phosphatase was from GE Healthcare

2.2.7 Electrophoresis

Multipurpose agarose was obtained from Roche, Nusieve agarose from Flowgen and acrylamide/bisacrylamide from Bio-Rad. 1kb DNA ladder and See Blue Plus2 Pre-stained protein ladder were supplied by Invitrogen.

2.2.8 Southern blotting

MegaPrime DNA labelling system was purchased from GE Healthcare. Zetaprobe GT membrane was purchased from BioRad.

2.2.9 Sequencing and fluorescent product sizing

Big Dye Terminator Cycle Sequencing kit version 3.1, POP6 polymer, HiDi formamide and Genescan 500-Rox size standard were purchased from Applied Biosystems. Montage SEQ_{96} sequencing reaction clean-up kits were purchased from Millipore.

2.2.10 Restriction enzymes

Restriction enzymes with appropriate buffer were supplied by New England Biolabs.

2.2.11 Radioisotopes and autoradiographic film

[α-^{32}P]dCTP and Kodak BioMax MR film was supplied by GE Healthcare.

2.2.12 Antibodies

Anti-murine Gelsolin was a kind gift from Prof. D. Kwiatkowski (Boston, MA). Cell Signalling Technologies supplied the anti-phospho-S6 ribosomal protein (Ser240/244), anti-mTOR and anti-phospho-mTOR (Ser 2448) antibodies. For Western blotting, donkey anti-rabbit-HRP secondary antibody was supplied by GE Healthcare. Anti-β actin loading control antibody was purchased from Abcam Ltd.

2.2.13 Immunohistochemistry

The rabbit VECTASTAIN ELITE ABC horseradish peroxidase kit and 3,3'-diaminobenzidine (DAB) peroxidase substrate kit were supplied by Vector Laboratories. Bovine albumin fraction V was purchased from VWR international. Cytomation wax pens were supplied by DAKO.

2.2.14 Protein analysis

RIPA lysis buffer was purchased from Santa Cruz Biotechnologies. Acrylamide gel cassette moulds (1.0mm) were purchased from Invitrogen. BioRad supplied 40% acrylamide/bisacrylamide 29:1 mixture. Immobilon-P transfer membrane was supplied by Millipore. Visualizer EC Western blot detection kits were purchased from Upstate cell signalling solutions. Ponceau S stain was purchased from VWR international. Bradford assay reagents were bought from Bio-Rad.

2.3 Equipment

2.3.1 Plastics

Sterile tips for Gilson pipettes were purchased from Starlabs. Bioquote supplied 0.6ml, 1.5ml and 2.0ml plastic eppendorf tubes. ThermoLife Sciences supplied thermo fast 96 well PCR plates. ABGene provided 0.2ml thermo strip tubes, adhesive PCR film and thermo fast 96 well detection plates. Sterile universal tubes were purchased from Bibby Sterling. Corning Costar Inc. supplied 5ml, 10ml and 25ml strippettes.

2.3.2 Histology

Fixed tissue was processed using a Thermo Shandon Citadel 2000 wax processor and embedded using a Thermo Shandon Histocentre 2. Paraffin sections were cut on a Thermo Shandon Finesse microtome and stained with H&E on a GLX Thermo Shandon automatic ministain. Frozen sections were cut on a Bright cryostat. Tissues were viewed using an Olympus BX51 BF light microscope or a Motic B3 professional series light microscope.

2.3.3 Laser microdissection

Laser capture microdissection was carried out using the PALM Microlaser system and visualised using the PALM Robo software.

2.3.4 Immunohistochemistry

Raymond A Lamb Ltd provided plastic slide racks and Coplin jars.

2.3.5 Protein analysis

Protein extraction was performed on the fast prep system from Thermo Savant. DNA and protein quantification was carried out using the GeneQuant Pro spectrophotometer from GE Healthcare.

2.3.6 Determining the level of radioactivity

The radioactivity levels of Southern blotting probe were determined on the Bioscan QC-2000.

2.3.7 Thermocycling

Thermocycling of single tubes was carried out in a DNA thermal cycler 480 from Applied Biosystems. Thermocycling of 96-well plates and strip tubes was carried out in a PTC-225 Peltier thermal cycler from GRI.

2.3.8 Electrophoresis

Agarose gel electrophoresis was carried out using Horizon 11.14 gel tanks from Invitrogen Life Technologies, a Model H4 large gel tank from Bethesda Research Laboratories or a 96-well gel apparatus from ABGene. Biorad supplied the power packs. Capillary gel electrophoresis of fluorescent sequencing or PCR products was performed on ABI 3100 or ABI 3730 Genetic analysers. Acrylamide gel electrophoresis and blotting was carried out using the XCell sure lock gel tank and blot module purchased from Invitrogen.

2.3.9 Photography

Macroscopic pictures were recorded using a Nikon Coolpix 4500. Agarose gels were photographed using a Gel Doc 2000 UV transilluminator from Bio Rad and printed using the Mitsubishi P91 video processor with high-density thermal paper. Micrographs were prepared using a Zeiss AxioVision/AxioCam digital camera system.

2.4 General solutions

Commonly used solutions included 1xTAE (0.4M Tris-acetate, 10mM EDTA, pH 8.0), 1xTE (10mM Tris HCL, 1mM EDTA, pH 8.0), 1xSSC (3M NaCl, 0.3M *tri*-NaCitrate) and 1xTBS (0.15 NaCl, 0.005M Tris).

2.5 Methods

2.5.1 Animal husbandry

All procedures with animals were carried out in accordance with Home Office guidelines. Mice were housed in filter top cages and received filtered food and water. Cages were kept at an ambient temperature of 22°C and maintained on a 12 hour light :12 hour dark cycle (7:30 hours to 19:30 hours). Mice were tagged using microchips and tail tips were cut from mice for genotyping using a local anaesthetic. Mice were killed by cervical dislocation.

2.5.2 Necropsy analysis

Necropsy analysis included macroscopic examination of the brain, heart, lungs, kidneys, liver, spleen and uterus (in females) in all animals. Half

of each organ was fixed and processed into paraffin wax. The other half of the organ was snap frozen.

2.5.3 Histology

2.5.3.1 Tissue fixation and paraffin embedding

Fresh tissue was immersed into 10% formal saline and fixed overnight at 4°C. Fixed tissue was placed into the processor for a period of 1½ hours in each of the following solutions; formaldehyde, 70% IMS, 90% IMS, 96% IMS, 100% IMS x 3, chloroform x 3, paraffin wax and paraffin wax under vacuum. Tissues were embedded cut plane down and stored at room temperature. Paraffin sections were routinely sectioned at 4µm and floated onto poly-L-lysine treated glass slides. Sections were dried onto slides overnight at 45°C and stored at room temperature.

2.5.3.2 Freezing and sectioning tissue

Tissue was placed onto cork disks and covered with OCT embedding medium. Disks were dropped into liquid nitrogen-cooled isopentane until frozen, and stored in cryotubes at -70°C. Frozen sections were routinely sectioned at 10µm on a Bright cryostat and placed onto either PEN membrane covered or glass slides. Sections were air-dried at room temperature for 2 hours and stored at -20°C.

2.5.3.5 Haematoxylin and eosin staining

Paraffin sections were stained with H&E by immersion for a period of ~40 seconds in each of the following solutions; xylene x3, IMS x3, running

water, instant heamotoxlyin x7, running water x3, 1% acid alcohol, running water, Scotts tap water substitute, running water, 1% aqueous eosin (acified) x2, running water, IMS x3 and xylene x3. Sections were mounted with DPX.

2.5.4 Staining for β-galactosidase activity

Staining was carried out on frozen tissue sections. Slides were washed in water and sections were fixed for 10 minutes in 0.5% gluteraldehyde. Sections were stained overnight at 20°C using Xgal staining solution from the LacZ Reporter Assay Kit, washed in PBS/$MgCl_2$ solution, counterstained in eosin, dehydrated and mounted with DPX.

2.5.5 Laser capture microdissection

Laser micromanipulation offers microscopic high-resolution control of sample composition by selecting or rejecting tissue areas. For laser capture microdissection, frozen tissue was sectioned onto poly-L-lysine and UV treated (254nm) PEN membrane covered slides. Sections were washed in tap water and immersed in toluidine blue for 2 seconds. Following a further wash with water, sections were passed through 50%, 70% and 100% ethanol for 15 seconds and air dried overnight. A pulsed ultra-violet laser is interfaced into the microscope and focused through an objective. The laser cuts the tissue without the heating of adjacent material and results in a clear-cut gap between the desired sample area and the surrounding tissue. After microdissection, the isolated specimens are ejected out of the object plane and catapulted directly into the cap of a microfuge tube containing 1µl of

mineral oil positioned above the slide. DNA was extracted from there tissue samples using QIAamp DNA micro kits as described in section 2.5.12.4.

2.5.6 Immunohistochemistry

Paraffin sections were deparaffinised and rehydrated by passing through xylene x3, 100% ethanol x2, 70% ethanol, 50% ethanol and water. For antigen retrieval, sections were boiled in 10 mM citrate buffer (pH 6.0) for 10 minutes. Endogenous peroxidase activity was blocked with 0.3% hydrogen peroxide for 30 minutes followed by 2x TBS washes for 5 minutes. Immunostaining of paraffin sections was performed in a humidity chamber using the rabbit VECTASTAIN ELITE ABC horseradish peroxidase kit. Sections were encircled with a wax ring and blocked in goat normal serum for 20 minutes. Primary antibodies were applied and incubated for 30 minutes at room temperature or overnight at 4°C, followed by 2x 5 minute TBS washes. A Secondary antibody was applied and incubated for 30 minutes followed by 2x 5 minute TBS washes. Avidin-biotin complex (ABC complex) was incubated for 30 minutes followed by 2x 5 minute TBS washes. Sections were developed using DAB, counterstained in Gills haematoxylin for 30 seconds, and blued in tap water. Sections were dehydrated through graded ethanols, cleared in xylene, mounted with DPX and air dried.

2.5.7 Protein extraction

Protein extraction from snap frozen and fresh tissues was performed using 500µl RIPA lysis buffer and homogenised on the fast prep system for

30 seconds. The sample was left to settle on ice, spun at 13000 rpm for 1 minute, and the supernatant collected and stored at -20°C.

2.5.8 Protein quantification

Proteins were quantified using the Bradford assay on the GeneQuant spectrophotometer.

2.5.9 SDS-PAGE

SDS-PAGE gels were cast at 5%, 8% or 10% depending upon the size of protein to be resolved and topped with a 4% stacking gel. Fifty micrograms of protein samples were solubilised by heating in Laemmli buffer (1ml 0.5M Tris/HCl pH6.8, 0.8ml glycerol, 1.6ml 10% SDS, 0.4ml β-mercaptoethanol, 0.2ml 0.05% bromophenol blue, 4ml distilled H_2O) at 80°C for 15 minutes prior to loading on the gel. Electrophoresis was carried out in SDS-PAGE buffer (192mM glycine, 25mM Tris, 0.1% SDS) at 100V for approximately 2 hours.

2.5.10 Western blotting

Prior to transfer, the Immobilon-P (PVDF) membrane was wetted with methanol. The gel, Whatman paper and sponges were soaked in transfer buffer (192mM gycine, 25mM Tris, 20% methanol) for 15 minutes. The resolved proteins in the SDS-PAGE gel were blotted onto the membrane at 30V for 1 hour in transfer buffer. The membrane was blocked with 5% Marvel (dried milk powder)/TBS-T (TBS and 0.001% Tween 20) for 30 minutes. Antibodies were diluted in 5% Marvel/TBS-T. The membrane was incubated

with primary antibody for 1 hour, followed by 3 washes in TBS-T and a final TBS wash for 5 minutes each. The membrane was then incubated with secondary antibody and washed as described above. Protein bands were detected with chemiluminescence by incubating the membrane in the Visualizer EC reagents for 1 minute and exposing the film for various times to obtain the optimal image.

2.5.11 Protein loading controls

Equal loading of protein was confirmed by incubation of membranes with an anti-β actin antibody and Ponceau S staining.

2.5.12 Nucleic acid extraction

2.5.12.1 DNA extraction from tail tips

For the purpose of mouse genotyping, DNA was extracted from 3mm tail tips that had been immediately frozen after cutting. Tail tips were incubated overnight at 65°C with 500µl tail buffer (500mM Tris, 100mM EDTA, 100mM NaCl, 1% SDS, pH 8.0) and 20µl of proteinase K (20mg/ml). An extra 20µl of proteinase K was added and vortexed in the morning if the tail tip was not fully digested. Two hundred and fifty micro litres of 6M supersaturated NaCl was added to the lysate, the mixture vortexed, and centrifuged at 13000 rpm for 10 minutes. The supernatant was collected into a fresh eppendorf and 500µl of isopropanol added. The tube was manually inverted until a DNA precipitate could be seen. Eppendorfs were left overnight at -20°C to aid precipitation, when required. The DNA precipitate was then separated by centrifugation for 5 minutes at 13000 rpms. The

supernatant was removed and the DNA pellet washed in 150µl of 70% ethanol. The pellet was air-dryed for 15 minutes to remove any remaining ethanol and re-suspended in 30-50µl of DNAase-free water overnight at 35°C.

Samples were stored at -20°C.

2.5.12.2 DNA extraction from fresh and frozen tissue

DNA was extracted from fresh and frozen tissue using the QIAamp DNA mini kit according to the manufacturers instructions. Small pieces of up to 25mg of tissue were incubated overnight at 56°C with 180µl buffer ATL contents a trade secret (CTS) and 20µl of proteinase K. Two hundred micro litres of AL (CTS) was added to the lysate and incubated at 70°C for 10 minutes. Two hundred micro litres of 100% ethanol was added and the solution was applied to the QIAamp silica gel based spin column and centrifuged at 13000 rpm for 1 minute. The column was transferred to a clean collection tube and 500µl of AW1 (CTS) wash buffer was added. The column was re-centrifuged at 13000 rpm for 1 minute. The elutant was discarded before a second wash was carried out using 500µl of AW2 (CTS). The column was re-centrifuged at 13000 rpm for 3 minutes followed by an extra 1 minute spin in a clean collection tube to remove any residual ethanol that may inhibit any downstream reactions. DNA was eluted in 200µl of DNAase free water by incubating for 1 minute at 25°C and centrifuging at 13000 rpm for 1 minute. Samples were stored at -20°C.

2.5.12.3 DNA extraction from paraffin embedded tissue

DNA was extracted from paraffin embedded tissue using the QIAamp DNA mini kit. Two or 3 sections of 4µm tissue were placed into an eppendorf tube. Tissue was incubated overnight at 65°C with 180µl buffer ATL (CTS) and 20µl of proteinase K. Two hundred micro litres of AL (CTS) was added to the lysate and incubated at 70°C for 10 minutes. Two hundred micro litres of 100% ethanol were added and the solution was left at 25°C for at least 3 hours to allow the wax set on the top of the sample. The solution was obtained by pipetteing through the wax, added to a QIAamp spin column and centrifuged at 13000 rpm for 1 minute. The column was then transferred to a clean collection tube and 500µl of AW1 (CTS) wash buffer was added. The column was re-centrifuged at 13000 rpm for 1 minute. The elutant was discarded before a second wash was carried out using 500µl of AW2. The column was re-centrifuged at 13000 rpm for 3 minutes followed by an extra 1 minute spin in a clean collection tube to remove residual ethanol. DNA was eluted in ~100µl of DNAase free water by incubating for 1 minute at 25°C and centrifuging at 13000 rpm for 1 minute. Samples were stored at -20°C.

2.5.12.4 DNA extraction from laser microdissected tissue

DNA was extracted from laser captured tissue using the QIAamp DNA micro kit. Tissue was catapulted onto the lids of 0.6ml tubes. Forty micro litres of ATL (CTS) buffer and 10µl of proteinase K were carefully placed into the lid of the tube and the tubes were left inverted at room temperature for ~3 hours. After the tissue was digested, 50µl of AL (CTS) buffer was added to the lysate and incubated at 70°C for 10 minutes. Fifty micro litres of 100% ethanol was added and the solution was applied to the QIAamp micro silica

gel based spin column and centrifuged at 13000 rpm for 1 minute. The column was transferred to a clean collection tube and 500µl of AW1 (CTS) wash buffer was added. The column was re-centrifuged at 13000 rpm for 1 minute. The elute was discarded before a second wash was carried out using 500µl of AW2 (CTS). The column was re-centrifuged at 13000 rpm for 3 minutes followed by an extra 1 minute spin in a clean collection tube to remove residual ethanol. DNA was eluted in ~40µl of DNAase free water by incubating for 1 minute at room temperature and centrifuging at 13000 rpm for 1 minute. Samples were stored at -20°C.

2.5.13 Quantification of nucleic acid

The concentration of DNA in samples was determined by UV spectrophotometry at wavelengths of 260nm and 280nm. This allowed the amount of DNA to be quantified and the protein concentration to be established.

2.5.14 Restriction enzyme digestion

For DNA digestion, a total reaction volume of 40µl containing 4-5µg of DNA, an appropriate 10X reaction buffer, 1X BSA and 10U of restriction enzyme was used. The reaction was incubated at 37°C overnight. Digestion was assessed using agarose gel electrophoresis. An extra 20U of restriction enzyme was added and the sample re-incubated, if required.

2.5.15 DNA purification by Gene clean

To prepare probes for Southern blotting, plasmid DNA was digested with appropriate restriction enzyme, run on a low melting point agarose gel and visualised under UV light. The correct band was excised, weighed and placed in a sterile tube. A volume of NaI equal to three times the gel slice weight was added. The tube was incubated for 5 minutes at 55°C and 5µl of glassmilk (CTS) was added and vortexed. DNA was allowed to bind to the silica matrix in the glassmilk by incubating on ice for 5 minutes with repeated vortexing. The matrix was centrifuged, the supernatant removed and the pellet washed 3x in 500µl of NEW wash solution containing a high concentration of NaCl (CTS). DNA was eluted from the silica matrix by incubating the pellet in 20µl of TE for 3 minutes at 55°C followed by centrifugation for 30 seconds and collection of the supernantant.

2.5.16 Southern blotting

For Southern blotting, digested DNA was run on a 0.7% agarose gel at 40V for 22 hours. The gel was then subjected to depurination (0.25M HCl) for 10 minutes, denaturation (0.5M NaOH, 1M NaCl) for 30 minutes and neutralisation (0.5M Tris, 3M NaCl, pH 7.4) for 40 minutes. Blotting was carried out using a Whatman paper wick dipped into 10x SSC and DNA was blotted onto the ZetaProbe membrane at room temerature for 16 hours. After blotting, the membrane was washed in 2x SSC and dried at 65°C for 45 minutes. The probes were labelled using the MegaPrime DNA labelling system. Briefly, the probe and random primer oligomers were denatured at 95°C for 10 minutes. The labelling buffer containing dATP, dGTP and dTTP nucleotides, Klenow polymerase enzyme and [α-^{32}P] dCTP were added to

make a 25µl reaction volume, which was incubated at 37°C for 30 minutes. Unincorporated nucleotides were removed by ethanol precipitation followed by probe resuspension in 200µl of TE. The radioactivity of the probe was then determined. The radiolabelled probe was denatured at 100°C for 10 minutes and added to pre-warmed (65°C) membrane in modified Church and Gilbert hybridisation buffer (7% SDS, 0.5M PO_4 [pH 7.2]), 10mM EDTA). Hybridisation was carried out for at least 16 hours. After hybridisation, the membrane was washed in 5x SSC and 0.1% SDS at 65°C for 30 minutes. The stringency of the washes were gradually increased until non-specific hybridisations were at a minimised. The membrane was then mounted on a plastic sheet, covered with cling film and placed in a cassette with X-ray film. The film was exposed at -70°C for 1 to 14 days depending on the strength of the signal obtained.

2.5.17 Primer design

Oligonucleotides were designed using Primer 3 (Rozen and Skaletsky 2000). Where possible, the melting temperatures of the primer pairs were within 2°C of each other. Primers were between 18 and 23 nucleotides in length, lacked repetitive motifs and had little predicted dimerisation or secondary structure formation. Primers used in fluorescent analyses were modified by the addition of a 5' FAM fluorescent label.

2.5.18 Polymerase chain reaction (PCR)

Standard conditions for PCR included 25ng of template DNA, 0.25mM dNTPs, 12.5 pmoles of forward and reverse primers, 10x GeneAmp PCR

buffer (100mM TrisHCl, pH8.3, 500mM KCl, 15nM $MgCl_2$, 0.01% w/v gelatin) and 0.5Units of AmpliTaq Gold DNA polymerase in a total reaction volume of 20µl. Reactions in tubes were scaled up to a 50µl total volume and overlaid with mineral oil. Cycling conditions were 94°C for 12 minutes, followed by 35 cycles of 94°C for 1 minute, annealing temperature of 50°C to 60°C for 1 minute, and 72°C for 1 minute. There was a final elongation step of 72°C for 12 minutes.

2.5.19 Agarose gel electrophoresis

Agarose gels of 0.8 to 2.5% w/v concentration were prepared using 1x TAE buffer and 0.05µg/ml ethidium bromide. The higher the gel concentration, the smaller the pore sizes and that ensures, the better, the separation for small DNA fragments. NuSieve agarose was used at 3% w/v to separate very small (<200bp) DNA fragments. Two micro litres of loading dye (15% ficol, 10mM Tris pH 8, 1mM EDTA, 2% orange G) were added to each sample before loading and electrophoresis was performed in 1x TAE buffer at 100V. A 1kb DNA ladder was used to allow fragment sizing. DNA was visualised on a UV transluminator at a wavelength of 300nm and photographed using the Gel Doc 2000 system.

2.5.20 Capillary electrophoresis

One micro litre of fluorescenty-labelled PCR product was mixed with 9µl of highly deionised formamide containing 40pM ROX GS500 size standard. The reaction was run on the 3100 Genetic Analyser and products were visualised and quantified using GeneScan software.

2.5.21 PCR purification

Fifteen micro litres of PCR product was purified by the addition of 5U exonuclease I and 0.5U shrimp alkaline phosphatase. The sample was incubated at 37°C for 1 hour followed by denaturation at 80°C for 15 minutes.

2.5.22 Cycle sequencing

Sequencing reactions were performed using the BigDye Terminator Cycle Sequencing kit (Version 3.1). A total reaction volume of 10µl was used containing 0.8-3.0µl of DNA (~5ng), 0.25pmoles of primers, 0.75µl of Terminator ready reaction mix (labelled A, C, G and T dye terminators, dNTPs, AmpliTaq DNA polymerase FS, $MgCl_2$ and Tris-HCl buffer, pH 9.0) and 2µl BigDye terminator sequencing buffer. Cycle sequencing conditions were 96°C for 1 minute followed by 25 cycles of 96°C for 10 seconds, 50°C for 5 seconds and 60°C for 3:30 minutes. Purification of sequencing products was performed using Montage SEQ_{96} sequencing reaction clean up kits. Twenty micro litres of injection fluid was added to sequencing reactions and transferred into the micro well filter plate. The samples were drawn thought the plate using a vacuum pump (20 inches Hg) until the wells were empty. Two additional washes with injection fluid (25µl) were performed using the vacuum pump. Purified sequencing products were re-suspended in 25µl of injection fluid by shaking for 10 minutes. Samples were run on an ABI 3100 Genetic Analyser.

2.6 Bioinformatic tools

Genebank (http://www.ncbi.nih.gov/Genbank/) accession numbers for the genes analysed in this project are as follows:

Tsc1 (*Mus musculus*) NT_039206

Blm (*Mus musculus*) NT_039428

BLAST searches were carried out against DNA sequences from Genbank (http://www.ncbi.nlm.nih.gov/BLAST/). Open reading frames (ORF) were identified using the ORF finder (http://www.ncbi.nlm.nih.gov/gorf/gorf.html). mRNA sequences were aligned to a single genomic sequence using Spidey (http://www.ncbi.nlm.nih.gov/IEB/Research/Ostell/Spidey/). Sequence data were viewed on Sequencher version 4.2. Microsatellite data were obtained from the Mouse Microsatellite Data Base of Japan (MMDBJ) (http://www.shigen.nig.ac.jp/mouse/mmdbj/top.jsp).

Chapter 3: Characterising a mouse model of tuberous sclerosis 1 deficiency

3.1 Introduction

Two groups have generated mouse lines with constitutively inactivated *Tsc1* (Kobayashi et al. 2001, Kwiatkowski et al. 2002) and *Tsc2* (Onda et al 1999, Kobayashi et al. 1999) alleles. These mice are predisposed to renal lesions; $Tsc1^{+/-}$ mice develop renal lesions by fifteen to eighteen months, whereas $Tsc2^{+/-}$ mice developed lesions by six months.

Here, we describe the development and characterisation of a further mouse model of tuberous sclerosis-1 deficiency, as a tool to determine the mechanisms by which hamartin deficiency leads to TSC-associated disease. This new model is more severely affected than the published *Tsc1* murine models, and heterozygotes exhibit increased early post-natal mortality and metastatic renal cell carcinoma.

3.2 Materials and methods

3.2.1 Targeted inactivation of the *Tsc1* gene and generation of *Tsc1*$^{+/-}$ mice

A replacement-type targeting vector was constructed in pUC19 using 129/Ola cloned genomic DNA containing the *Tsc1* gene (Cheadle *et al.* 2000). This comprised a 1.3kb region spanning exon 5 and part of exon 6 of *Tsc1* for the 5' homology arm, and a 1.9kb region spanning exon 9 for the 3' homology arm. A reporter/positive selection cassette, $(TAG)_3$/IRES-*lacz*-polyA/*loxP*/MC1*neo*-polyA/*loxP*, was inserted between the homology arms. This cassette (a newer version of that previously described (Nehls *et al.* 1996) modified to contain *loxP* sites) therefore disrupted exon 6 inserting TAG codons in all three reading frames at the junction and introduced a *lacz* reporter preceded by an internal ribosome entry site (IRES) and followed by an SV40 polyadenylation sequence. This allows expression of the reporter from the IRES but under control of the endogenous targeted gene's promoter. The positive selection marker (MC1*neo*-polyA) contained in the cassette is independently expressed using its own enhancer/promoter and polyadenylation sequence. A negative selection cassette (MC1tk^2), which consists of two copies of the HSV thymidine kinase gene independently expressed using its own enhancer/promoter and polyadenylation sequence (Smith *et al.* 1995), was appended to the end of the right homology arm. The vector was linearised at a unique *Sal*I site. The knock-out construct was prepared by Jeremy Cheadle and Shelley Idziaszczyk.

Seventy five micrograms of linearised targeting construct were electroporated into $4.5x10^7$ E14 Tg2aIV ES cells (from 129/Ola strain). Cells

were selected on 160μg/ml G418 containing medium from one day after electroporation and then on G418 + Ganciclovir (GANC, 2.5μM) containing medium after a further four days, in order to enrich for targeted clones by positive-negative selection (Mansour *et al.* 1988). After 10 days, 700 G418 + GANC resistant colonies were picked into 96 well plates, and subsequently replica plated for freezing and DNA isolation. DNA was digested with *Eco*RI, and analysed by Southern blotting and hybridisation with external 5' and 3' flanking probes to identify correctly targeted clones. Gene Targeting was performed by Andrew Smith and Rosemary Bayne in The Gene Targeting Laboratory, Institute for Stem Cell Research, University of Edinburgh.

Tsc1$^{+/-}$ ES cell clones were injected into C57BL/6 blastocysts, transferred into pseudo-pregenant (CBA x C57BL/6) females and chimeric pups identified. Male chimeras were mated with inbred C57BL/6 females to generate F1 mice (50% 129ola/ 50% C57BL/6) carrying the targeted mutation, identified by coat colour and subsequent genotyping on tail biopsied DNA. *Tsc1*$^{+/-}$ F1 mice were backcrossed (N≥3) with inbred C57BL/6J Ola Hsd (C57BL/6), Balb/c Ola Hsd (Balb/c) and C3H HeN Hsd (C3H) mice (Harlan UK Limited). Blastocyst manipulation was performed by Andrew Smith and Rosemary Bayne in The Gene Targeting Laboratory, Institute for Stem Cell Research, University of Edinburgh.

3.2.2 Southern blotting and PCR genotyping

DNA was extracted from ES cells, yolk sacs, whole embryo paraffin sections or tail tips using QIAamp DNA mini kits (Qiagen) or NaCl/ isopropanol extraction methods (chapter 2). Southern blot analysis was

performed as previously described (chapter 2 section 2.5.16). A ~0.7kb *Pst*I fragment cut from the vector pMC1*neo*-polyA, a ~0.8kb fragment containing exon 4 of *Tsc1* and a ~0.6kb fragment containing exons 11 and 12 of *Tsc1*, were used as the neomycin probe, and 5' and 3' external flanking probes, respectively.

PCR genotyping of DNA from tail tips and embryo yolk sacs was performed by amplification of the wild type and mutant *Tsc1* alleles using the following primers in a 35 cycle PCR reaction with AmpliTaq gold DNA polymerase (Applied Biosystems): wild type allele, 44F 5'–ATTCACCCGGAATTAGTGACTG-3' & 45R 5'–GCGTCCTCTTCTCCTTTTACAC-3' (1730bp product), and, for the mutant allele, either 16F 5'-AGCGTTGGCTACCCGTGATATTG-3' & 21R 5'-GTGTTGATGGGGAACTCAAACTCT-3' (2306bp product), or, sh2F 5'–GCCGAATATCATGGTGGAAA-3' & sh2R 5'-ACGAAGGTGATCAGGGAATG-3' (1100bp product). Products were analysed on 1% agarose gels. Some genotyping assistance was provided by Shelley Idziaszczyk and Carol Guy.

An independent PCR of DNA extracted from paraffin embedded embryo sections was performed to validate the yolk sac genotypes. PCR was performed by amplification of the wild type and mutant alleles using the following primers in a 35 cycle PCR reaction: wild type allele, EXON 8F 5'-TGCCTGGAAGCCCAGGAAGGT-3' & EXON 8R 5'-CTGCAGGGCCCATGGTGGTT-3' (183bp product), and, mutant allele, IRES F 5'-TAACGTTACTGGCCGAAG-3' & IRES R 5'-GTCGCTACAGACGTTGTT-3' (237bp product).

3.2.3 RT-PCR analysis

RNA was extracted from tissues and embryos after snap freezing and grinding in liquid nitrogen using the RNAeasy kit (Qiagen). 50ng-1μg RNA was used for first strand cDNA synthesis using oligo $(dT)_{15}$ and Superscript II RNase H^- Transcriptase (Invitrogen Life Technologies). Second strand synthesis was carried out in 50μl reaction volumes using 1μl cDNA, 25pmol primers, 0.2mM dNTPs, 5μl reaction buffer and 2U AmpliTaq Gold DNA polymerase in 35 cycle PCR reactions. Four reactions were carried out: (i) KO34 (exon 4 F) 5'–ACGTGGGCCTATGCTTGTCAACA-3' & KO35 (exon 7 R) 5'–AGCGCAGGAAGGAGACGAAGTTA–3', (ii) KO34 & IRES_R2 5'–TCCTTCAGCCCCTTGTTGAATAC–3', (iii) LACZ_F 5'–AAACCCTGGCGTTACCCAACTTA–3' & LACZ_R 5'–ACCGTCGATATTCAGCCATGTTC–3', and, (iv) KO34 & KO21 (exon 10 R) 5'–GTGTTGATGGGGAACTCAAACTCT-3'. Products were analysed on 1% agarose gels, cloned into pGEM-T (Promega) and sequenced. RT-PCR analysis was performed by Lee Parry.

3.2.4 Animal care, necropsy and pathology

Animal care, necropsy and pathology was carried out as previously described (chapter 2). Tissues from 10, 15 and 20 *Tsc1*$^{+/-}$ mice and wild type littermates on each background were analysed at 3-6, 9-12 and 15-18 months, respectively. Half of each organ was fixed and processed into paraffin wax. The other half of the organ was snap frozen. To estimate the average number of microscopically visible kidney lesions per mouse, ten

Tsc1$^{+/-}$ mice were analysed per background at 3-6, 9-12 and 15-18 months - five representative sections ~200μm apart from each half kidney were stained with H&E and anti-gelsolin and inspected on an Olympus BX51 BF light microscope (lesions crossing more than one section were counted once and total numbers were doubled to generate a mean number per mouse). Animals that died before weaning were collected, genotyped and processed into paraffin wax, sectioned at 4μm and stained with H&E for microscopic analysis. Staining for β-galactosidase activity was carried out as described in chapter 2, section 2.5.4.

Embryos were removed at 9.5, 10.5, 11.5, 12.5 and 13.5 days post fertilisation (noon on the day on which the vaginal plug was formed was defined as embryonic day 0.5). Yolk sacs were removed for genotyping and whole embryos were processed into paraffin wax, sectioned at 4μm and stained with H&E for microscopic analysis.

3.2.5 Immunohistochemistry and immunoblotting

Immunostaining of paraffin sections was performed as described (chapter 2, section 2.5.6) using the rabbit VECTASTAIN ELITE ABC horseradish peroxidase kit (Vector Laboratories). Primary antibodies were incubated for 30 minutes at room temperature for anti-murine gelsolin (Onda *et al.* 1999) and overnight at 4°C for anti-Phospho-S6 Ribosomal protein (Ser240/244) and anti-Phospho-mTOR (Ser 2448) (Cell Signalling Technologies).

Immunoblotting was performed as previously described (chapter 2 sections 2.5.7 to 2.5.11). Primary antibodies used included anti-mTOR, anti-

phospho-mTOR (Ser 2448), or, anti-phospho-S6 ribosomal protein (Ser 240/244) (Cell Signalling Technonlogies).

3.2.6 Somatic loss of heterozygosity analysis

Snap frozen tissue was sectioned at 10μm onto PEN (PALM) membrane covered slides, and stained with toluidine blue. Tumour and normal tissue were microdissected (PALM LCM) and DNA extracted using the QIAamp DNA micro kits (Qiagen). PCR of microdissected DNA was performed by simultaneous amplification of both the wild type (EXON 8F-5'FAM labelled & EXON 8R) and mutant (IRES F-5'FAM labelled & IRES R) alleles in a 25 cycle PCR reaction. 2μl of PCR products were mixed with an ABI GS500 internal size standard and formamide loading buffer, and run on an ABI3100 genetic analyser. Results were analysed using Genescan v.3.7 software. DNA extracted from 8 different normal tissue sections from *Tsc1*$^{+/-}$ mice was used to normalise the assay (comparison of wild type:mutant allele peak heights). Loss of heterozygosity was defined as a wild type:mutant peak ratio of ≥2.0.

3.2.7 Statistical analysis

Comparisons of numbers of *Tsc1*$^{+/-}$ to *Tsc1*$^{+/+}$ mice were calculated using the Chi-square test with 1d.f. Lesion counts per mouse were compared using the Kruskal-Wallis and Mann-Whitney confidence interval tests. Survival over 18 months was compared using Kaplan-Meier cumulative survival plots.

3.3 Results

3.3.1 Generation of *Tsc1*$^{+/-}$ mice

The murine *Tsc1* locus from the 129/Ola strain was previously cloned, sequenced and characterised (Cheadle *et al.* 2000). A replacement-type targeting vector for homologous recombination in mouse ES cells was constructed. This vector was designed to inactivate an endogenous *Tsc1* gene by deleting an internal region of the gene comprising the 3' half of exon 6 and all of exons 7 and 8, and substituting this with a β-galactosidase reporter/neomycin selection ((TAG)$_3$/IRES*lacz*-polyA/*loxP*/MC1*neo*-polyA/*loxP*) cassette (Nehls *et al.* 1996) (Fig. 3.1a). Insertion of this cassette was predicted to truncate the *Tsc1* coding sequence in exon 6 by introducing TAG stop codons in all three frames, and also create a bicistronic mRNA in which expression of the β-galactosidase coding sequence was brought under the control of *Tsc1* transcriptional regulatory sequences via an IRES. The linearised vector was electroporated into E14 Tg2aIV ES cells and correctly targeted clones identified by Southern blot analysis of *Eco*RI digested DNA, using 5' and 3' probes external to, and flanking, the vector homology arms. Targeting efficiency was ~3.4%. Chimeric male mice generated from two independently derived targeted ES cell lines (I/F5 and I/G11) fathered offspring with the ES cell coat colour in test crosses with C57BL/6 females and germ line transmission of the targeted allele was confirmed in 50% of these by Southern blot analysis on tail DNA (Figs. 3.1b-c). Further confirmation of successful targeting was obtained by carrying out long distance PCR using a primer within the neomycin coding sequence and a

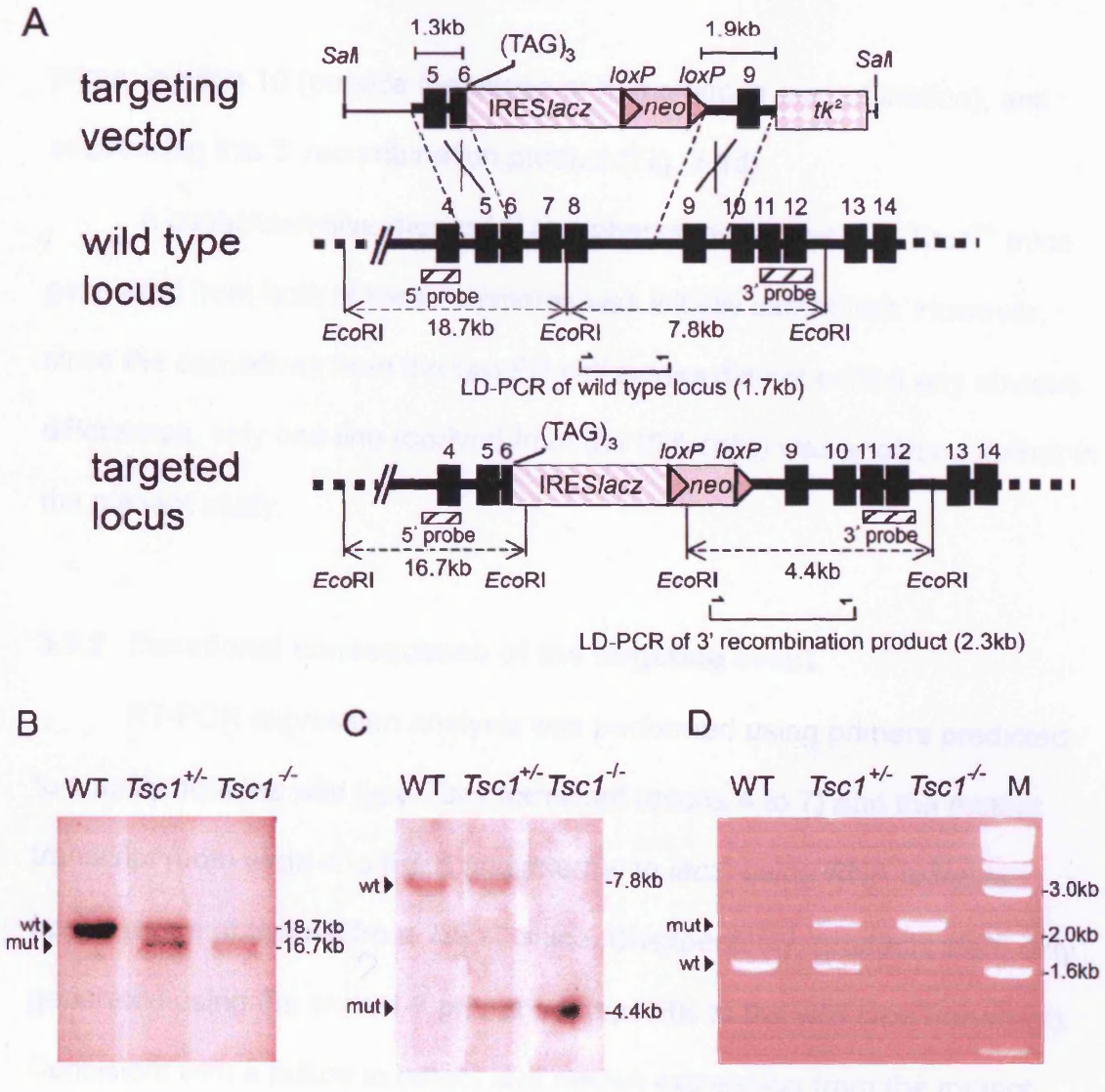

Figure 3.1: (A) Schematic illustration of the *Tsc1* replacement targeting vector (upper panel), the wild type *Tsc1* locus (middle panel) and the targeted locus (lower panel). The vector was comprised of cloned 129/Ola genomic DNA consisting of a 1.3kb region spanning exon 5 and part of exon 6 of *Tsc1* for the 5' homology arm and a 1.9kb region spanning exon 9 of *Tsc1* for the 3' homology arm, flanking a $(TAG)_3$/IRES-*lacz*-polyA/*loxP*/MC1*neo*-polyA/*loxP* reporter/ positive selection cassette in the same transcriptional orientation. A negative selection cassette MC1-*tk*^{2} consisting of two copies of the HSV thymidine kinase (*tk*) gene was positioned at the outer end of the 3' homology arm. The vector was linearised at a unique *Sal*I site in the plasmid backbone. The regions of homology in which cross-overs (denoted X) can occur between the linearised vector and the *Tsc1* locus to result in a replacement event are indicated by the dashed lines. The predicted targeted locus contains the reporter/positive selection cassette inserted into exon 6 of *Tsc1* and introduces stop codons $(TAG)_3$ into all three reading frames of the *Tsc1* coding sequence. The targeting event also simultaneously deletes the 3' part of exon 6 and all of exons 7 and 8 of *Tsc1*. Exons are shown as numbered black rectangles, introns as a thick black line, flanking genomic regions as a thick dashed line, plasmid vector sequence as a thin black line. The reporter/selection cassette is shown as a large light grey striped rectangle (IRES-*lacz* component) and a large filled light grey rectangle (MC1*neo*-polyA component), with dark grey triangles indicating *loxP* sites. The negative selection cassette is shown as a grey chequered rectangle. The positions of relevant *Eco*RI sites and the predicted sizes of *Eco*RI restriction fragments (thin dashed lines with arrows) detected with the 5' and 3' probes (small black striped rectangles) before and after targeting, and the long distance (LD) PCR products spanning the wild type locus and the 3' recombination junction, are shown below the wild type and targeted loci. (B) Southern blot analysis of *Eco*RI digested DNA from wild type (wt) and *Tsc1*$^{+/-}$ mice and *Tsc1*$^{-/-}$ embryos, analysed with the 5' probe. The 18.7 kb wild type fragment is present in only wild type and *Tsc1*$^{+/-}$ mice, and the 16.7 kb targeted fragment is present in only *Tsc1*$^{+/-}$ mice and *Tsc1*$^{-/-}$ embryos, as expected. (C) Southern blot analysis of *Eco*RI digested DNA from wild type (wt) and *Tsc1*$^{+/-}$ mice and *Tsc1*$^{-/-}$ embryos, analysed with the 3' probe. The 7.8 kb wild type fragment is present in only wild type and *Tsc1*$^{+/-}$ mice, and the 4.4 kb targeted fragment is present in only *Tsc1*$^{+/-}$ mice and *Tsc1*$^{-/-}$ embryos, as expected. (D) Multiplex PCR of long distance PCR products generated from the wild type locus (using primers in exon 8 and intron 8 to amplify a 1.7 kb product) and from the targeted locus (using primers in the neomycin cassette and exon 10 to amplify a 2.3 kb product). The 1.7 kb wild type fragment is present in only wild type and *Tsc1*$^{+/-}$ mice, and the 2.3 kb targeted fragment is present in only *Tsc1*$^{+/-}$ mice and *Tsc1*$^{-/-}$ embryos.

primer in exon 10 (outside the region of homologous recombination), and sequencing this 3' recombination product (Fig. 3.1d).

A comprehensive molecular and phenotypic analysis of *Tsc1*$^{+/-}$ mice generated from both of these chimeras was initially carried out. However, since the derivatives from the two ES cell clones did not exhibit any obvious differences, only one line (derived from the I/F5 cells) was analysed further in the present study.

3.3.2 Functional consequence of the targeting event

RT-PCR expression analysis was performed using primers predicted to amplify both the wild type *Tsc1* transcript (exons 4 to 7) and the mutant transcript (both exon 4 to IRES and internal to *lacz*) using RNA extracted from a range of tissues from *Tsc1*$^{+/-}$ mice. Unexpectedly, products were only generated using the exon 4-7 primer set (specific to the wild type transcript). Consistent with a failure to detect *lacz* mRNA expression from the mutant allele, β-galactosidase activity in kidneys from *Tsc1*$^{+/-}$ mice was not detected (Fig. 3.2) (although β-galactosidase activity in kidneys from *Pkd1*$^{+/-}$ mice that also carried a *lacz* expression construct was detected; Boulter *et al.* 2001).

RT-PCR was then performed with primers in exons 4 and 10, which lie outside the regions of homologous recombination, so that any aberrant expression products from the modified locus could be detected. A product corresponding to correctly spliced exon 4-10 transcripts was detected in RNA extracted from wild type and *Tsc1*$^{+/-}$ mice, but not in RNA extracted from *Tsc1*$^{-/-}$ embryos. A strongly expressed truncated transcript was also detected in RNA extracted from *Tsc1*$^{+/-}$ mice and was the only product detected in

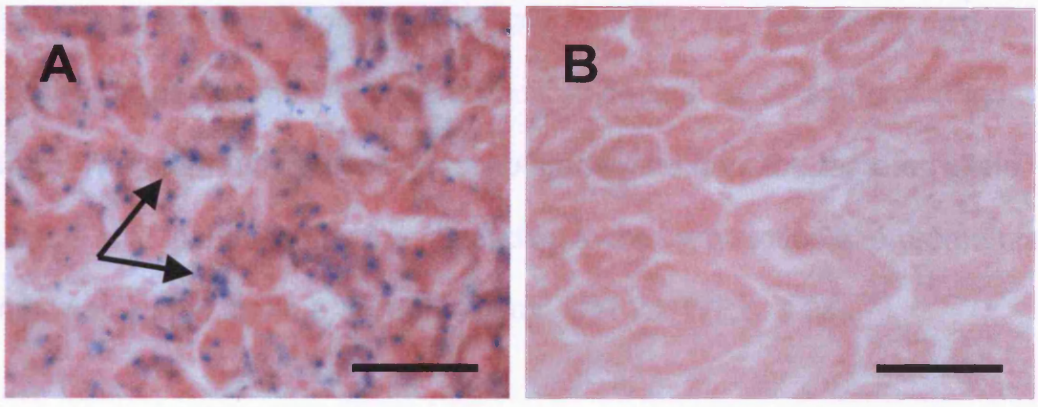

Figure 3.2: *LacZ* staining for β-galactosidase activity. (A) Renal tissue from *Pkd1*$^{+/-}$ mice carrying a *lacZ*-neomycin fusion gene with known β-galactosidase activity (Boulter *et al.* 2001). Blue staining (arrows) indicates positive β-galactosidase activity (B) *Tsc1*$^{+/-}$ renal tissue showing no β-galactosidase activity. Bars are 50μm.

Tsc1$^{-/-}$ embryos. This aberrant transcript was not present in RNA extracted from wild type mice. Cloning and sequencing of these products confirmed the presence of normal, correctly spliced *Tsc1* transcripts in wild type and *Tsc1*$^{+/-}$ mice, and revealed an unpredicted spliced transcript that lacked exons 6, 7 and 8, and joined exons 5 and 9, in *Tsc1*$^{+/-}$ mice and *Tsc1*$^{-/-}$ embryos (Figs. 3.3a-b). The aberrantly spliced transcript generated from the targeted allele causes a shift in the reading frame, leading to the introduction of a premature termination codon at the 8th codon of exon 9 of *Tsc1* (Fig. 3.3c).

3.3.3 *Tsc1*$^{-/-}$ mice die during embryonic development

Tsc1$^{+/-}$ intercrosses (*Tsc1*$^{+/-}$ x *Tsc1*$^{+/-}$) were set up using F1 mice generated from the chimera test crosses (50% 129ola/ 50% C57BL/6). From eleven intercrosses, 138 progeny were obtained, 47 of which were *Tsc1*$^{+/+}$, 86 were *Tsc1*$^{+/-}$ and 0 were *Tsc1*$^{-/-}$ (5 mice failed to be genotyped). This ratio differs significantly from expected ($P<0.0001$) indicating that the *Tsc1* mutant allele has a recessive, embryonic lethal phenotype. *Tsc1*$^{+/-}$ mice were backcrossed (*Tsc1*$^{+/-}$ x *Tsc1*$^{+/+}$) onto a C57BL/6 background ($N\geq4$) and 15 *Tsc1*$^{+/-}$ intercrosses were set up for timed matings to study the embryonic development of *Tsc1*$^{-/-}$ animals. *Tsc1*$^{-/-}$ embryos died between embryonic day (E) 9.5 to E12.5 and no viable null embryos were observed at E13.5 (Table 3.1). *Tsc1*$^{-/-}$ embryos were generally smaller and developmentally retarded as compared to wild type and heterozygous littermates (for example, mean size of *Tsc1*$^{-/-}$, *Tsc1*$^{+/+}$ and *Tsc1*$^{+/-}$ embryos was 2.8, 4.3 and 3.8mm at E10.5, respectively). Two out of 12 (17%) null embryos displayed

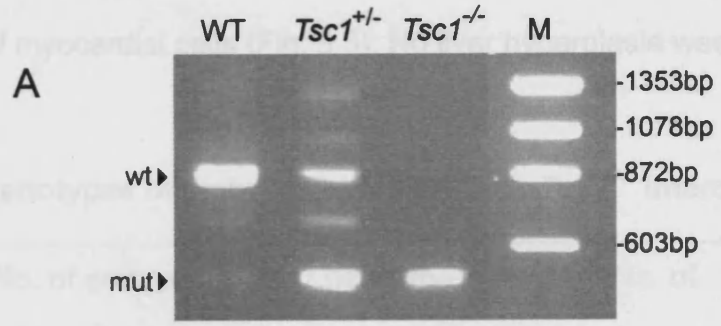

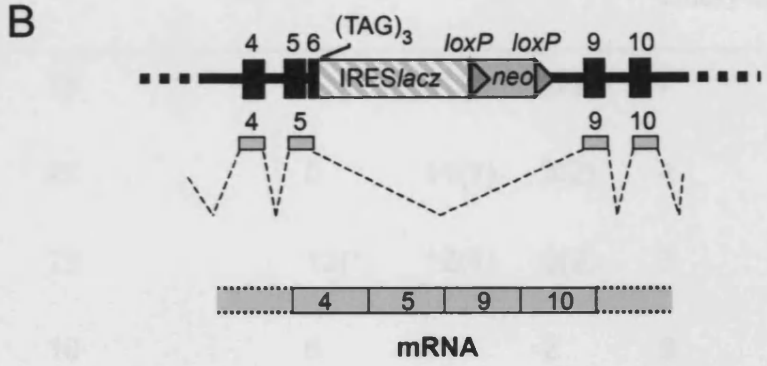

C

wild type

```
      exon 5    |  exon 6          exon 8    |   exon 9
... Cys Leu Lys|Met Asp Thr ... Pro Arg Arg  Trp Lys Thr Leu Glu Thr His Asp ...
... TGT CTC AAG|ATG GAC ACT ... CCT CGA AG|G TGG AAG ACA TTA GAA ACT CAT GAT ...
               |                          |
```

mutant

```
      exon 5    |   exon 9
... Cys Leu Lys|Val Glu Asp Ile Arg Asn Ser STOP
... TGT CTC AAG|GTG GAA GAC ATT AGA AAC TCA TGA ...
               |
```

Figure 3.3: Functional consequence of homologous recombination with the knockout vector. (A) RT-PCR analysis using primers in exons 4 and 10 of *Tsc1*. Full length, normally spliced products of ~900 bp were detected only in RNA extracted from wild type and *Tsc1*$^{+/-}$ mice. Truncated products were detected only in RNA extracted from *Tsc1*$^{+/-}$ mice and *Tsc1*$^{-/-}$ embryos. Further faint bands that were not seen in wild type mice and *Tsc1*$^{-/-}$ embryos were detected in RNA from *Tsc1*$^{+/-}$ mice; these were shown to correspond to heteroduplex species formed between wild type and mutant RT-PCR products. (B) Sequence analysis of cloned RT-PCR products from *Tsc1*$^{+/-}$ mice and *Tsc1*$^{-/-}$ embryos identified the presence of a mutant *Tsc1* transcript lacking exons 6, 7 and 8 and fusing exons 5 and 9 as a consequence of an aberrant splicing event, thus excluding the coding sequence of the 5' region of exon 6 and the IRES-*lacz* sequence in the mRNA. DNA sequences are indicated as in Figure 3.1 and RNA exon sequences are indicated by grey rectangles. (C) Mutant transcripts were predicted to cause a shift in the reading frame and introduce a premature termination codon at the 8th codon in exon 9 of *Tsc1*, and were thus considered to be inactivating.

exencephaly (Fig. 3.4) and, at E12.5, 2 out of 2 null embryos had abnormal vacuolation of myocardial cells (Fig. 3.5). No liver hyperplasia was observed.

Table 3.1: Genotypes of embryos obtained from *Tsc1*$^{+/-}$ intercrosses

Embryonic day	No. of embryos genotyped	*Tsc1* genotype			[a]No. of resorbed embryos
		+/+	+/-	-/-	
9.5	18	7	8	2(1)	7
10.5	22	5	11(1)	3(2)	4
11.5	28	12(1)	12(1)	0(2)	3
12.5	19	6	11	2	8
13.5	18	8	10	0	10

Number in parentheses refers to resorbing embryos that could be genotyped.

[a]Number of resorption sites for which no material was available for genotyping.

3.3.4 Some *Tsc1*$^{+/-}$ mice on a C57BL/6 background die post-natally

Tsc1$^{+/-}$ mice were backcrossed (N≥3) with inbred (wild type) C57BL/6 mice. Genotyping showed that, out of the 253 offspring that survived until weaning, 103 were *Tsc1*$^{+/-}$ and 142 were wild type (8 failed to be genotyped), which is significantly different from the expected 1:1 ratio (P= 0.014) (Table 3.2). This indicated ~27% excess mortality among *Tsc1*$^{+/-}$ mice before weaning. To investigate the point at which these *Tsc1*$^{+/-}$ mice died (*in utero* or post-natally), additional crosses between *Tsc1*$^{+/-}$ mice at this backcross

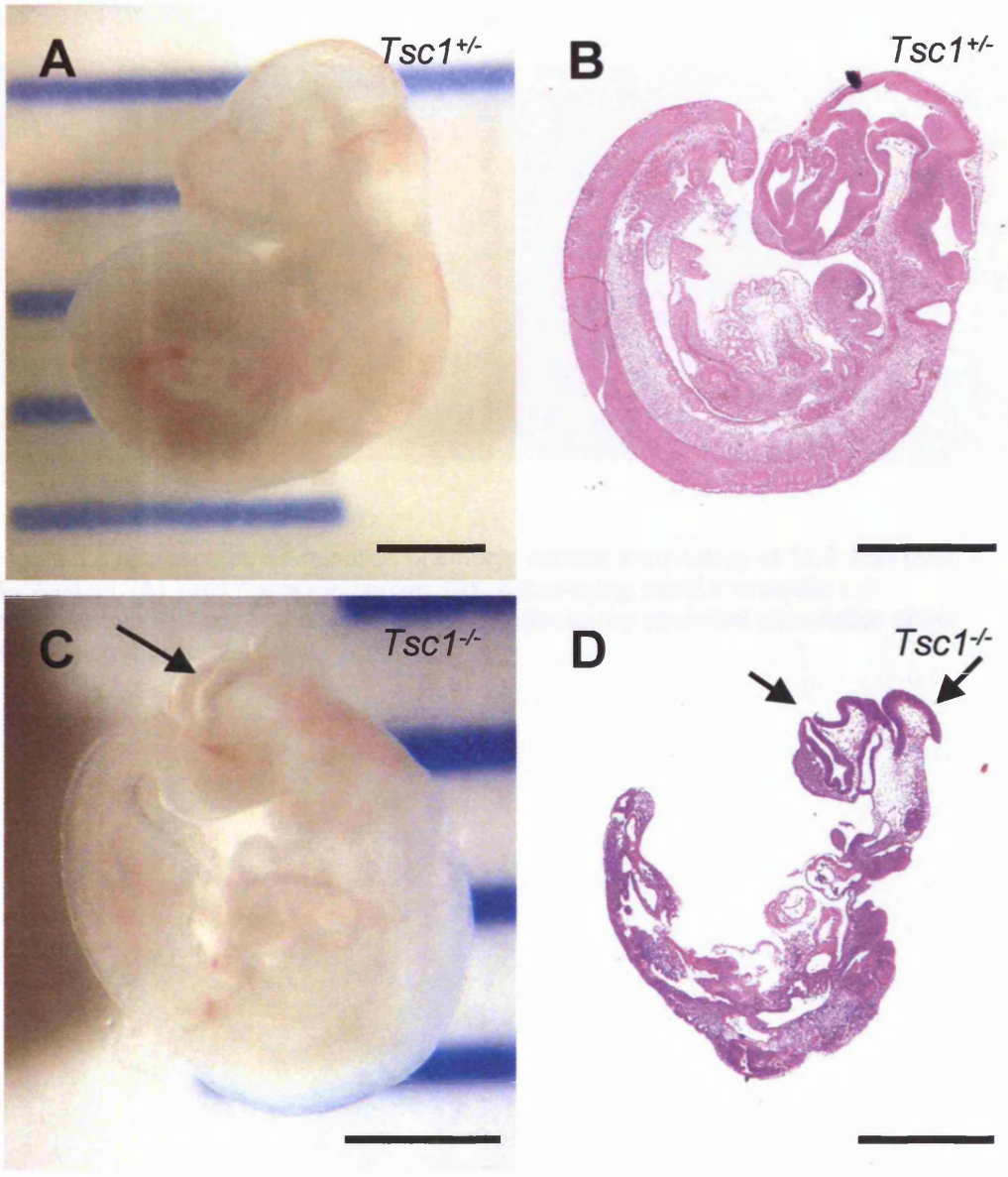

Figure 3.4: Macroscopic and microscopic examination of mouse embryos at 10.5 days post fertilisation. (A and B) A *Tsc1*$^{+/-}$ mouse embryo displaying full neural tube closure and substantial organ differentiation. (C and D) *Tsc1*$^{-/-}$ mouse embryos were smaller and developmentally retarded, as compared to heterozygous littermates. Some had neural exencephaly (arrows). Bars are 1mm.

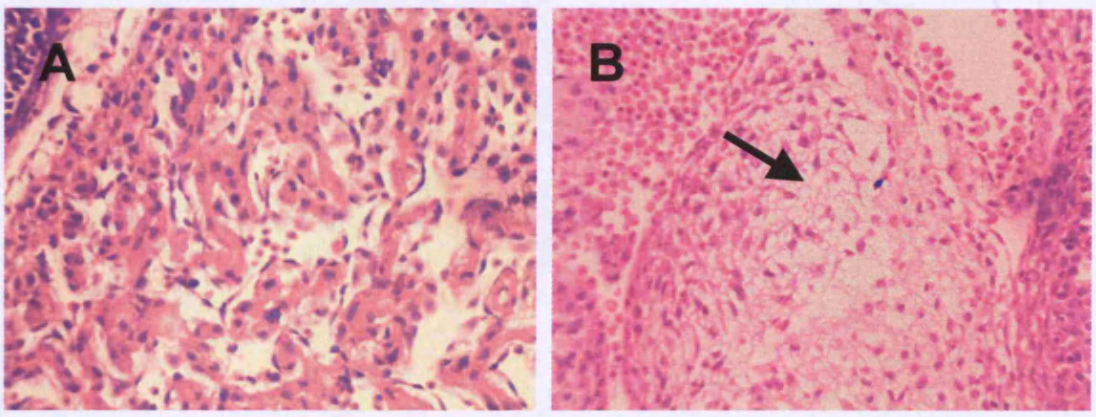

Figure 3.5 Microscopic examination of embryo cardiac morphology at 12.5 days post fertilisation. (A) *Tsc1*$^{+/+}$ embryo cardiac tissue displaying intact myocardial cell morphology. (B) *Tsc1*$^{-/-}$ embryo cardiac tissue displaying abnormal vacuolation of the developing myocardial cells.

generation and wild type C57BL/6 mice were set up and offspring genotyped at birth. Out of 184 new born pups, 95 were *Tsc1*$^{+/-}$ and 88 were wild type (1 mouse failed to be genotyped), thus excluding *in utero* mortality. Close examination of another cohort of mice revealed that a significant proportion of animals died soon after birth. The carcasses of 37 of these animals were collected and genotyped; 25 were *Tsc1*$^{+/-}$ and 12 were wild type, which is significantly different from the expected 1:1 ratio (*P*= 0.033) (Table 3.2).

Table 3.2: Genotypes of offspring from *Tsc1*$^{+/-}$ and *Tsc1*$^{+/+}$ crosses (N≥3 C57BL/6)

[a]Cohort of mice	No. of animals assayed	[b]*Tsc1* genotype		Failed to genotype	P
		+/-	+/+		
Analysed at birth	184	95	88	1	NS
Analysed at weaning	253	103	142	8	0.014
[c]Died between birth and weaning	37	25	12	-	0.033

[a]Three independent cohorts of mice were analysed (one cohort was analysed at birth, one was analysed at weaning, and one was set up to collect and analyse animals that died between birth and weaning). [b]Expected a 1:1 ratio of *Tsc1*$^{+/-}$:*Tsc1*$^{+/+}$ offspring in each cohort. [c]Whole litters that died overnight on day 1 (normally due to maternal rejection) were excluded from this analysis; if included, 53 carcasses were collected, 34 of which were *Tsc1*$^{+/-}$ and 19 were *Tsc1*$^{+/+}$ (*P*=0.04). NS – not significant.

Tsc1$^{+/-}$ mice were backcrossed (N≥3) onto two further genetic backgrounds (C3H and Balb/c). No evidence of increased post-natal mortality of *Tsc1*$^{+/-}$ mice was observed on either of these backgrounds (144 *Tsc1*$^{+/-}$ and 138 *Tsc1*$^{+/+}$ mice on the Balb/c background and 120 *Tsc1*$^{+/-}$ and 120 *Tsc1*$^{+/+}$ mice on the C3H background survived until weaning), indicating that this phenotype was specific to the C57BL/6 background.

3.3.5 Survival of *Tsc1*$^{+/-}$ mice between weaning and 18 months

Survival of *Tsc1*$^{+/-}$ mice backcrossed onto 3 different backgrounds was tracked from weaning until 18 months of age. Twenty-nine out of 106 (27%) *Tsc1*$^{+/-}$ mice on a Balb/c background died prematurely, 5 out of 92 (5%) *Tsc1*$^{+/-}$ mice on a C3H background died prematurely, 8 out of 97 (8%) *Tsc1*$^{+/-}$ mice on a C57BL6 background died prematurely (mean age of death= 10.1, 10.3, and 12.9 months respectively). In contrast, *Tsc1*$^{+/+}$ mice from each background had low levels of premature death varying between 2% to 11%. Therefore, *Tsc1*$^{+/-}$ mice on a Balb/c background had significantly more deaths between weaning and 18 months ($P< 0.001$) than *Tsc1*$^{+/-}$ mice on a C3H or C57BL6 background (Fig. 3.6a), and significantly more deaths between weaning and 18 months ($P= 0.038$) than their *Tsc1*$^{+/+}$ littermate controls (Fig. 3.6b). Post mortem examination could not be performed on all animals due to autolysis or cannibalism by cage mates. Twenty four percent (7/29) of *Tsc1*$^{+/-}$ mice on a Balb/c background that had died before 18 months had heart abnormalities (Fig. 3.7a and b) that were classified as atrial thrombi by expert pathologist Charles H. Frith. Thrombosis of the heart artria commonly involved the left atrium which was enlarged and often

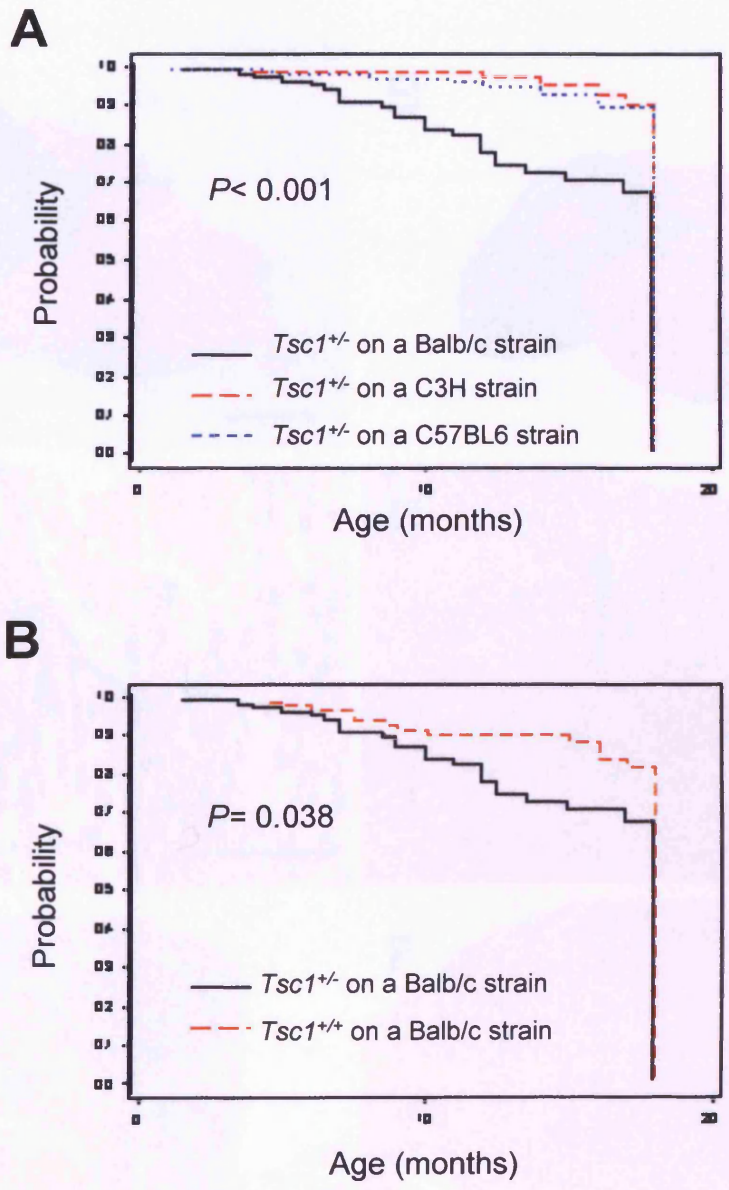

Figure 3.6 Kaplan-Meier cumulative survival plots of *Tsc1* mice from weaning to 18 months. (A) Comparing survival rate of $Tsc1^{+/-}$ mice on the 3 study backgrounds: Balb/c, C3H and C57BL6 from weaning to18 months. (B) Comparing survival rate of $Tsc1^{+/-}$ to $Tsc1^{+/+}$ mice on a Balb/c background from weaning to18 months.

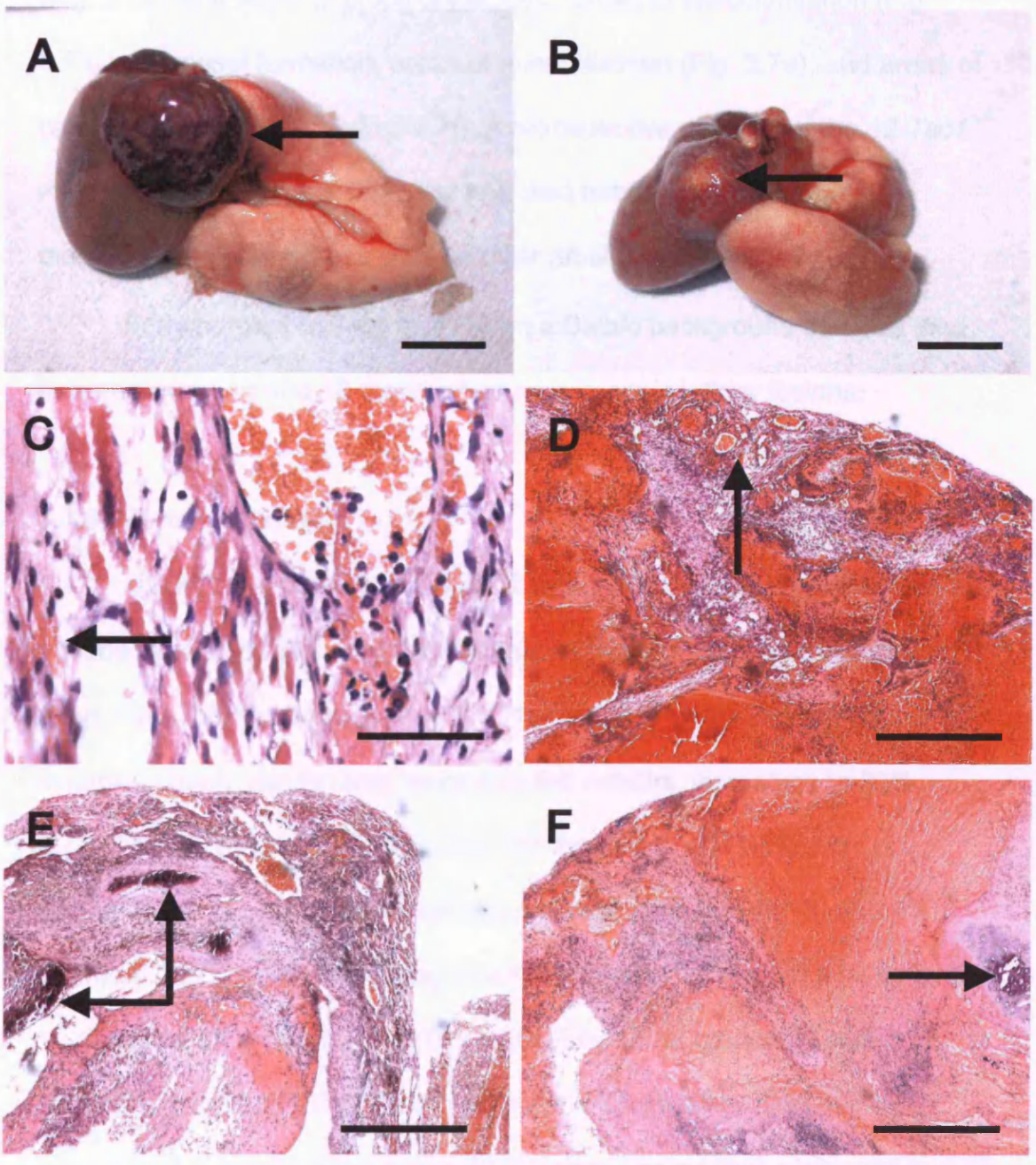

Figure 3.7 Macroscopic and microscopic examination of heart abnormalities in *Tsc1*$^{+/-}$ mice on a Balb/c background. (A and B) Macroscopic view of heart and lungs from *Tsc*$^{+/-}$ mice on a Balb/c background that had died between weaning and 18 months, arrows indicating large atrial thrombosis on top of hearts (bars are 5mm). (C-F) Microscopic view of atrial thrombosis showing (C) hemosiderin pigment (bar is 50μm) (D) vascularisation (E) mineralisation (F) cartilaginous metaplasia (bars are 500μm).

occluded by organising thrombi. The thrombi contained hemosiderin pigment (Fig. 3.7c) as a result of blood breakdown, areas of vascularisation (Fig. 3.7d) with vessel formation, areas of mineralisation (Fig. 3.7e), and areas of cartilaginous metaplasia (Fig. 3.7f). A retrospective analysis of the 12 *Tsc1*$^{+/+}$ mice on a Balb/c background that had died between weaning and 18 months, revealed 1 mouse with a similar atrial thrombosis.

Forty percent of *Tsc1*$^{+/-}$ mice on a Balb/c background that had died between weaning and 18 months had macroscopic kidney lesions.

3.3.6 Renal pathology

The kidneys of mice at 3-6, 9-12 and 15-18 months were examined by macroscopic inspection and microscopic analysis of five sections ~200μm apart. On a C3H background, 44% (7/16) of *Tsc1*$^{+/-}$ mice developed macroscopically visible renal lesions by 3-6 months, increasing to 95% (37/39) by 15-18 months (Table 3.3). On the Balb/c and C57BL/6 backgrounds, the phenotype was less dramatic with 13% (2/16) and 8% (1/13) of *Tsc1*$^{+/-}$ mice developing macroscopically visible renal lesions by 3-6 months, and 88% (35/40) and 67% (29/43) by 15-18 months (Table 3.3). Microscopically, all (10/10) *Tsc1*$^{+/-}$ mice on a C3H background had renal lesions by 3-6 months (average of 10.2 lesions per mouse) compared to 90% (9/10) (6.2 lesions) and 60% (6/10) (2.0 lesions) on Balb/c and C57BL/6 backgrounds, respectively. By 15-18 months, all mice had microscopically visible lesions regardless of background (with 29, 26.8 and 14.8 lesions per mouse on C3H, Balb/c and C57BL/6 backgrounds, respectively). None of the

wild type littermates had macro- or microscopic kidney lesions by 15-18 months.

Renal lesions varied from pure cysts through to solid anaplastic carcinomas and were classified as either cysts (simple cysts lined with one layer of epithelium), atypical cysts (cysts with single papillary projections into the lumen), branching cysts (cystadenomas with branching papillary projections), mixed cystic/solid carcinomas and solid carcinomas (examples shown in Figs. 3.8a-f). Solid carcinomas often displayed pleomorphic nuclei, which are characteristic of a malignant neoplasm (Fig. 3.8g). The majority of lesions expressed gelsolin (a proposed marker for *Tsc*-associated renal lesions, Onda *et al.* 1999), with staining intensities similar to distal tubules and collecting ducts; however, some did not (Fig. 3.8h). The distribution in the size of the lesions, with simple cysts tending to be smaller and more numerous than branching cysts, mixed cysts and solid carcinomas (Table 3.4), suggests that some small cysts progressed to carcinomas. In addition, there was a preponderance of cysts in younger animals and a morphological continuity of lesions further supporting this progression (Fig 3.8b-f). By 15-18 months, $Tsc1^{+/-}$ mice on a C3H background had significantly more cystic lesions (simple, atypical and branching cysts) compared to mice on a C57BL/6 background (P= 0.013), and those on a Balb/c background had significantly more solid lesions (mixed cystic/solid lesions and solid carcinomas) compared to mice on C3H (P= 0.014) or C57BL/6 (P= 0.004) backgrounds.

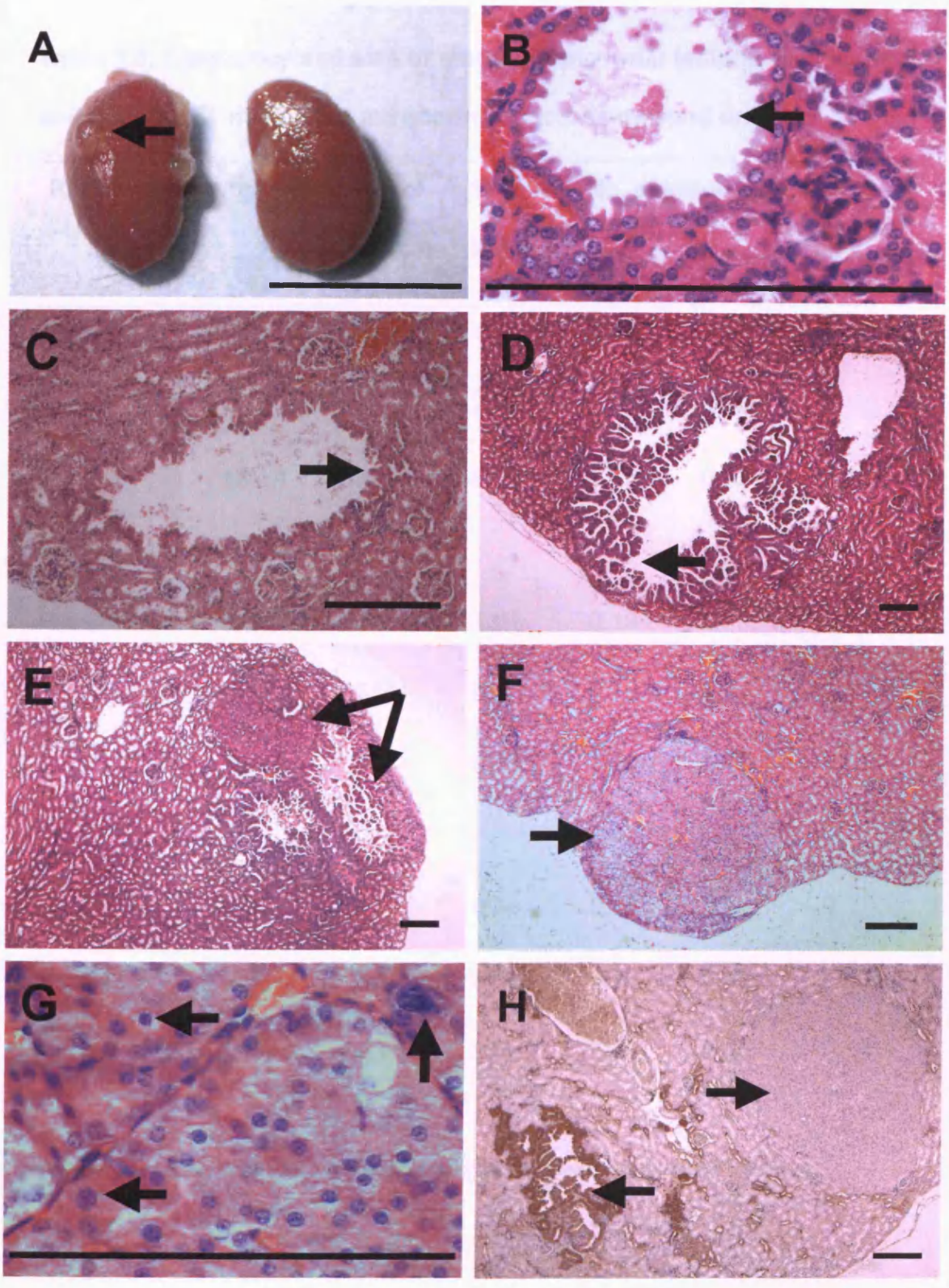

Figure 3.8: Macroscopic and microscopic analysis of renal lesions from *Tsc1*$^{+/-}$ mice. (A) Kidneys from an 18 month old mouse showing macroscopic renal cystadenomas (indicated by an arrow). (B) Microscopic view of a cyst with a single layer of cuboidal lining cells. (C) Microscopic view of an atypical cyst with papillary growths into the centre of the cyst. (D) Microscopic view of a cystadenoma with branching papillae filling the centre of the cyst. (E) Mixed cystic solid lesion, complex cystadenoma with branching cystic region and kidney carcinoma that appears to have developed from the adjacent cyst. (F) Solid renal cell carcinoma. (G) Close up view of kidney carcinoma displaying pleomorphic nuclei. (H) Immunostaining with an anti-gelsolin antibody showed gelsolin expression (indicated by brown staining) in a papillary cystadenoma (arrow on left) and lack of expression in a solid carcinoma (arrow on right). Macroscopic bars are 1cm and microscopic bars are 200μm.

Table 3.3: Frequency and size of macroscopic renal lesions (cystic and solid) in *Tsc1*$^{+/-}$ mice grouped according to background and age

Background	Age (months)	No. of animals	% with lesions	No. of lesions per mouse		
				≤2 mm	3-4 mm	≥5mm
C3H	3-6	16	44%	0.81	0	0
	9-12	28	79%	2.68	0.04	0
	15-18	39	95%	5.15	0.33	0.08
Balb/c	3-6	16	13%	0.19	0	0
	9-12	37	81%	2.73	0.14	0.03
	15-18	40	88%	4.70	0.98	0.68
C57BL/6	3-6	13	8%	0.08	0	0
	9-12	35	37%	0.46	0.06	0
	15-18	43	67%	1.56	0.21	0.14

No wild type littermates had macroscopic (or microscopic) kidney lesions.

Table 3.4: Number and histological classification of microscopic renal lesions in *Tsc1*$^{+/-}$ mice grouped according to background and size

		No. of microscopic lesions				
Background	Size (mm)	Simple cyst	Atypical cyst	Branching cyst	Mixed cystic/solid	Solid RCC
C3H	≤0.49	**103**	**44**	14	0	3
	0.5-0.99	13	6	21	1	1
	1-1.99	7	3	**30**	**7**	**4**
	≥2	0	0	2	0	0
Balb/c	≤0.49	**78**	**12**	7	0	3
	0.5-0.99	19	9	**21**	4	7
	1-1.99	4	0	18	**8**	10
	≥2	0	0	0	4	**21**[a]
C57BL/6	≤0.49	**56**	**15**	2	**1**	**3**
	0.5-0.99	8	2	3	**1**	2
	1-1.99	3	3	**4**	**1**	2
	≥2	0	0	0	**1**	0
Total	≤0.49	**237**	**71**	23	1	9
	0.5-0.99	40	17	45	6	10
	1-1.99	14	6	**52**	**16**	16
	≥2	0	0	2	5	**21**

Numbers based on the analysis of five sections (~200μm apart) from half kidneys of ten *Tsc1*$^{+/-}$ mice at 3-6, 9-12 and 15-18 months (30 mice in total for each strain). In general, severity of lesion increased with size (numbers in bold represent the highest number in each histological group), providing evidence for progression of cysts through cystadenomas (atypical/branching cysts) to solid carcinomas. [a]Four solid tumours had a sarcomatoid morphology.

3.3.7 *Tsc1*$^{+/-}$ mice develop renal cell carcinomas, resulting in grossly deformed kidneys

Eighty percent (16/20) of *Tsc1*$^{+/-}$ mice on a Balb/c background exhibited solid renal cell carcinomas (RCC) by 15-18 months and in 41% (17/40), RCCs were ≥5mm, which resulted in grossly deformed kidneys of up to 2.5cm in size (Figs. 3.9a-c). One mouse displayed this distinctive phenotype as early as 11 months. *Tsc1*$^{+/-}$ mice on C57BL/6 and C3H backgrounds rarely harboured RCCs ≥5mm at 15-18 months (7 and 3%, respectively, $P<0.002$). Four out of nine (44%) RCCs ≥5mm (analysed from different mice) had a sarcomatoid morphology consisting of spindle cells with nuclear anaplasia arranged in whorled patterns (Fig. 3.9d); three of these had metastasized to the lungs (the only lung tumours observed in this study) (Figs. 3.9e-f).

3.3.8 Extra-renal tumours

Microscopic liver hemangiomas were observed in 18% of 15-18 month *Tsc1*$^{+/-}$ mice, regardless of background or sex; these lesions were not seen in wild type littermates. Histologically, hemangiomas consisted of abnormal vascular channels and a proliferation of smooth muscle cells (Figs. 3.10a and b). Liver hepatomas were seen at equal frequency (24%) in *Tsc1*$^{+/-}$ and wild type littermates, suggesting that their pathogenesis is independent of *Tsc1* mutation status. One *Tsc1*$^{+/-}$ mouse (Balb/c background) had a splenic hemangioma and two (C3H background) had isolated uterine leiomyoma/leiomyosarcomas (Figs. 3.10c and d).

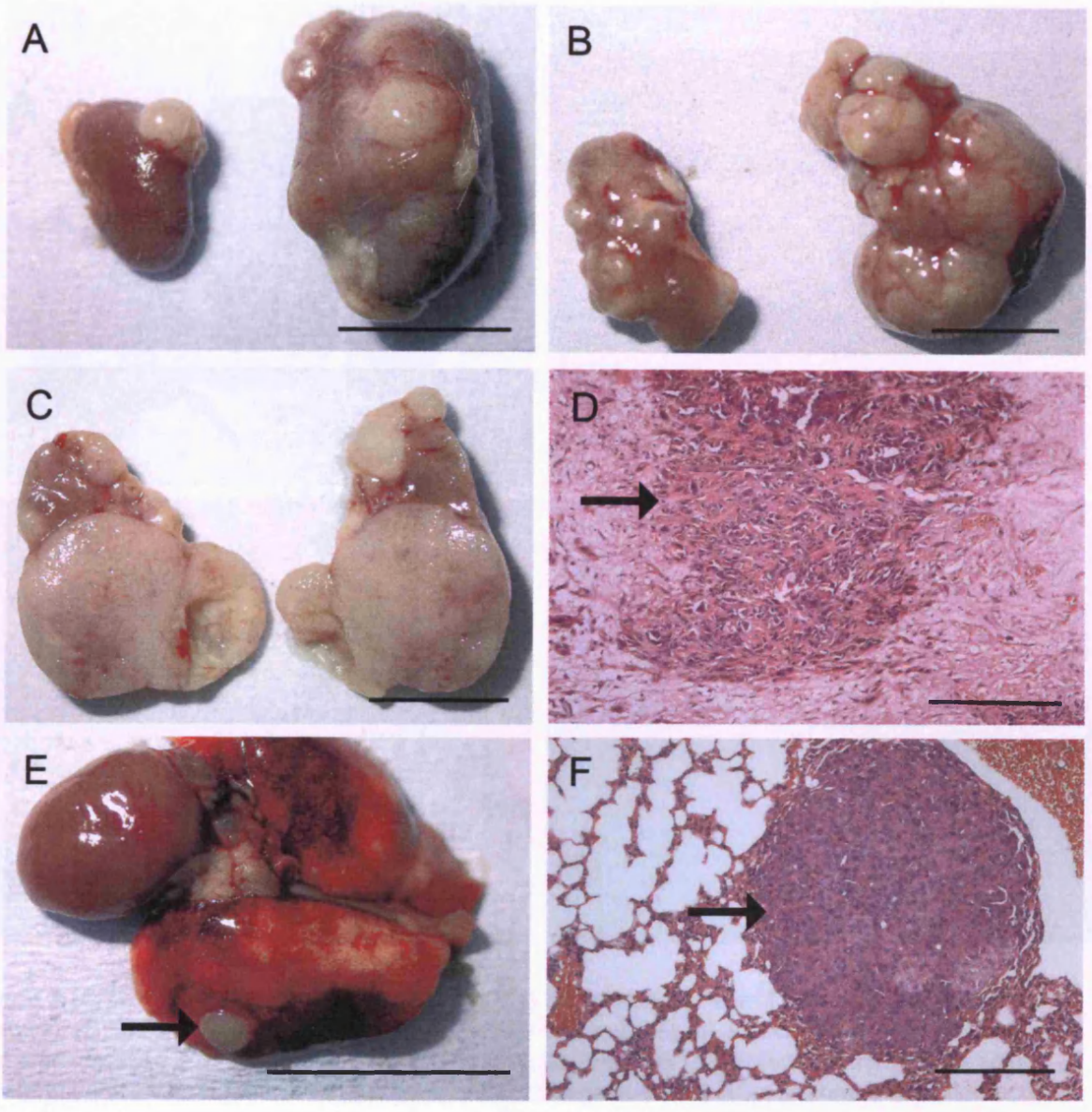

Figure 3.9: Renal cell carcinoma (RCC) in *Tsc1*$^{+/-}$ mice on a Balb/c background resulting in grossly deformed kidneys and metastases in the lungs. (A, B) Paired kidneys from 18 month old *Tsc1*$^{+/-}$ mice with RCC ≥5mm. (C) Section through a kidney displaying RCC. (D) Microscopic view of a sarcomatoid RCC with elongated sheets of spindle cells intermingled with more typical carcinomatous areas. (E) Macroscopic, and, (F) microscopic RCC metastases in the lungs (the metastatic nature of lesions was determined by the histological appearance of cells with renal tubular morphology in the lungs). Macroscopic bars are 1cm and microscopic bars are 200μm.

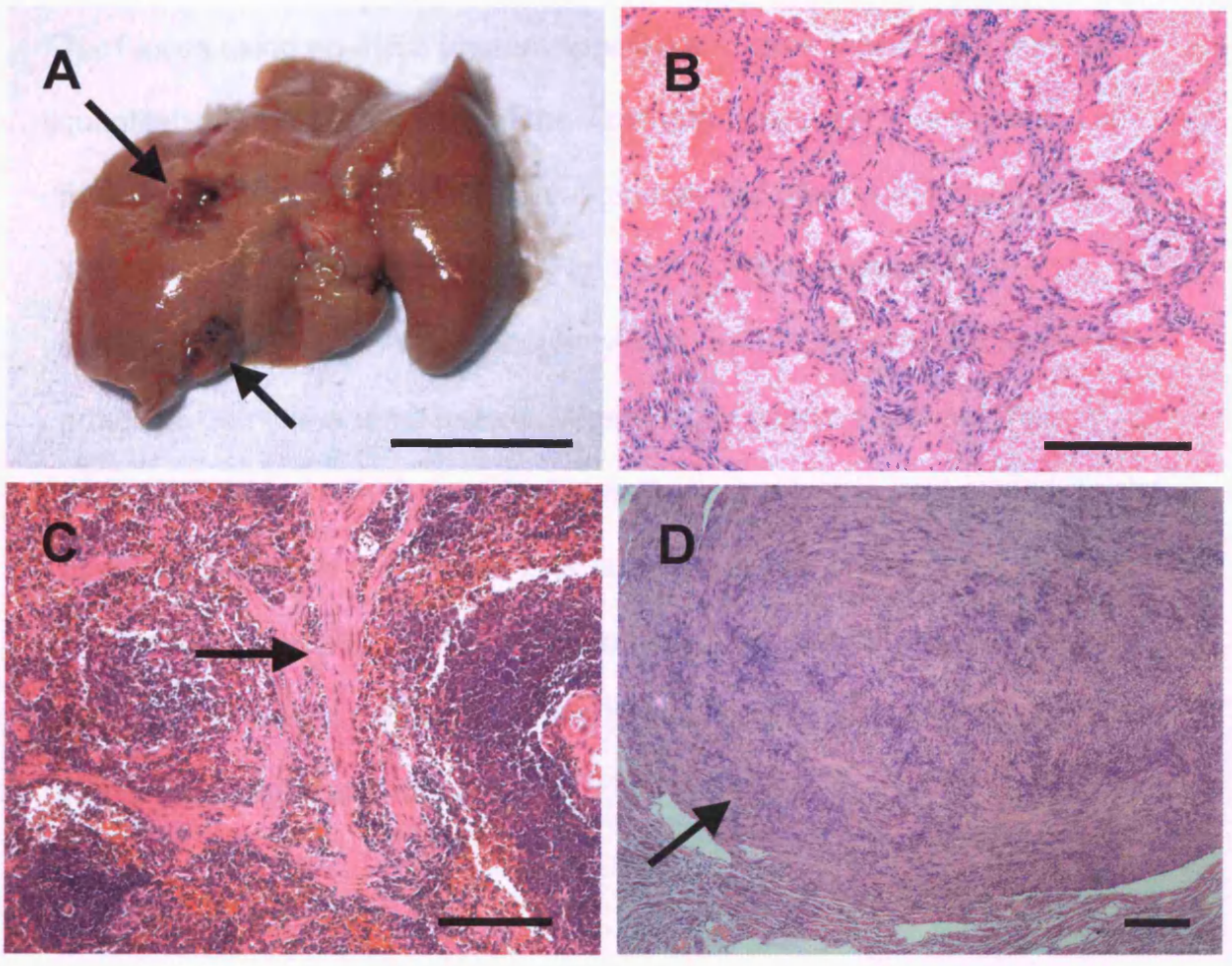

Figure 3.10: Extra renal lesions in *Tsc1*$^{+/-}$ mice. (A) Macroscopic view of liver hemangiomas (arrows) (B) Microscopic view of a liver hemangioma consisting of abnormal vascular channels and a proliferation of smooth muscle cells (C) Microscopic view of a splenic hemangioma with proliferation of smooth muscle cells neighbouring disorganised vascular channels (D) Microscopic view of a uterine leiomyoma/leiomyosarcomas. Macroscopic bars are 1cm and microscopic bars are 200μm

3.3.9 Molecular and immunological analysis of lesions

DNA was extracted from LCM kidney, liver, uterine and lung (a kidney metastasis) lesions and analysed for loss of heterozygosity (LOH) at the *Tsc1* locus using an IRES (mutant specific) and exon 8 (wild type specific) quantitative PCR assay. Loss of the *Tsc1* wild-type allele was observed in 5/12 renal lesions, 2/5 hepatic hemangiomas, 1/2 uterine lesions and 1/1 lung lesion (a kidney metastasis) (Fig. 3.11a). We investigated the expression levels of mTOR, phosphorylated (p)-mTOR and p-S6 ribosomal protein (p-S6) in the renal lesions. Western blot analysis showed that although levels of mTOR were the same in normal kidney and adjacent solid tumours, levels of p-mTOR and p-S6 were increased substantially in all lesions examined (Fig. 3.11b). Immunohistochemical analysis also showed increased expression of p-mTOR and p-S6 in renal cystadenomas as compared to adjacent normal tissue (Figs. 3.11c and d).

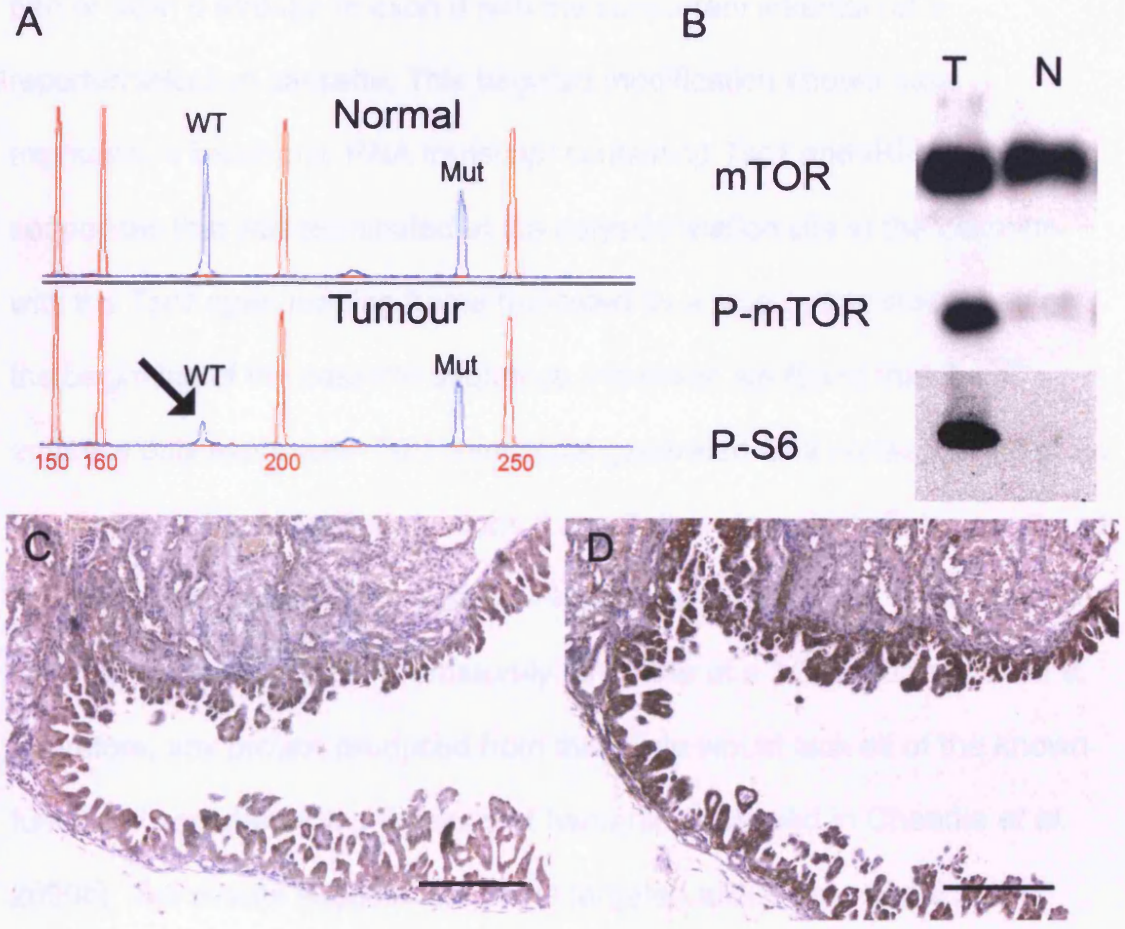

Figure 3.11: Molecular and immunological analysis of renal lesions in *Tsc1*$^{+/-}$ mice on a Balb/c background. (A) Detection of LOH in a microdissected renal tumour. Loss of the wild type *Tsc1* allele in the tumour, but not in adjacent normal tissue, is indicated by an arrow (WT – wild type allele, Mut - mutant allele). The red trace is an ABI GS500 internal size standard. (B) Western blot analysis showing relative expression levels of mTOR, phosphorylated mTOR (P-mTOR) and phosphorylated S6 ribosomal protein (P-S6) in tumour (a cystadenoma) (T) and normal (N) kidney tissue. (C,D) Immunostaining of a papillary cystadenoma using (C) an anti-Phospho-mTOR antibody, and, (D) an anti-Phospho-S6 ribosomal protein antibody. Expression of Phospho-mTOR and Phospho-S6 around the periphery of the cyst is indicated by brown staining. Microscopic bars are 200μm.

3.4 Discussion

3.4.1 Generation of *Tsc1*$^{+/-}$ mice

Mice bearing a targeted disruption of *Tsc1* were generated by deleting part of exon 6 through to exon 8 with the concurrent insertion of a reporter/selection cassette. This targeted modification should have expressed a bicistronic RNA transcript containing *Tsc1* and IRES-*lacz* sequences that was terminated at the polyadenylation site in the cassette, with the *Tsc1* open reading frame truncated by a stop codon introduced at the beginning of the cassette sequence. However, we found that *Tsc1*$^{-/-}$ embryos only expressed *Tsc1* transcripts generated as a consequence of an aberrant splicing event fusing exons 5 and 9, therefore excluding exon 6 and the IRES-*lacz* sequence. The exon 5-9 fusion alters the *Tsc1* reading frame, which is then predicted to prematurely terminate at a TGA codon in exon 9. Therefore, any protein produced from this allele would lack all of the known functional and interacting domains of hamartin (reviewed in Cheadle *et al.* 2000b). The results suggest that in the targeted allele, the exon 9 splice acceptor is utilised in preference to that of exon 6 and therefore a transcript containing the IRES-*lacz* sequence is not produced efficiently. This explains the failure to detect β-galactosidase activity in kidneys from *Tsc1*$^{+/-}$ mice.

3.4.2 *Tsc1*$^{+/-}$ mice are a valid model of hamartin deficiency

The targeted mouse strain was confirmed to be a valid model for tuberous sclerosis-1 deficiency, by several criteria: (i) *Tsc1*$^{-/-}$ embryos die *in utero* at a similar stage to other murine models of *Tsc1*-deficiency (Kobayashi *et al.* 2001, Kwiatkowski *et al.* 2002). (ii) Somatic mutation

analysis of DNA extracted from microdissected renal and extra renal lesions showed loss of the wild type *Tsc1* allele. (iii) Western blot analysis and immunostaining showed increased levels of phosphorylated mTOR and phosphorylated S6 ribosomal protein in kidney lesions (in agreement with the findings of Kwiatkowski *et al.* 2002).

3.4.3 Some *Tsc1*$^{+/-}$ mice on a C57BL/6 background die post-natally

Approximately 27% of *Tsc1*$^{+/-}$ mice on a C57BL/6 background were found to die before weaning and this mortality appeared to occur in the post-natal period, primarily 1-2 days after birth. At birth, the trans-placental nutrient supply is suddenly interrupted and neonates face severe starvation until a supply can be restored through milk nutrients. It has been shown that neonates adapt to these adverse circumstances by immediately inducing autophagy in a number of tissues (Kuma *et al.* 2004). Autophagy is the primary means for the degradation of cytoplamic constituents within lysosomes. The materials in vesicles are degraded and recycled to general nutrient stores to maintain essential cellular functions under starvation conditions (Inoki *et al.* 2005). Interestingly, it has recently been shown that autophagy is under mTOR control (Kamada *et al.* 2004). In normal growth situations, mTOR inhibits autophagy and stimulates cell proliferation. Under cellular stress mTOR becomes inactive, allowing the cell to induce autophagy, thus releasing valuable nutrients for cell survival. Therefore, some neonatal *Tsc1*$^{+/-}$ mice may be unable to effectively inhibit mTOR, leading to inability to stimulate autophagy at this critical period of starvation.

Further studies are necessary to determine if lack of autophagy is the critical factor in the death of these *Tsc1*$^{+/-}$ neonates.

3.4.4 Survival analysis

Survival analysis demonstrated that some *Tsc1*$^{+/-}$ mice on a Balb/c background died prematurely between weaning and 18 months when compared to both *Tsc1*$^{+/+}$ littermate controls ($P< 0.038$) and *Tsc1*$^{+/-}$ mice on a C3H or C57BL6 background ($P< 0.001$). Upon post mortem examination, 24% of *Tsc1*$^{+/-}$ mice on a Balb/c background and 8% of *Tsc1*$^{+/+}$ mice on a Balb/c background that had died prematurely between weaning and 18 months were shown to have atrial thrombi. Atrial thrombosis has been reported as a strain associated disease in female Balb/c mice and Balb/c crosses (Ayers and Jones 1978, Frith *et al.* 1983). In addition, factors such as sex, age, diet and pregnancy may have some role in the development of thrombi in the atria (Carlton and Engelhardt 1991). Interestingly 40% of *Tsc1*$^{+/-}$ mice on a Balb/c background that had died prematurly also had macroscopic kidney lesions. Characteristic symptoms of RCC in humans include secretion of vasoactive substances (e.g. renin) that may cause arterial hypertension, and release of erythropoietin that causes polycythemia (increased production of red blood cells). The potential extra physiological stress from renal lesions in the *Tsc1*$^{+/-}$ mice on a Balb/c background may have contributed to the increased number of thrombosis-related events.

3.4.5 Renal phenotype in *Tsc1*$^{+/-}$ mice

The *Tsc1*$^{+/-}$ mice described herein have a more severe renal phenotype as compared to the published models (Kobayashi *et al.* 2001, Kwiatkowski *et al.* 2002). By 3-6 months, 44% of the *Tsc1*$^{+/-}$ mice on a C3H background developed macroscopically visible renal lesions and 100% had microscopic lesions. In contrast, Kobayashi *et al.* (2001) failed to identify any macroscopic renal lesions in their *Tsc1*$^{+/-}$ mice by 9-12 months. Furthermore, 80% of the 15-18 month mice on a Balb/c background showed progression to RCC, which is considerably higher than described by Kwiatkowski *et al.* (2002) (up to 31% depending on the background), and in 41%, RCCs were ≥5mm which resulted in grossly deformed kidneys. Some of these carcinomas had a sarcomatoid morphology of spindle cells in whorled patterns and, unlike other *Tsc1*$^{+/-}$ mice, metastasized to the lungs. Further molecular and cellular studies are necessary to determine whether the phenotypic differences between the *Tsc1*$^{+/-}$ strain described herein and the published strains are due to the precise nature of the targeted modifications and/or to the presence or absence of modifiers in the various genetic backgrounds in which the mutated gene was studied. The *Tsc1*$^{+/-}$ mice produced by Kwiatkowski *et al.* (2002) had a targeting modification close to the 3' end of *Tsc1.* However, Immunoblot analysis indicated that no hamartin was produced from the mutant allele. The *Tsc1*$^{+/-}$ mice produced by Kobayashi *et al.* (2001) bear a similar targeting modification to the mice described herein. Therefore the phenotypic differences are likely to be due to the different genetic backgrounds rather than the nature of this targeting event. It should be noted that the *Tsc1*$^{+/-}$ mice analysed here were extensively backcrossed so that any random genetic changes introduced

during ES cell culture are likely to have been segregated from the targeted allele (Kumar et al. 2004). By contrast, the *Tsc1*$^{+/-}$ mice studied by Koybayashi *et al.* (2001) and Kwiatkowski *et al.* (2002) were F1s of mixed genetic backgrounds.

The distribution in the size of lesions (Table 3.4) and the morphological continuity between cystic, mixed, benign and malignant solid lesions (Fig.3.8) provides evidence for sequential progression from simple cyst through to solid lesions and metastasis. This progression may result from an accumulation of somatic mutations in key target genes involved in tumourigenesis. A model that already exemplifies this progressive pathway from benign lesion to carcinoma is colorectal cancer (CRC). The model has indicated that CRCs arise initially from biallelic inactivation of APC. However, Mutations in at least 4 or 5 different genes are then required for the formation of a malignant tumour (Fearon and Vogelstein 1990). Therefore the *Tsc1*$^{+/-}$ mice renal lesions may provide a powerful model to examine renal tumour progression.

Chapter 4: Induction of renal tumourigenesis with increased somatic deletions in *Tsc1*$^{+/-}$ mice

4.1 Introduction

4.1.1 Bloom's syndrome

Bloom's syndrome (BS) is a rare recessively inherited genetic disorder first described in 1954 (Bloom 1954). Only ~220 cases have been confirmed since 1975, of which many affected individuals are of Ashkenazi Jewish origin (*Blm*^{Ash}) (Hickson 2003). Patients are predisposed to cancer, particularly leukaemias, from an early age. The BS gene, *BLM*, encodes the BLM RecQ helicase homolog protein, which plays an important role in the maintenance of genomic stability in somatic cells.

4.1.2 BS manifestations

BS patients have a variable spectrum of manifestations that include growth retardation, microcephaly, immune deficiency and a characteristic high pitch voice. Skin abnormalities include hyper- and hypo-pigmented spots, and sun-sensitive telangiectatic erythema (German 1993). BS patients have an increased neoplastic risk: out of 150 patients on the Bloom's syndrome registry from 1933-1991, there were 118 instances of cancer recorded (mean age 24.4 years), of which 86 were malignant (German 1993). The cancers were characterised by multiplicity and diversity in site and type. BS cells show an elevated frequency of several types of chromosomal aberrations that include breaks, quadriradials and translocations. However, the hallmark feature of BS is an ~10-fold elevation

in the frequency of sister-chromatid exchanges (SCEs) (German 1993, Cheok *et al.* 2005). SCE arise from crossing-over of chromatid arms during homologous recombination, a ubiquitous process that exists to repair DNA double stranded breaks and replication forks (Wu and Hickson 2003). SCEs by themselves are non-mutagenic and therefore unlikely to be harmful. However, this may not hold true for aberrant recombination events such as unequal SCE that occur between homologous chromosomes or repetitive sequences at ectopic sites (Fig. 4.1). The resultant somatic deletions/duplications may contribute to the genomic instability seen in BLM cancer cells (Mankouri and Hickson 2004).

4.1.3 *BLM* gene

BLM is located on human chromosome 15q26.1 (German *et al.* 1994). It encodes a 1417 amino acid protein that belongs to a family of proteins called the RecQ helicases. The RecQ family is highly conserved in evolution from bacteria to humans. The centrally-located helicase domain that contains seven characteristic sequence motifs is particularly well conserved (Cheok *et al.* 2005). The family contains two other proteins that are defective in human disorders associated with cancer predisposition; WRN is defective in Werner's syndrome and RECQ4 is defective in Rothmund-Thomson syndrome (Rassool *et al.* 2003). Helicases are enzymes that separate the complementary strands of nucleic acid duplexes using the energy derived from ATP hydrolysis (Hickson 2003). The RecQ helicases are one family of these proteins that have the ability to recognise and unwind a wide variety of different DNA structures. The BLM gene product forms part of a muti-enzyme

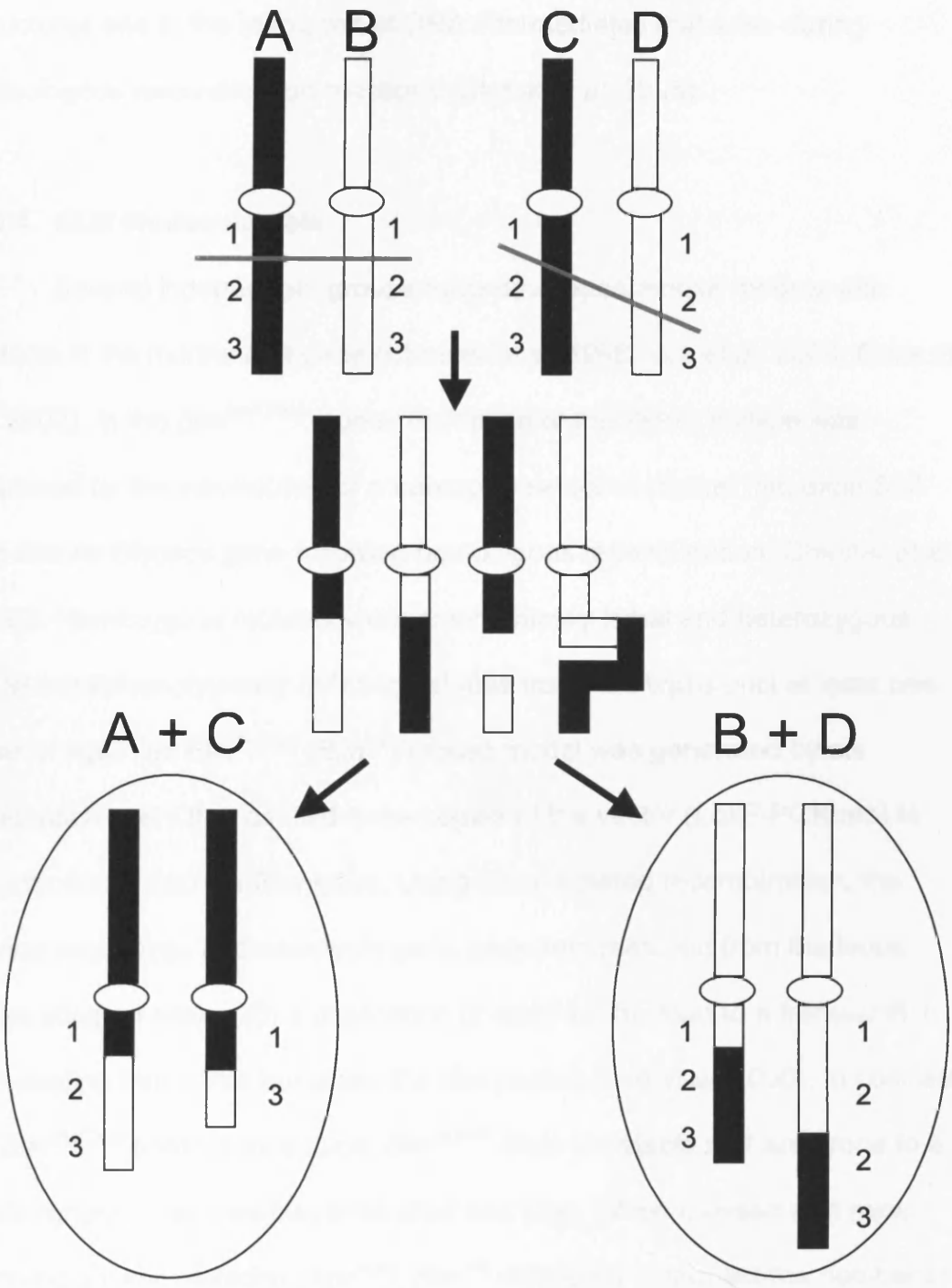

Figure 4.1: Schematic representation of theoretically possible genetic consequences of equal and unequal sister-chromatid exchange (SCE). Two homologous chromosomes are drawn with 3 lower regions denoted 1-3. In chromosomes A and B (left) SCE occurs between regions 1 and 2, and at mitosis, each daughter cell receives an identical chromosome. In chromosome C and D unequal SCE occurs between 1 and 2 (Chrm C) as well as 2 and 3 (Chrm D), and at mitosis, genetically different chromosomes will be transmitted to each daughter cell with either a segmental chromosome deletion or duplication (adapted from German 1993). Such rearrangements could be detected by dosage analysis.

complex that appears to play roles both in the disruption of alternative DNA structures and in the resolution of DNA intermediates that arise during homologous recombination reactions (Cheok *et al.* 2005).

4.1.4 BLM Mouse models

Several independent groups have developed mouse models with defects in the murine *Blm* gene (Chester *et al.* 1998, Luo *et al.* 2000, Goss *et al.* 2002). In the $Blm^{tm1Ches}$ model, disruption of the Bloom's allele was achieved by the introduction of a neomycin selection marker into exon 8 of the murine Bloom's gene following homologous recombination (Chester *et al.* 1998). Homozygous mutants were embryonically lethal and heterozygous mice were phenotypically indistinguishable from wild types until at least one year of age. The Blm^{tm3Brd} (Blm^{m3}) mouse model was generated by an integration event that caused three copies of the vector (*LoxP*-PGKneo) to be introduced into the *Blm* locus. Using Cre mediated recombination, the vector sequences and neomycin gene were then removed from the locus, generating an allele with a duplication of exon 4. This lead to a frameshift in the reading frame that truncated the *Blm* protein (Luo *et al.* 2000). In contrast to $Blm^{tm1Ches}$ homozygous mice, $Blm^{m3/m3}$ mice are viable and are prone to a wide variety of cancers that arise after one year. When crossed with mice carrying an *Apc* mutation (Apc^{min}), Blm^{m3} deficiency increased the number of intestinal tumours formed (Luo *et al.* 2000). Luo *et al.* (2000) confirmed that the major mechanism of LOH leading to the loss of the *Apc* wild type allele in the Apc^{min} Blm-deficient mice was mediated by mitotic recombination (Luo *et al.* 2000). The Blm^{m3} allele has now been shown to be a hypomorph, which

produces sufficient *Blm* protein to rescue the embryonic lethality seen in the $Blm^{tm1Ches}$ homozygous mice. Quantification of the Blm protein suggests that each Blm^{m3} allele produces 12.5% of wild type levels (McDaniel *et al.* 2003). A third bloom deficient mouse (Blm^{Cin}) was developed to mimic human Blm^{Ash}. Gene targeting was used to replace exons 10, 11 and 12 of the *Blm* allele with a hypoxantine phosphoribsyltransferase (*Hprt*) cassette (Goss *et al.* 2002). Homozygous mutants were embryonically lethal. Heterozygous mice developed lymphoma earlier than wild types in response to challenge with murine leukemia virus and they developed twice the number of intestinal tumours when crossed with mice carrying an *Apc* mutation. This data suggest that haploinsufficiency for *Blm* is associated with tumour predisposition (Goss *et al.* 2002).

4.1.5 Modulation of the somatic mutation spectra

Normally, a diverse range of mechanisms including nonsense, frameshift and deletion mutations and epigenetic silencing, are implicated in the somatic inactivation of the wild type allele of TSGs. This diversity of somatic alterations makes genetic mapping of loci involved in tumour progression problematic. Mutant mouse models can be used as powerful tools to modulate the type of somatic mutations found in TSGs. Modulation of the somatic mutation spectra has been achieved in *Msh2*-, *Msh6*- and *Msh3*-deficient mouse models that were crossed with Apc^{1638N} or Apc^{min} mice (Smits et al. 2000, Kuraguchi et al. 2001). Intestinal lesions of the *Apc*-mutant mice usually show inactivation of the wild-type *Apc* allele by complete loss of chromosome 18. However, complete loss of a chromosome does not

allow any differentiation in specific sequences. Therefore somatic mutation site cannot be analysed within the *Apc* gene (Smits et al. 2000). By crossing onto the *Msh*-deficient backgrounds LOH is reduced and somatic point mutations are increased (Smits et al. 2000, Kuraguchi et al. 2001), allowing the mapping of mutant alleles. Therefore, investigators have been able to look for the interdependence of 2 hits on the *Apc* gene. Such an interdependence has been shown in humans with FAP and sporadic colorectal tumours where mutation combination results in different growth advantages (Lamlum et al. 1999, Albuquerque et al. 2002, Cheadle et al. 2002, Sieber et al. 2006).

4.1.6 Aims

The study reported here investigated whether *Blm*$^{m3/m3}$ mice could be used to induce tumourigenesis in extra-colonic tissue by crossing with *Tsc1*$^{+/-}$ mice that are predisposed to renal cystadenomas and carcinomas (Chapter 3). We hypothesized that by crossing our *Tsc1*$^{+/-}$ mice onto a *Blm*-deficient background we would modulate the somatic mutation spectra observed at the *Tsc1* locus by increasing the frequency of large somatic deletions. If so this would provide a convenient means of directly mapping other genes involved in Tsc-associated tumourigenesis.

4.2 Methods

4.2.1 Animal care, genotyping, necropsy and pathology

Tsc1$^{+/-}$ mice on a Balbc background (N≥3) (chapter 3) were crossed with *Blm*$^{m3/m3}$ mice on a C57BL6 background (Luo et al. 2000) and *Tsc1*$^{+/-}$ *Blm*$^{+/m3}$ offspring were intercrossed to generate mice for subsequent analyses. DNA was extracted from mouse tail tips using the Qiagen QIAamp DNA mini kits and genotyping was performed as previously described (Luo *et al.* 2000, chapter 3). Necropsy analysis included macroscopic examination of the brain, heart, lungs, kidneys, liver, spleen and uterus in 20 *Tsc1*$^{+/-}$ *Blm*$^{+/m3}$ and 20 *Tsc1*$^{+/-}$ *Blm*$^{m3/m3}$ mice at 3-6 and 9-12 months. Half of each organ was fixed and processed into paraffin wax, sectioned at 4μm and stained with H&E for microscopic inspection (tissues from 10 mice per genotype were analysed microscopically at 3-6 and 9-12 months). Estimations of the average number of kidney lesions per mouse were determined as previously described (chapter 3). The other half of the organs were snap frozen in liquid nitrogen-cooled isopentane for LCM.

4.2.2 Immunohistochemistry

Immunohistochemistry using anti-phospho-S6 ribosomal protein (Ser240/244) (Cell Signalling Technologies) was performed as previously described (chapter 2 section 2.5.6).

4.2.3 Somatic mutation analysis

Snap frozen tissue was sectioned at 10μm onto PEN (PALM) membrane covered slides, and stained with toluidine blue. cystadenoma

(CA), RCC and normal tissue was microdissected (PALM LCM) and DNA extracted using the QIAamp DNA micro kits (Qiagen). LOH at the *Tsc1* locus was assayed as previously described (Chapter 3) using wild type:mutant peak ratios of <0.67 or ≥1.3 as indicative of LOH (Zhou *et al.* 2004). To search for intragenic somatic *Tsc1* mutations, the entire *Tsc1* ORF was amplified as 25 fragments and sequenced directly (Table 4.1). LOH at the *Blm* locus was assayed by amplifying and directly sequencing the region encompassing the variant 4109-152 G>A, located in intron 18 of the *Blm* gene, using the primers rs8248591/2F 5'–ACAGTTCTGAGAGGGGCTCA-3' and rs8248591/2R 5'–CCTAGCTTTCCACAGGCACT-3'. LOH of the *Blm* WT allele was determined by visual inspection of the 4109-152 G>A variant on the sequencing chromatograms by two independent investigators.

4.2.4 Simple sequence length polymorphism (SSLP) markers flanking *Tsc1*

Six highly polymorphic SSLP markers flanking *Tsc1* (*D2Mit484*, *D2Mit451*, *D2Mit63*, *D2Mit37*, *D2Mit433* and *D2Mit431,* Table 4.2) were analysed in 18 and 14 tumours with LOH of the *Tsc1* WT allele from $Tsc1^{+/-}$ $Blm^{m3/m3}$ and $Tsc1^{+/-}$ $Blm^{+/+}$ mice, respectively. Amplification of DNA from tumours was performed as previously described (chapter 3) using a 25 cycle PCR reaction. 2μl of PCR products were mixed with an ABI GS500 internal size standard and formamide loading buffer, and run on an ABI3100 genetic analyser. Results were analysed using Genescan v.3.7 software and LOH determined as previously described (Zhou *et al.* 2004).

Table 4.1: Primer sequences, product sizes and amplification temperatures used to screen for mutations in the *Tsc1* ORF

Primer name/exon	Primer sequence (5'-3')	Product size (bp)	Annealing temp. (°C)
mTsc1ex3F	GCTTGTTTTCCTGCAGGTTT	395	54
mTsc1ex3R	TCCAGGCTAATTTGGAATGC		
mTsc1ex4F	GACAGCCACTGAGGGAAAAG	242	54
mTsc1ex4R	ACTATGGATGAGCTGCTGTGG		
mTsc1ex5F	AGGAAGACTTGAGGCCTTGG	350	54
mTsc1ex5R	GAGACCCACATGGTCGAAAG		
mTsc1ex6F	TTTCAGTGCTGTCCCTCAAAT	350	54
mTsc1ex6R	CTTCCTTCCCGCATACACAT		
mTsc1ex7F	AGAGCTTCCGAGAGAAAGCA	427	54
mTsc1ex7R	GACTCGGACTCAGAAAGACGA		
mTsc1ex8F	TGCTGCATTCCTTTTTGTTG	362	54
mTsc1ex8R	TTCCAGGCACAGGCAGTAG		
mTsc1ex9F	TGCCACTGAGCTAGCCTCTT	373	54
mTsc1ex9R	CAGTTACGCTTGAAGGACAGAA		
mTsc1ex10F	AGCCAACGGTTTTAAGCAGA	266	54
mTsc1ex10R	GAGGTGAAGGCATGCTGAGT		
mTsc1ex11F	GCAACTTGTCTCGCGGTAA	465	54
mTsc1ex11R	CCAAGCAATCAAGTCCACCT		
mTsc1ex12F	CTGAGGCTGATCTGGATTCTG	388	54
mTsc1ex12R	CCTGGTCTGTACCGTGACCT		
mTsc1ex13F	CTCTGCGACACAGAACATGC	340	54

mTsc1ex13R	TCTCAGGCCGAAATGTCTCT		
mTsc1ex14F	TGGTCCCAACTTTCTCTGCT	366	54
mTsc1ex14R	TTGGCATTCCTTTCCCTGTA		
mTsc1ex15aF	ACGAACGTTCCCTGTAGTGC	406	54
mTsc1ex15aR	AAGGGCTGGGAGTGAGGATA		
mTsc1ex15bF	CTCCCATAGACCCACCCTCT	434	54
mTsc1ex15bR	CTGCCTTGGGTATAGGTGGA		
mTsc1ex16F	CGGCAGGAGACTCTCAAAAC	211	54
mTsc1ex16R	AAGCCAAAGAAGTCCCTTCC		
mTsc1ex17F	CCTTCCAAGACCCCAAGAAT	398	54
mTsc1ex17R	CCATGCACATCTGTTCCTCA		
mTsc1ex18F	TGTGCTAATGTGCAGTTTGGA	484	54
mTsc1ex18R	TTCTGTCCTCGGATCCATTC		
mTsc1ex19F	GGATCAGGTCTTTGGGAAGG	440	54
mTsc1ex19R	ACTCGAACCAACGTCTCCAG		
mTsc1ex20F	TGGACTCAGTGGGAATGGTT	392	56
mTsc1ex20R	CATGTAGCCTGGACCTCTGC		
mTsc1ex21F	GCCAGGAAGTCCTCCTCACT	404	56
mTsc1ex21R	GCCTCATACCTGCTCTCTGC		
mTsc1ex22F	TTCTGGCCAAGAAAGACCAC	414	54
mTsc1ex22R	GGCAGACTGAGTACAGCCAAC		
mTsc1ex23aF	GTTTCAGGCAGGCACATACA	447	54
mTsc1ex23aR	CCAGGAAGCTTTTGGAACTG		
mTsc1ex23bF	AGCAGCATCCCCACCACT	384	54
mTsc1ex23bR	CTGCTCAGACCCTGGAAACA		

4.2.5 Statistical analysis

Comparisons of numbers of mice were performed using the Chi-square test. Lesion counts per mouse were compared using the Mann-Whitney confidence interval tests and frequencies of LOH were compared using Fisher's exact test.

Table 4.2: Primer sequences, chromosomal positions, product sizes and amplification temperatures used to analyse SSLP markers flanking *Tsc1*

Primer name/exon	Primer sequence (5'-3')	cM	Size (bp)	Temp. (°C)
D2Mit484F	AGGAGTGGTAAGCATGGTGG	57.8	112	54
D2Mit484R	TGCTGCAGGGAGGTAACAG			
D2Mit451F	CATTAGATAGACTGGGCAAGGG	75.6	116	54
D2Mit451R	TCCTCCCTCCAAACCCTC			
D2Mit63F	GCAGTCTACCAGGAGCAACC	56.69	209	54
D2Mit63R	TGGATGTAGGCATGTGCCT			
D2Mit37F	TGTGCAAGCCAGAAAAGTTG	46.66	141	54
D2Mit37R	GAAGGGGATTGTAAATTGGTACC			
D2Mit433F	CTGTCTATCCTCATATTAGGAAATGG	33.18	173	54
D2Mit433R	AACTTTTAAAGACCATTTTATAGCCTT			
D2Mit431F	AAATAGTCTGTTCTGACTCCAGGG	23.12	98	54
D2Mit431R	GCCAGGCAGTGGTAAAAAGA			
D2Mit484F	AGGAGTGGTAAGCATGGTGG	57.8	112	54
D2Mit484R	TGCTGCAGGGAGGTAACAG			

Primer sequences were obtained from the Mouse Microsatellite Data Base of Japan (MMDBJ) (http://www.shigen.nig.ac.jp/mouse/mmdbj/top.jsp).

4.3 Results

4.3.1 *Blm*-deficiency has no effect on *Tsc1*$^{+/-}$ mortality

Tsc1$^{+/-}$ *Blm*$^{+/m3}$ mice were intercrossed. Genotyping showed that out of the 360 offspring that survived until weaning, 204 were *Tsc1*$^{+/-}$ and 134 were wild type (22 failed to be genotyped). Indicating that all *Tsc1*$^{-/-}$ and ~24% of *Tsc1*$^{+/-}$ mice died before weaning (P=0.016). Genotyping of the *Blm* allele in *Tsc1*$^{+/-}$ animals showed no deviation from the expected 1:2:1 ratio (42 *Blm*$^{+/+}$, 90 *Blm*$^{+/m3}$, 52 *Blm*$^{m3/m3}$ mice (20 failed to be genotyped)).

4.3.2 Renal tumour analysis in *Tsc1*$^{+/-}$ mice on a *Blm*-deficient background

The kidneys of mice at 3-6 months were examined by macroscopic inspection and microscopic analysis of five sections ~200μm apart. A significant increase in renal tumours in *Tsc1*$^{+/-}$ mice on a *Blm*-deficient background was observed; 70% (14/20) of *Tsc1*$^{+/-}$ *Blm*$^{m3/m3}$ mice developed macroscopically visible renal lesions (average 4.2 lesions per mouse), compared to only 15% (3/20) of *Tsc1*$^{+/-}$ *Blm*$^{+/m3}$ mice (average 0.2 lesions per mouse, P=0.0003) (Table 4.3, Fig. 4.2). At a microscopic level, *Tsc1*$^{+/-}$ *Blm*$^{m3/m3}$ mice had an average of 23.2 lesions per mouse compared to 5.4 for *Tsc1*$^{+/-}$ *Blm*$^{+/m3}$ mice (P=0.0203). Renal lesions from *Tsc1*$^{+/-}$ *Blm*$^{m3/m3}$ mice stained positively with anti-phospho-S6 ribosomal protein (Ser 240/244) (Fig. 4.2).

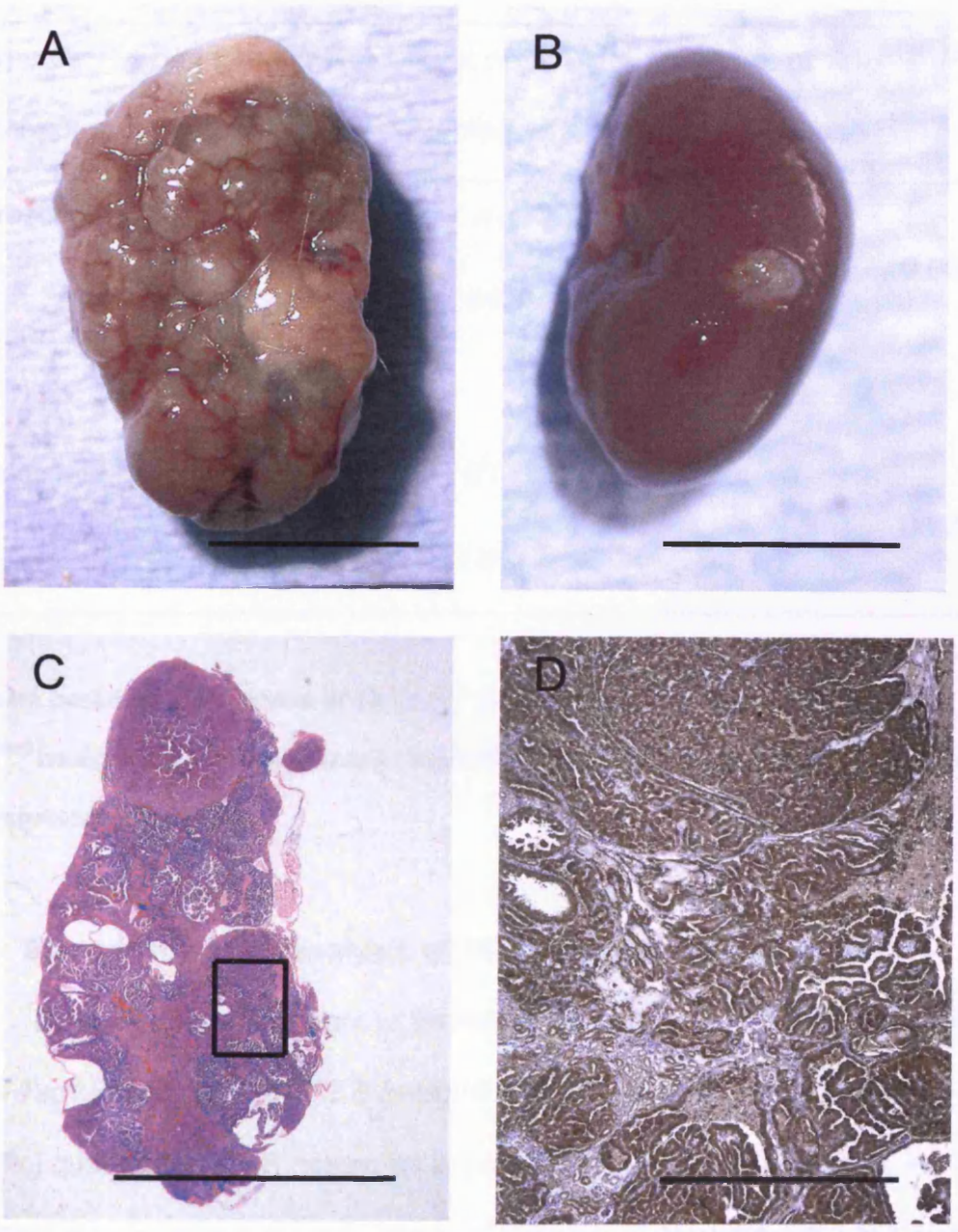

Figure 4.2: Renal cystadenomas in *Tsc1*$^{+/-}$ mice on a *Blm*-deficient background. (A) An example of a kidney from a *Tsc1*$^{+/-}$ *Blm*$^{m3/m3}$ mouse at 3-6 months showing significantly more macroscopically visible lesions compared to (B) a kidney from a *Tsc1*$^{+/-}$ *Blm*$^{+/m3}$ mouse. (C,D) Microscopic view of cystadenomas from *Tsc1*$^{+/-}$ *Blm*$^{m3/m3}$ mice stained with H&E (C) and immunostained with an anti-phospho-S6 ribosomal protein (p-S6) antibody (D) (region shown in D is a magnified view of the region boxed in C). Lesions on a *Blm*-deficient background showed increased expression of p-S6 (indicated by brown staining) suggesting that these lesions develop through the normal pathway of Tsc-associated tumourigenesis. Scale bars are 5mm (in A, B and C) and 1mm (in D).

Table 4.3: Frequency of renal lesions in 3-6 month old *Tsc1*$^{+/-}$ mice on *Blm*$^{+/m3}$ and *Blm*$^{m3/m3}$ backgrounds

Type of analysis	*Blm* genotype of *Tsc1*$^{+/-}$ mice	Total no. of tumours	Mean no. of tumours per mouse	*P*
Macroscopic	*+/m3*	4	0.2	0.0003
	m3/m3	84	4.2	
Microscopic	*+/m3*	27	5.4	0.0203
	m3/m3	116	23.2	

Numbers based on the analysis of 20 *Tsc1*$^{+/-}$ mice on *Blm*$^{+/m3}$ background and 20 on a *Blm*$^{m3/m3}$ background for macroscopic inspection and 10 *Tsc1*$^{+/-}$ mice in each category for microscopic inspection.

4.3.3 Somatic mutation analysis of *Tsc1* and mechanism of LOH

DNA was extracted from LCM kidney lesions and analysed for LOH at the *Tsc1* locus using an IRES (mutant specific) and exon 8 (wild type specific) quantitative PCR assay, as previously described (Chapter 3). We observed significantly increased levels of somatic LOH of the *Tsc1* WT allele in renal lesions from *Tsc1*$^{+/-}$ *Blm*$^{m3/m3}$ mice (53/61, 87%) as compared to renal lesions from *Tsc1*$^{+/-}$ *Blm*$^{+/+}$ mice (61/118, 52%) (*P*<0.0001) (Fig. 4.3). To determine the mechanism of increased somatic LOH in these lesions, we analysed the extent of the LOH events using 6 SSLP markers on mouse chromosome 2, on which *Tsc1* resides. Two out of 18 tumours showing loss

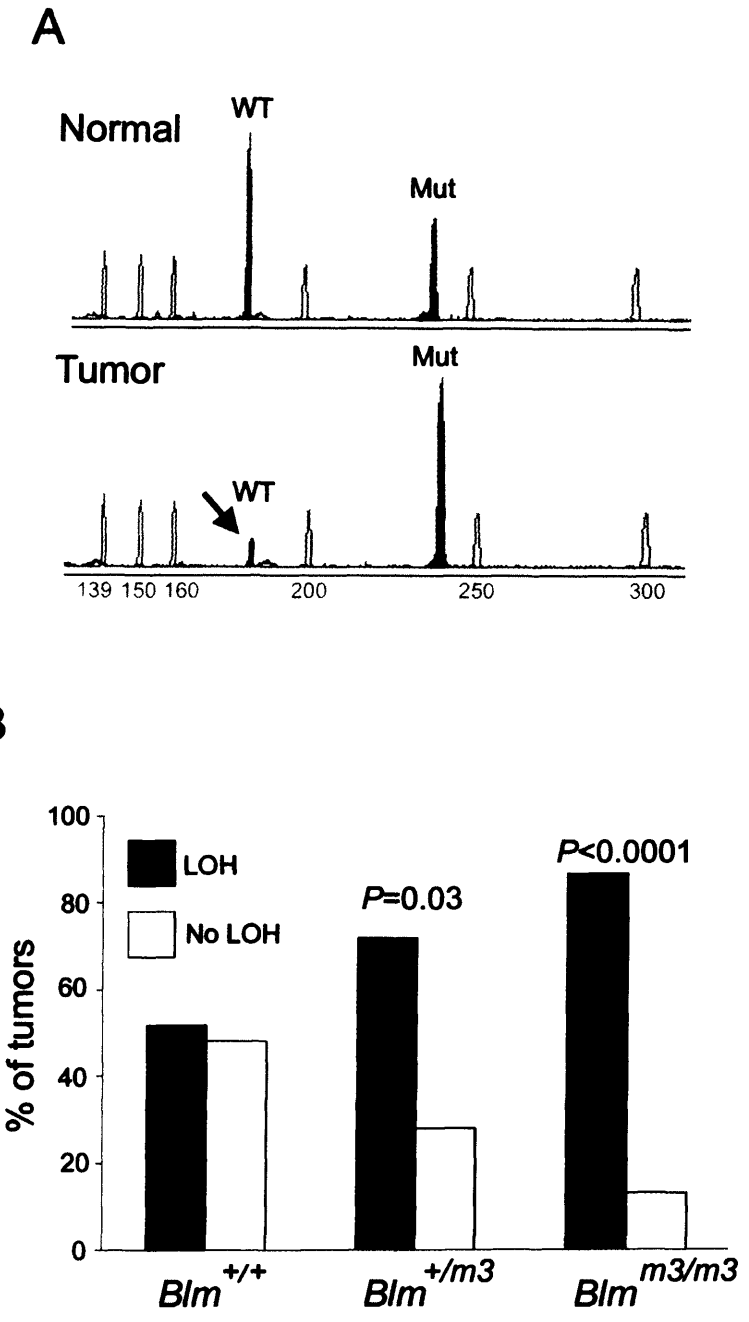

Figure 4.3: LOH analysis of renal lesions from *Tsc1*$^{+/-}$ mice on *Blm*-proficient (*Blm*$^{+/+}$), haploinsufficient (*Blm*$^{+/m3}$) and deficient (*Blm*$^{m3/m3}$) backgrounds. (A) Example of LOH in a microdissected renal tumour. Loss of the wild type *Tsc1* allele in the tumour (lower panel), but not in adjacent normal tissue (upper panel), is indicated by an arrow (WT – wild type allele, Mut - mutant allele). The unshaded trace is an ABI GS500 internal size standard. (B) Graph showing the percentage of lesions with LOH versus those without LOH, from *Tsc1*$^{+/-}$ *Blm*$^{+/+}$, *Tsc1*$^{+/-}$ *Blm*$^{+/m3}$ and *Tsc1*$^{+/-}$ *Blm*$^{m3/m3}$ mice. *P* values reflect differences in the frequency of LOH in *Tsc1*$^{+/-}$ *Blm*$^{+/m3}$ and *Tsc1*$^{+/-}$ *Blm*$^{m3/m3}$ mice as compared to *Tsc1*$^{+/-}$ *Blm*$^{+/+}$ mice.

of the *Tsc1* WT allele from *Tsc1*$^{+/-}$ *Blm*$^{m3/m3}$ mice remained heterozygous at the marker *D2Mit431* located ~5cM upstream of *Tsc1* (Fig. 4.4), whereas no tumours with loss of the *Tsc1* WT allele from *Tsc1*$^{+/-}$ *Blm*$^{+/+}$ mice retained heterozygosity at any of the markers tested. Intragenic somatic *Tsc1* mutations were sought in DNA from the eight tumours from *Tsc1*$^{+/-}$ *Blm*$^{m3/m3}$ mice that retained the *Tsc1* WT allele, by direct sequence analysis of the entire *Tsc1* ORF. High quality sequencing for ≥89% of the *Tsc1* ORF was generated for each tumour and identified a single intragenic somatic mutation, characterised as a 2bp deletion in exon 22 (*Tsc1* del 2872-2873) (Fig. 4.5).

4.3.4 *Tsc1*$^{+/-}$ *Blm*$^{+/m3}$ mice do not show increased tumour burden?

We did not observe significantly more renal lesions in *Tsc1*$^{+/-}$ *Blm*$^{+/m3}$ mice at 3-6 months when compared to *Tsc1*$^{+/-}$ *Blm*$^{+/+}$ mice that had previously been backcrossed (N>3) onto two different backgrounds (Balb/c and C57BL6) (chapter 3). However, we did observe significantly increased levels of somatic LOH of the *Tsc1* WT allele in renal lesions from *Tsc1*$^{+/-}$ *Blm*$^{+/m3}$ mice (23/32, 71%) as compared to *Tsc1*$^{+/-}$ *Blm*$^{+/+}$ mice (61/118, 52%)(P=0.03). To determine whether tumours from *Tsc1*$^{+/-}$ *Blm*$^{+/m3}$ mice had lost the *Blm* WT allele, we analysed of polymorphism 4109-152 G>A which lies within intron 18 of the *Blm* gene. Nineteen out of 20 (95%) renal lesions from *Tsc1*$^{+/-}$ *Blm*$^{+/m3}$ mice that had lost the *Tsc1* WT allele and were informative for this marker, retained the *Blm* WT allele, indicating that the increased somatic LOH at the *Tsc1* locus in these mice was mediated by *Blm* haploinsufficiency.

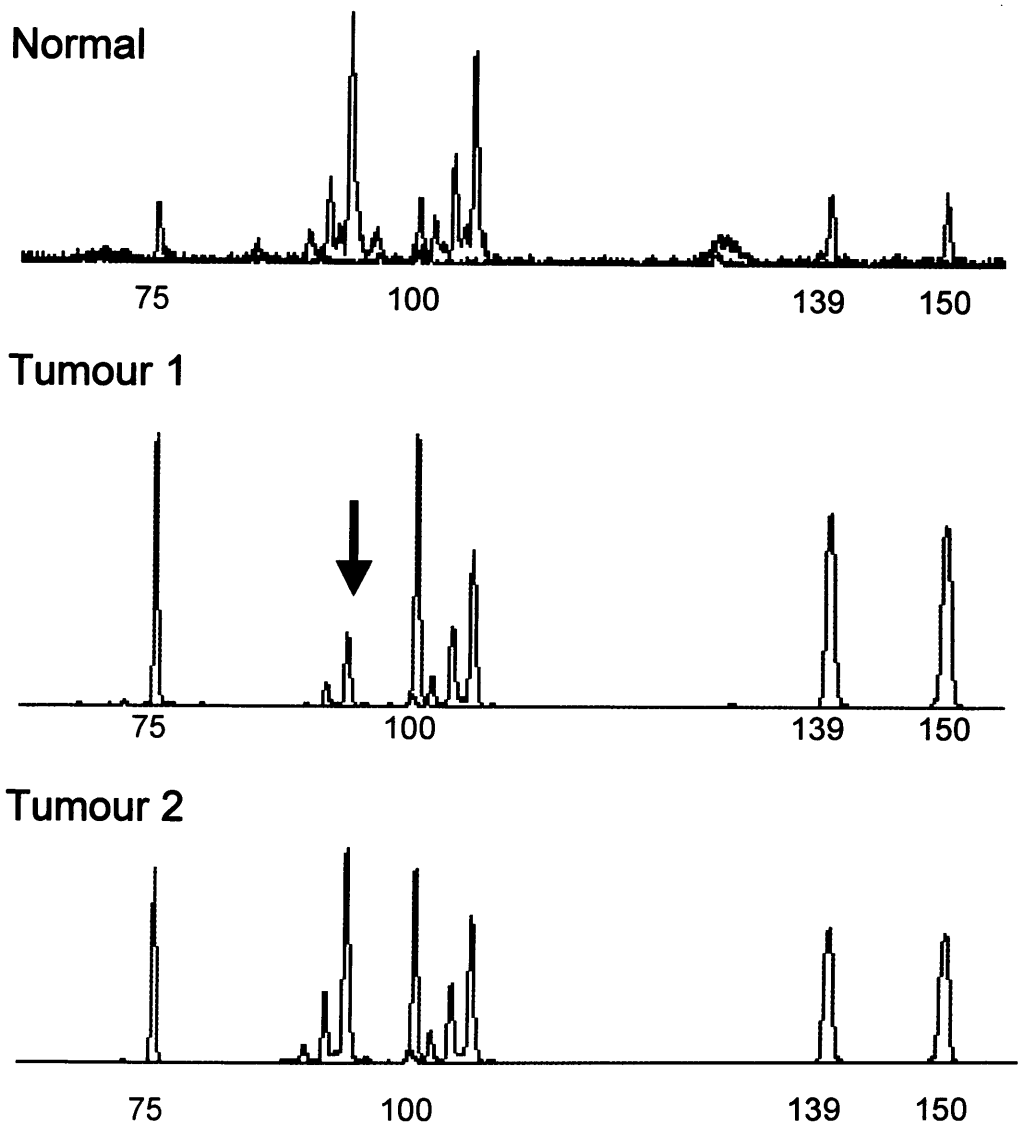

Figure 4.4: Analysis of the extent of LOH on mouse chromosome 2 in *Tsc1*$^{+/-}$ *Blm*$^{m3/m3}$ mice advanced lesions. Lesions had known LOH at *Tsc1* and were heterozygous at the SSLP marker D2Mit431. Loss of the wild type D2Mit431 allele in tumour 1, is indicated by an arrow (middle panel), but is not in adjacent normal tissue (upper panel). Tumour 2 (lower panel) has no LOH of the wild type D2Mit431 allele. This result indicates the lesion retained heterzygosity of the chromosomal region immediately surrounding the LOH at the *Tsc1* locus, suggesting that the LOH of *Tsc1* was mediated by mitotic recombination. Stutter peaks can be observed which occur during amplification of microsatellite loci (they are thought to be caused by polymerase slippage during elongation).

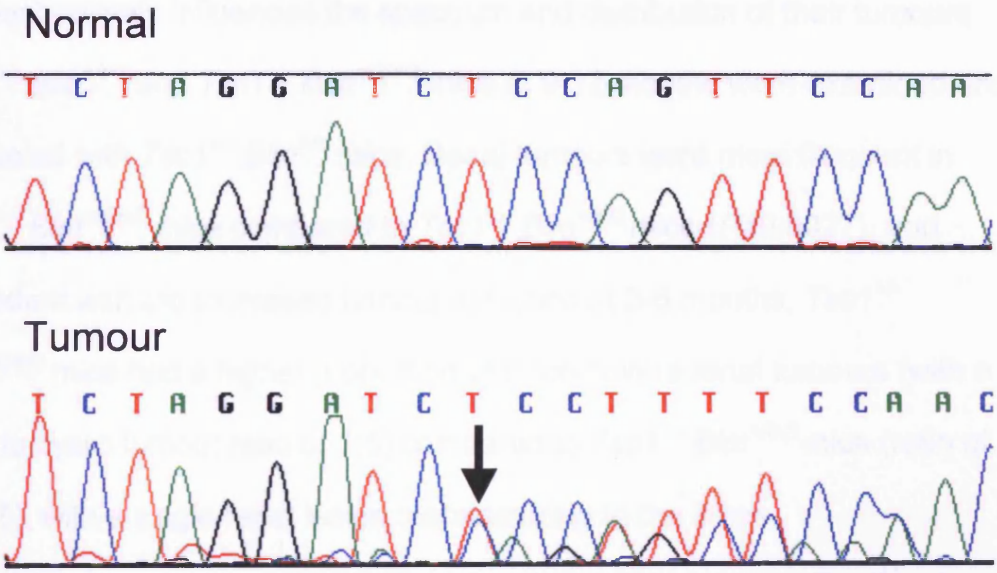

Figure 4.5: An example of an intragenic frame shift mutation in a microdissected CA from a *Tsc1*$^{+/-}$ *Blm*$^{-/-}$ mouse. A 2 base pair deletion in exon 22 (*Tsc1* del 2872-2873) in the tumour (lower panel), but not in adjacent normal tissue (upper panel), is indicated by an arrow.

4.3.5 The nature of the second hit does not influence the spectrum and distribution of *Tsc*-associated lesions

To study whether the increased frequency of LOH at *Tsc1* in the *Blm*-deficient animals influenced the spectrum and distribution of their tumours $Tsc1^{+/-}$ $Blm^{+/m3}$ and $Tsc1^{+/-}$ $Blm^{m3/m3}$ mice at 9-12 months were examined and compared with $Tsc1^{+/-}$ $Blm^{+/+}$ mice. Renal tumours were more frequent in $Tsc1^{+/-}$ $Blm^{m3/m3}$ mice compared to $Tsc1^{+/-}$ $Blm^{+/m3}$ mice (P=0.0027), and consistent with the increased tumour induction at 3-6 months, $Tsc1^{+/-}$ $Blm^{m3/m3}$ mice had a higher proportion of more severe renal tumours (with a solid to cystic tumour ratio of 1:5) compared to $Tsc1^{+/-}$ $Blm^{+/m3}$ mice (ratio of 1:11.5), with a single renal lesion metastasizing to the lungs.

The spectrum and distribution of extra-renal tumours in $Tsc1^{+/-}$ mice on $Blm^{+/m3}$ or $Blm^{m3/m3}$ backgrounds was not significantly different to $Tsc1^{+/-}$ mice on a $Blm^{+/+}$ background – only an isolated liver hemangioma was observed in a single $Tsc1^{+/-}$ $Blm^{m3/m3}$ mouse and no other lesions were seen after macro and microscopic examination of the brain, heart, lungs, spleen and uterus.

4.4 Discussion

4.4.1 Exploiting the power of the *Blm*-deficient model

N-ethyl-N-nitrosourea (ENU) has been used in whole animal mutagenesis systems to discover novel alleles for studying human disease in mice (Hrabe de Angelis and Balling 1998). However, despite rewarding results these screens are costly and time consuming (Chen et al. 2000). Homozygous mutations in cultured ES cells provide both a source of cells that can generate mice for *in vivo* studies and an *in vitro* model for understanding disease. Therefore producing a system that creates a genome wide library of homozygous mutant ES cells will prove invaluable. Recently, several investigators have exploited the high rate of mitotic recombination in Blm-deficient ES cells to allow these powerful recessive genetic screens to be carried out (Guo et al. 2004, Yusa et al. 2004). Guo et al. (2004) and Yusa et al. (2004) used ES cells with the *Blm* allele under conditional control of tetracycline (Blm^{tet}). Consequently transient inactivation of the Blm protein can be produced using doxycycline, minimising changes to the ES cell phenotype. Transient loss of Blm caused an 18-27-fold increase in the rate of bi-allelic mutations (Guo et al. 2004, Yusa et al. 2004), and allowed the identification of the novel MMR gene *Dnmt1* (Guo et al. 2004).

The high rate of mitotic recombination induced by *Blm* deficiency has also been used *in vivo*. Luo *et al.* (2000) crossed Apc^{min} mice with mice on a Blm deficient background. $Apc^{min/+}$ $Blm^{m3/m3}$ mice developed an average of 80 more polyps (larger than 1mm) than $Apc^{min/+}$ $Blm^{m3/+}$ mice. In this study we have also exploited the high rate of mitotic recombination in Blm-deficient mice. We investigate whether $Blm^{m3/m3}$ mice could induce tumourigenesis in

extra-colonic tissue by crossing with *Tsc1*$^{+/-}$ mice that are predisposed to renal cystadenomas and carcinomas. We show that *Tsc1*$^{+/-}$ mice on a *Blm*-deficient background have a significantly increased number of renal lesions. In addition, we show that renal lesions from *Tsc1*$^{+/-}$ *Blm*$^{m3/m3}$ mice stained positively with anti-phospho-S6 ribosomal protein (Fig. 4.2). Together with the investigations by Luo et al. (2000), this study shows the value of the Blm-deficient mice in inducing lesions in cancer prone models of disease. Furthermore, *Tsc1*$^{+/-}$ *Blm*$^{m3/m3}$ lesions seem to develop through the normal pathway of Tsc-associated tumourigenesis.

4.4.2 Increased levels of somatic LOH mediated by mitotic recombination

It has been hypothesised that the underlying mechanism leading to cancer predisposition in Bloom's syndrome is an increase in LOH resultant from uneven SCEs (Mankouri and Hickson 2004). Luo et al. (2000) hypothesised that elevated recombination processes in the intestine of *Apc*$^{min/+}$ *Blm*$^{m3/m3}$ mice leads to an increase in LOH, therefore elevating the incidence in tumours. However, because intestinal lesions of the *Apc*-mutant mice normally show inactivation of the wild-type *Apc* allele by complete loss of chromosome 18 (Smits et al. 2000) studying changes in LOH was not possible. In our study we were able to show significantly increased levels of somatic LOH of the *Tsc1* wild type allele in renal lesions from *Tsc1*$^{+/-}$ *Blm*$^{m3/m3}$ mice (87%) as compared to renal lesions from *Tsc1*$^{+/-}$ *Blm*$^{+/+}$ mice (52%) (P<0.0001). We have therefore provided evidence for the first time that increased LOH is the major mechanism of somatic mutagenesis in *Blm*-

deficient mice. Furthermore, analysis of the extent of the LOH events using 6 SSLP markers on mouse chromosome 2 suggested that the LOH on a *Blm*-deficient background was mediated by mitotic recombination, in agreement with Luo *et al.* (2000).

Intragenic mutation analysis of the *Tsc1* ORF in eight tumours from $Tsc1^{+/-}$ $Blm^{m3/m3}$ mice that retained the *Tsc1* wild type allele, identified a single intragenic somatic mutation. Therefore, 11% of advanced tumours from $Tsc1^{+/-}$ $Blm^{m3/m3}$ mice have no detected LOH or coding region variations. Since these animals are on a background with increased LOH, these *Tsc1*- mutation negative lesions may have large deletions elsewhere in the genome. Deletions may be affecting the promoter region of the *Tsc1* gene or genes that regulate the expression of the *Tsc1* transcript. Further studies are necessary to verify these deletions

4.4.3 *Blm* haploinsufficiency

Goss *et al.* (2002) showed that mice heterozygous for a targeted null mutation of *Blm* developed lymphoma earlier than wild-type littermates when challenged with murine leukemia virus and developed twice the number of intestinal tumours when crossed with $Apc^{+/Min}$ mice. Furthermore, Gruber *et al.* (2002) demonstrated that carriers of a BLM mutation have more than a twofold-increased risk for colorectal cancer. However, we did not observe significantly more renal lesions in $Tsc1^{+/-}$ $Blm^{+/m3}$ mice at 3-6 months when compared to $Tsc1^{+/-}$ $Blm^{+/+}$, although, we did observe significantly increased levels of somatic LOH of the *Tsc1* wild type allele in renal lesions from $Tsc1^{+/-}$ $Blm^{+/m3}$ mice (P=0.03). McDaniel *et al.* (2003) recently showed that the Blm^{m3}

allele is in fact hypomorphic and expresses a low level of normal Blm protein. This may explain the failure to find significantly increased tumour burden in *Tsc1*$^{+/-}$ *Blm*$^{+/m3}$ mice. However, our results indicate that the previously reported tumour predisposition associated with *Blm* haploinsufficiency (Goss *et al.* 2002, Gruber *et al.* 2002) may be mediated by increased somatic LOH.

4.4.4 The nature of the 2nd hit does not affect the spectrum and distribution of extra-renal lesions in *Tsc1*$^{+/-}$ mice

To date, investigators have induced renal lesions in *Tsc1*$^{+/-}$ mice (Kobayashi *et al.* 2001) using ENU, which causes a high frequency of somatic point mutations on the *Tsc1* wild type allele. These animals do not appear to develop any unusual extra-renal tumours. We sought lesions in *Tsc1*$^{+/-}$ mice on *Blm*$^{+/m3}$ or *Blm*$^{m3/m3}$ background to investigate if nature of the 2nd hit (large deletions) influences the spectrum and distribution of extra renal lesions. *Tsc1*$^{+/-}$ mice on the *Blm*$^{+/m3}$ or *Blm*$^{m3/m3}$ backgrounds did not appear to develop any unusual extra-renal tumours. Lesions have also been induced in *Apc*^{min} mice by loss of the MMR genes *Msh*3, *Msh6* and *Msh2* (Smits et al. 2000, Kuraguchi et al. 2001). *Apc*^{min} mice are prone to intestinal lesions that normally occur because of large deletion events inactivating the *Apc* wild type allele. Loss of the MMR genes in *Apc*^{min} mice increased the frequency of somatic point mutations on the wild type *Apc* allele (Smits et al. 2000, Kuraguchi et al. 2001). Consistent with our studies, there was no reported unusual extra-colonic tumours as a result of different 2nd hits in the *Apc* mutant mice. Together, these data indicate that the nature of the 2nd hit does

not affect the spectrum and distribution of lesions in either of the TSG-deficient mouse models.

4.4.5 Conclusion

This study confirms the utility the *Blm*$^{m3/m3}$ mouse for inducing LOH by mitotic recombination. It also confirms utility of the *Blm*$^{m3/m3}$ mouse for inducing tumourigenesis in cancer prone mouse models in agreement with Luo et al. (2000). The high levels of LOH in the resultant tumours (and consequently low level of intragenic mutations) will help facilitate the mapping of TSG loci that may play a role in tumour progression.

Chapter 5: *Tsc1*-haploinsufficiency is sufficient for renal cyst formation in *Tsc1*$^{+/-}$ mice

5.1 Introduction

Several studies have identified somatic mutations in the wild type *TSC1* or *TSC2* alleles (so called '2nd hits') in TSC-associated renal angiomyolipomas (Niida et al. 2001), in accordance with Knudson's 'two-hit' hypothesis of tumourigenesis (Knudson 1971). However, somatic mutations appear to be very uncommon in the majority of TSC-associated brain lesions (Niida et al. 2001), although physiologically inappropriate phosphorylation tuberin may act as a 2nd hit in some of these (Han et al. 2004).

In studies using the Eker rat, somatic LOH at the *Tsc2* locus was found in only 21% (4/19) of single altered renal tubules (Kubo et al. 1995), raising the possibility that although 2-hits are present in some early lesions, haploinsufficiency for *Tsc2* may be sufficient for their initiation. Here, we investigated the role of *Tsc1* haploinsufficiency in Tsc-associated renal tumourigenesis by examining cysts, cystadenomas (CAs) and RCCs from *Tsc1*$^{+/-}$ and *Tsc1*$^{+/-}$ *Blm*$^{-/-}$ (Bloom-deficient) mice using a combination of complementary mutation screening strategies and IHC.

5.2 Materials and methods

5.2.1 Animal care, genotyping, necropsy and pathology

All procedures with animals were carried out in accordance with Home Office guidelines. Kidneys were collected from *Tsc1*$^{+/-}$ and *Tsc1*$^{+/-}$ *Blm*$^{-/-}$ mice as previously described (chapter 3, chapter 4). Half of each kidney was snap frozen in liquid nitrogen-cooled isopentane for LCM and the other half was processed into paraffin wax and sectioned at 4μm for H&E or IHC.

5.2.2 Somatic mutation analysis

DNA was extracted from renal lesions after LCM from kidneys of 55 *Tsc1*$^{+/-}$ and 31 *Tsc1*$^{+/-}$ *Blm*$^{-/-}$ mice. LOH at the *Tsc1* locus was assayed by simultaneous amplification of both the wild type and mutant alleles in a 25 cycle PCR reaction, as previously described (chapter 3), using 3ng of DNA (multiple sections of the same lesion were sometimes required to provide sufficient yields of DNA). LOH was defined as a change in wild type:mutant peak ratios of <0.67 or ≥1.3 (chapter 4). To search for intragenic somatic *Tsc1* mutations, the entire *Tsc1* ORF was amplified as 23 fragments (Table 4.1) and sequenced directly. The Wales Gene Park assisted with sequencing and somatic mutation detection.

5.2.3 Immunohistochemistry

IHC using anti-mTOR, anti-phospho-mTOR (Ser 2448), anti-S6 ribosomal protein and anti-phospho-S6 ribosomal protein (Ser240/244) (Cell Signalling Technologies) was performed as previously described (chapter 3). Renal lesions were identified after H&E staining and adjacent sections were

stained with antibodies to p-mTOR or p-S6 (kidneys from 36 *Tsc1*$^{+/-}$ and 30 *Tsc1*$^{+/-}$ *Blm*$^{-/-}$ mice were used for the p-mTOR analyses and 44 *Tsc1*$^{+/-}$ mice were used for the p-S6 analyses). Staining intensities were ranked blind by two independent investigators as little/absent or strong (there was 70.4% and 81.2% concordance in staining estimates for p-mTOR and p-S6, respectively). Cleo Bonnet assisted with some paraffin sectioning and p-S6 IHC.

5.2.4 Determination of cyst and cell size

Total cyst area was measured using Motic image plus 2.0 software in 17 p-S6 positively stained cysts and 9 p-S6 negatively stained cysts. Cell areas were estimated by measuring the height and width of 20 adjacent cells within 12 p-S6 positively stained cysts, 9 p-S6 negatively stained cysts, 6 CAs and 6 RCCs (positively stained for p-S6), and 20 normal tubule cells selected at random within the same kidneys.

5.2.5 Determining the sensitivity of the LOH assay for detecting the level of mutant alleles

LCM of cysts is technically challenging due to their small size and proximity to normal renal cells. Therefore, DNA extracted from cysts may have relatively high levels of contaminating wild type alleles. Theoretically, the LOH assay would be able to detect LOH of the wild type allele down to 12.5% tumour tissue if LOH is defined as a change in wildtype: mutant peak ratios of ≥1.3. However in practice tissue is heterogeneous. To determine the lowest level of mutant alleles that could be detected by the LOH assay, RCC

tissue with known LOH was excised and mixed with different amounts of normal renal tissue. DNA extracted from these mixed samples was assayed as previously described. Mutant to wild type allele proportions were estimated to vary between 25% to 97% (n=60). As expected, increasing the amount of wild type allele decreased the LOH ratio for the samples (Fig. 5.1). This data indicated LOH could be detected with 95% confidence when the proportion of mutant alleles was as low as 25%.

5.2.6 Statistics

Comparisons between numbers of somatic mutations was performed using Fisher's Exact test. Comparisons between staining grades were performed using the Mann-Whitney confidence interval test. Determinations of cyst and cell sizes were compared using the ANOVA followed by a Tukey test.

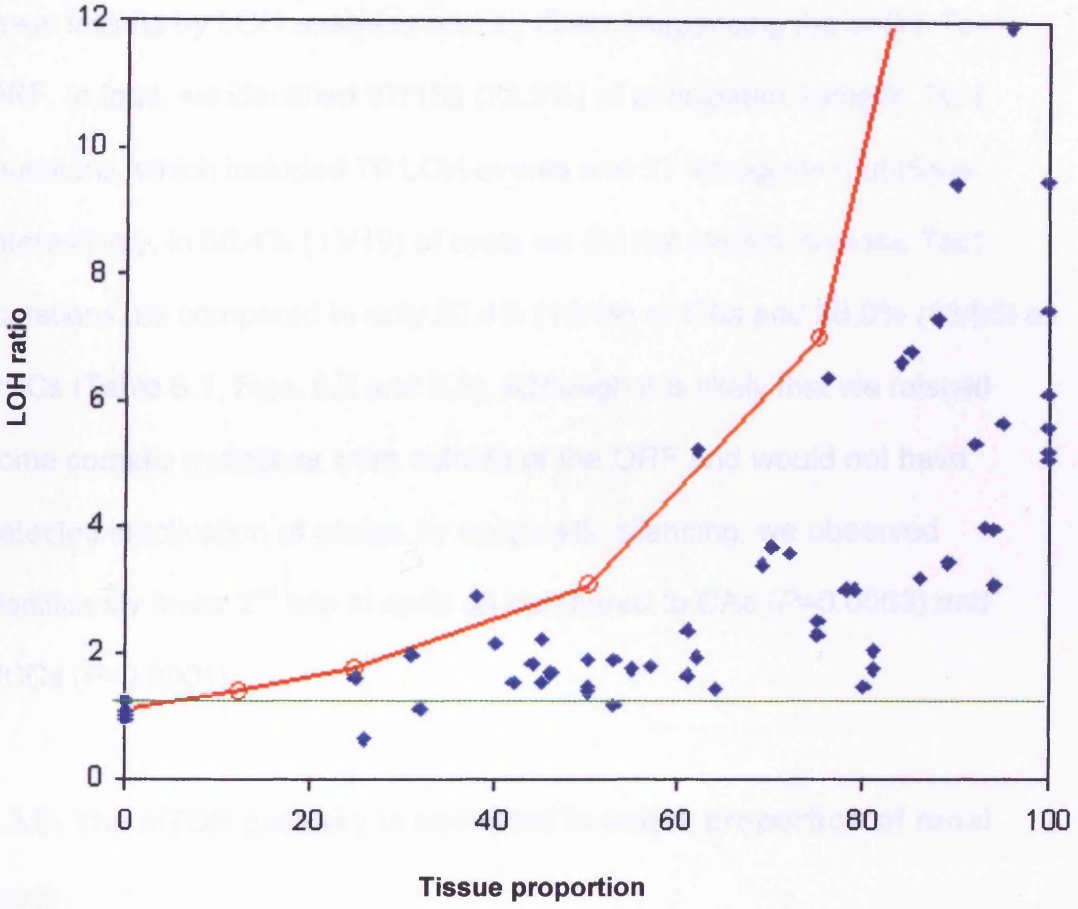

Figure 5.1: Determining the sensitivity of the LOH assay to detect low levels of mutant allele. Plot of LOH ratios obtained from DNA extracted from RCC tissue (with known LOH) mixed with differing amounts of normal renal tissue (n=60). DNA extracted from 8 different normal tissue sections from *Tsc1*$^{+/-}$ mice was used to normalise the assay (comparison of wild type:mutant allele peak heights). Red curved line indicates theoretical values expected. LOH was defined as a change in wild type:mutant peak ratios ≥1.3 (green line).

5.3 Results

5.3.1 Somatic *Tsc1* mutations are not abundant in renal cysts from *Tsc1*$^{+/-}$ mice

DNA was extracted from 19 renal cysts, 49 renal CAs and 65 RCCs from *Tsc1*$^{+/-}$ mice after LCM. We sought somatic *Tsc1* mutations in DNA from these lesions by LOH analyses and by direct sequencing the entire *Tsc1* ORF. In total, we identified 97/133 (72.9%) of anticipated somatic *Tsc1* mutations, which included 70 LOH events and 27 intragenic mutations. Interestingly, in 68.4% (13/19) of cysts we did not identify somatic *Tsc1* mutations, as compared to only 20.4% (10/49) of CAs and 20.0% (13/65) of RCCs (Table 5.1, Figs. 5.2 and 5.3). Although it is likely that we missed some somatic mutations lying outside of the ORF and would not have detected inactivation of alleles by epigenetic silencing, we observed significantly fewer 2nd hits in cysts as compared to CAs (P=0.0003) and RCCs (P=0.0001).

5.3.2 The mTOR pathway is activated in only a proportion of renal cysts

We investigated whether the low level of somatic *Tsc1* mutations in cysts correlated with low levels of mTOR activation. We assessed the expression levels of phosphorylated (activated) (p-)mTOR in 45 renal cysts, 51 renal CAs and 27 RCCs from *Tsc1*$^{+/-}$ mice by IHC. In total, 94/123 (76.4%) lesions showed strong staining for p-mTOR. However, 53.3% (24/45) of cysts showed little or no p-mTOR staining, compared to only 3.9% (2/51) of CAs and 11.1% (3/27) of RCCs, the majority (>88.9%) of which

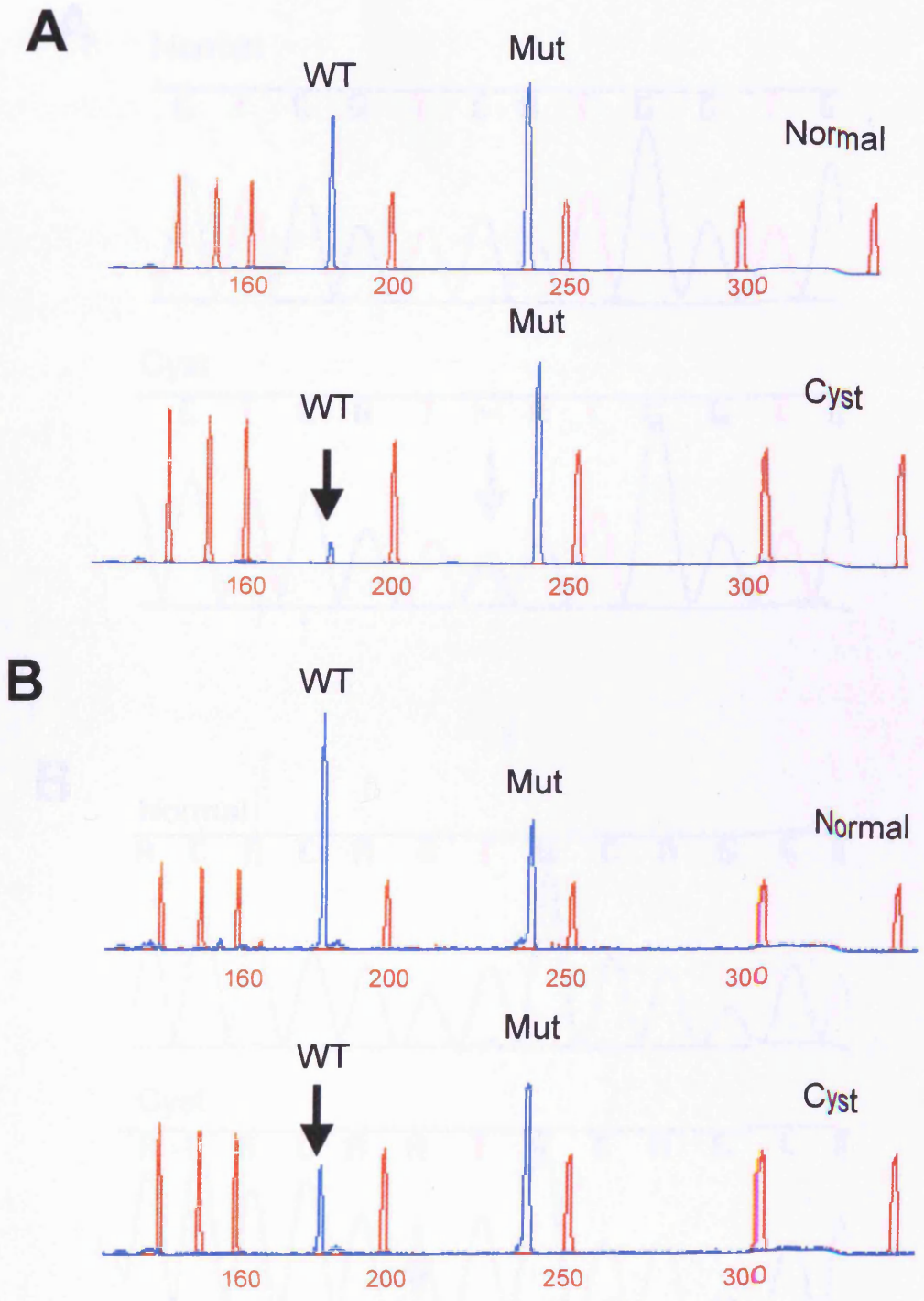

Figure 5.2: (A and B) Examples of somatic LOH identified in cysts from *Tsc1*$^{+/-}$ mice. Loss of the wild type *Tsc1* allele in the cyst (lower panel), but not in adjacent normal tissue (upper panel), is indicated by an arrow (WT – wild type allele, Mut - mutant allele).

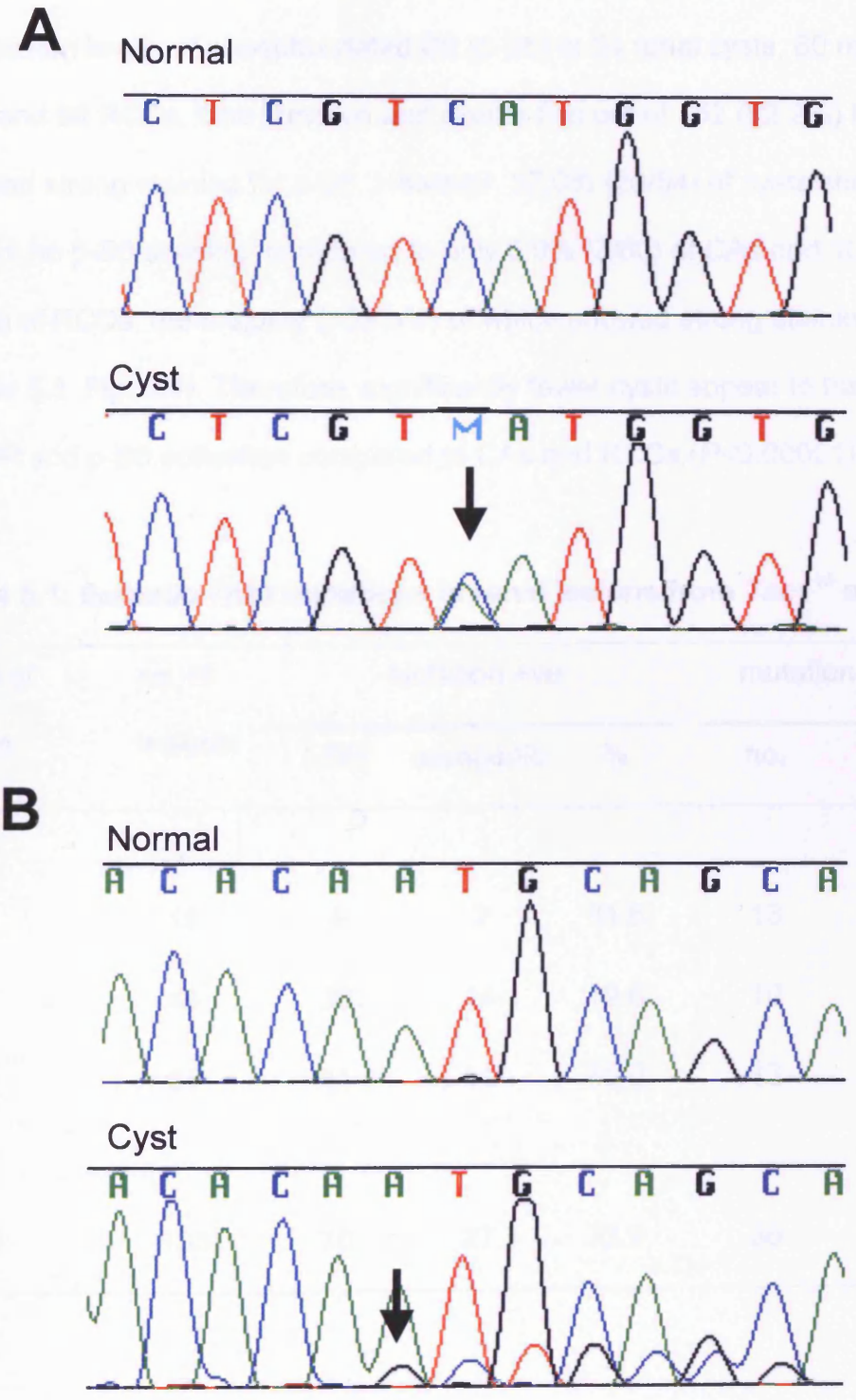

Figure 5.3: Examples of somatic intragenic mutations identified in cysts from *Tsc1*$^{+/-}$ mice. (A) An example of an intragenic nonsense mutation (S163X) in a renal cyst. The C to A substitution at nucleic acid position 488 was identified in the cyst (lower panel), but not in the adjacent normal tissue (upper panel) (indicated by an arrow). (B) An example of an intragenic 58 base pair deletion in exon 17 was identified in the cyst (lower panel), but not in the adjacent normal tissue (upper panel) (indicated by an arrow).

showed strong staining (Table 5.2, Fig. 5.4). We also assessed the expression levels of phosphorylated S6 (p-S6) in 54 renal cysts, 60 renal CAs and 38 RCCs. One hundred and twenty-five out of 152 (82.2%) lesions showed strong staining for p-S6. However, 37.0% (20/54) of cysts showed little or no p-S6 staining, compared to only 5.0% (3/60) of CAs and 10.5% (4/38) of RCCs, the majority (>89.5%) of which showed strong staining (Table 5.3, Fig. 5.4). Therefore, significantly fewer cysts appear to have p-mTOR and p-S6 activation compared to CAs and RCCs ($P<0.00001$).

Table 5.1: Somatic *Tsc1* mutations in renal lesions from *Tsc1*$^{+/-}$ mice

Type of lesion	no. of lesions	mutation +ve			mutation –ve	
		LOH	intragenic	%	no.	%
cyst	19	4	2	31.6	13	68.4
CA	49	25	14	79.6	10	20.4
RCC	65	41	11	80.0	13	20.0
Total	133	70	27	72.9	36	27.1

5.3.3 Detailed analysis of renal cysts

We determined the pattern of p-S6 activation throughout individual renal cysts from *Tsc1*$^{+/-}$ mice by staining consecutive serial sections. Seventeen out of 26 (65%) cysts studied in this way showed consistently

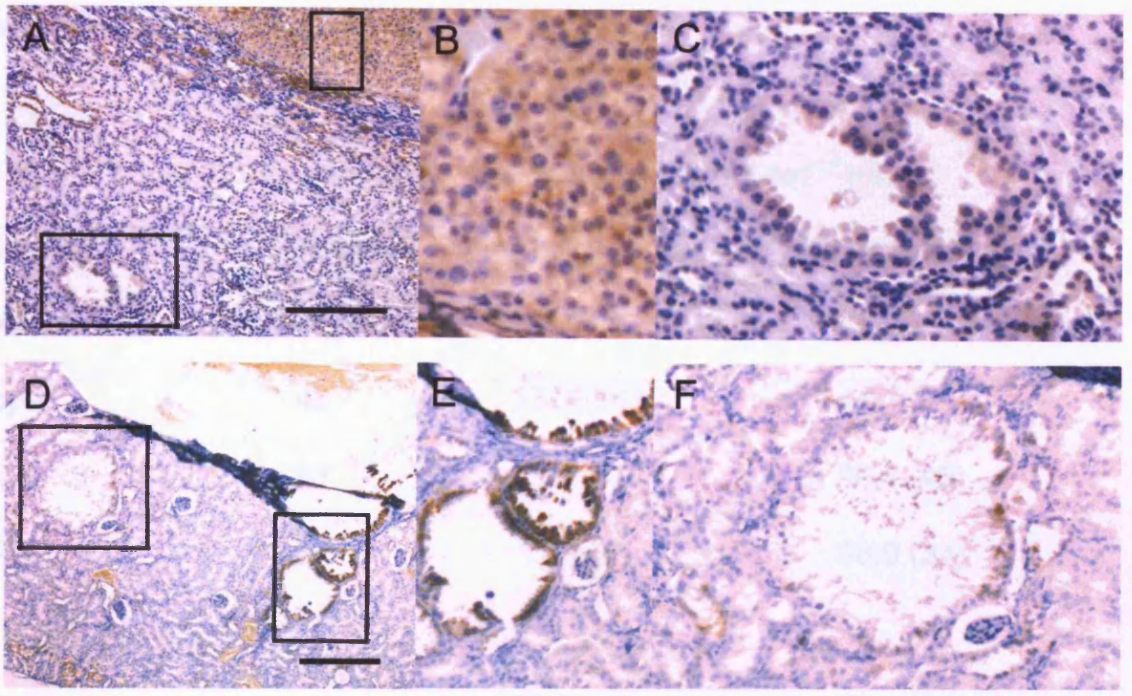

Figure 5.4: IHC of renal lesions from *Tsc1*$^{+/-}$ mice using an anti-p-mTOR (A-C) and anti-p-S6 (D-F) antibodies. (A) A RCC (*top right hand corner*) shows intense (brown) staining with p-mTOR (boxed region enlarged in B), whereas a cyst (*lower left hand corner*) shows little or no staining (boxed region enlarged in C). (D) Some cysts (*right hand side*) showed staining with p-S6 (boxed region enlarged in E), whereas others (*left hand side*) showed little or no staining (boxed region enlarged in F). Control staining using S6 and mTOR antibodies showed consistent staining throughout the kidney and all lesions studied (data not shown). N.B. cysts that did not stain for either p-mTOR or p-S6 were rarely adjacent to RCCs (that might have contributed to their formation). Scale bars are 200μm.

strong p-S6 staining and the remaining 9 (35%) showed consistently little or no staining, in every serial section (Fig. 5.5). Three of the cysts with little or no p-S6 staining had some sections in which single cells displayed strong positivity (e.g. in Fig. 5.5D); however, this pattern was also seen in some normal tubular epithelial cells.

Table 5.2: p-mTOR analysis of renal lesions from *Tsc1*$^{+/-}$ mice

Type of lesion	no. of lesions	% with little or no staining*	% with strong staining*
cyst	45	53.3 (24)	46.7 (21)
CA	51	3.9 (2)	96.1 (49)
RCC	27	11.1 (3)	88.9 (24)
Total	123	23.6 (29)	76.4 (94)

*numbers of lesions are shown in parentheses

Table 5.3: p-S6 analysis of renal lesions from *Tsc1*$^{+/-}$ mice

Type of lesion	no. of lesions	% with little or no staining*	% with strong staining*
cyst	54	37.0 (20)	63.0 (34)
CA	60	5.0 (3)	95.0 (57)
RCC	38	10.5 (4)	89.5 (34)
Total	152	17.8 (27)	82.2 (125)

*numbers of lesions are shown in parentheses

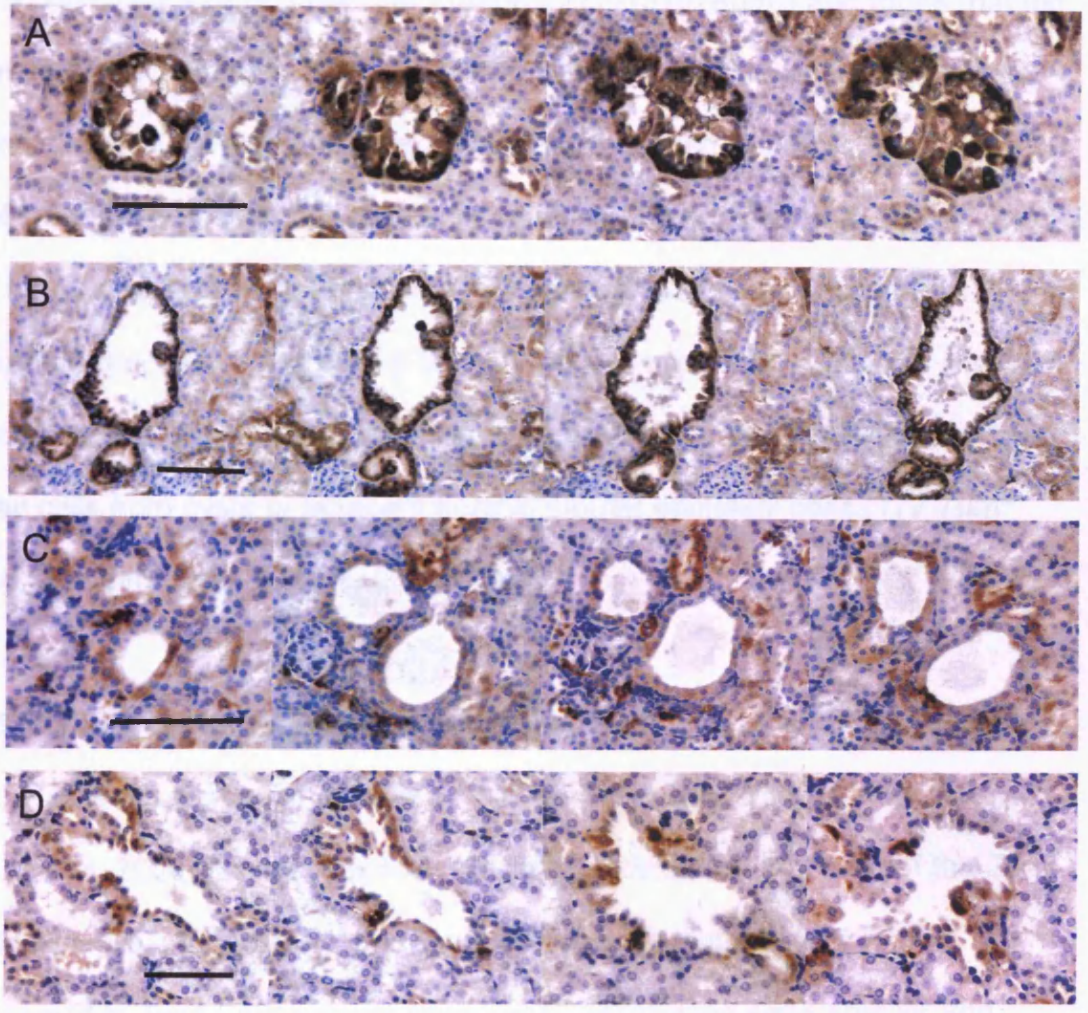

Figure 5.5: IHC of consecutive serial sections of renal cysts from *Tsc1*$^{+/-}$ mice using a p-S6 antibody. Examples of serial sections through cysts that consistently either stained (A and B), or, that did not stain strongly (C and D). Note: other lesions present in other parts of sections shown in C and D stained for p-S6 (data not shown), confirming that the antibody worked successfully. Scale bars are 100μm.

5.3.4 Size and morphology of p-S6 stained and unstained cysts

We found no significant difference in the size of cysts that stained for p-S6 (average size of 21441μm^2, range 3177-151578μm^2) and those that did not (average 10615μm^2, range 3264-25661μm^2), nor did we find any gross morphological differences. In terms of cells that lined the cysts, p-S6 stained cells were of a similar size to unstained cells (100.4μm^2 vs. 106.8μm^2), and of a similar size to adjacent normal tubular epithelial cells (98.9μm^2). Furthermore, cells lining both p-S6 stained and unstained cysts had similar morphologies. In contrast, cells from CAs and RCCs were significantly larger than cells from cysts or adjacent normal tubular epithelial cells (172.7μm^2 and 188.3μm^2, respectively, P<0.001).

5.3.5 Analysis of renal lesions from *Tsc1*$^{+/-}$ *Blm*$^{-/-}$ mice

We have crossed our *Tsc1*$^{+/-}$ mice onto a *Blm*-deficient background (Luo et al. 2000), which increases the frequency of somatic LOH of the *Tsc1* wild type allele (chapter 4), thereby facilitating the detection of 2nd hits. As observed in *Tsc1*$^{+/-}$ mice, cysts from *Tsc1*$^{+/-}$ *Blm*$^{-/-}$ mice were smaller and more numerous than CAs and RCCs, supporting the model of tumour progression. We sought somatic LOH events and intragenic mutations at the *Tsc1* locus in DNA extracted from 23 renal cysts, 38 renal CAs and 24 RCCs after LCM from *Tsc1*$^{+/-}$ *Blm*$^{-/-}$ mice. In total, we identified 82.4% (70/85) of somatic *Tsc1* mutations, which included 69 LOH events and 1 intragenic mutation. However, in 34.8% (8/23) of cysts we did not identify any somatic *Tsc1* mutations, as compared to only 13.2% (5/38) of CAs and 8.3% (2/24) of

RCCs (Table 5.4); therefore, in agreement with our studies on *Tsc1*$^{+/-}$ mice, somatic *Tsc1* mutations were significantly less frequent in cysts as compared to CAs (P=0.048) and RCCs (P=0.03) on a *Tsc1*$^{+/-}$ *Blm*$^{-/-}$ background. We also assessed the expression levels of p-mTOR in 23 renal cysts, 42 renal CAs and 9 RCCs from *Tsc1*$^{+/-}$ *Blm*$^{-/-}$ mice by IHC, and, consistent with our previous findings, we observed that significantly fewer cysts had activation of the mTOR pathway as compared to the more advanced lesions (P=0.02).

Table 5.4: Somatic *Tsc1* mutations in renal lesions from *Tsc1*$^{+/-}$ *Blm*$^{-/-}$ mice

Type of lesion	no. of lesions	mutation +ve			mutation -ve	
		LOH	intragenic	%	no.	%
cyst	23	15	0	65.2	8	34.8
CA	38	32	1	86.8	5	13.2
RCC	24	22	0	91.7	2	8.3
Total	85	69	1	82.4	15	17.6

5.4 Discussion

5.4.1 Sensitivity of the LOH assay and methodological drawbacks

LCM of cysts is technically challenging and DNA extracted from cysts may therefore have a relatively high level of contaminating wild type alleles. However, we show that our assay could detect LOH in samples with as low as 25% mutant alleles with 95% confidence. Furthermore, we have found many examples of cysts with high levels of mutant alleles (Figs. 5.2 and 5.3), confirming mutations in cysts could be easily located.

Unfortunately, in this study there were a number of reasons why we were unable to undertake both mutation analysis and IHC on the same cysts. Firstly, the small size of cysts makes LCM and extraction of sufficient amounts of DNA difficult. Secondly, p-S6 staining did not work on frozen tissue. Thirdly, DNA extracted from paraffin embedded tissue was not reliable in LOH assays. Finally, immunohistochemical staining of paraffin and frozen tissue hinders DNA extraction. Therefore, paraffin embedded p-S6 stained cysts could not be used for DNA extraction and frozen cysts could not be stained for p-S6.

5.4.2 *Tsc1*-haploinsufficiency in a proportion of renal cysts

A wide range of mutational mechanisms may cause somatic inactivation of the wild-type allele of tumour suppressor genes. Consequently, reports of tumour haploinsufficiency at tumour suppressor loci may sometimes be incorrect and simply reflect an inability to find second mutations. We have utilised two complimentary approaches to demonstrate *Tsc1*-haploinsufficiency in a proportion of renal cysts from $Tsc1^{+/-}$ mice.

Firstly, we have shown by staining for p-mTOR and p-S6, that there is little or no activation of the mTOR pathway in ~37-53% of cysts. Secondly, we have crossed *Tsc1*$^{+/-}$ mice onto a *Blm*-deficient background which dramatically increases the frequency of somatic LOH of the wild type *Tsc1* allele, making the identification of 2nd hits straightforward (chapter 4); on this background ~34.8% of cysts appeared to be haploinsufficient for *Tsc1*. Interestingly, 2nd hits at *Tsc1* and activation of the mTOR pathway were found in the vast majority of more advanced renal tumours suggesting that although these are important steps in Tsc-associated renal tumourigenesis, they may not be key initiating events in this process.

5.4.3 Haploinsufficiency in tuberous sclerosis

Other studies have also suggested that haploinsufficiency for *TSC1* or *TSC2* has both biochemical and phenotypic consequences. Microscopically normal renal tubular epithelial cells from TSC mutation carriers have significant differences in gene expression profiles compared to similar cells from controls. *TSC* renal epithelial cells showed increased expression of transcripts for several factors involved in protein synthesis including eukaryotic translation initiation factor 3 and upregulation of several ribosomal protein genes (S6, S25, L6, L21) (Stoyanova et al. 2004). These data suggest that heterozygous *TSC* renal epithelial cells may have compromised inhibition of mTOR signalling. In addition, heterozygous *TSC* renal epithelia had altered HIF signalling, shown by increased expression of the HIF1α subunit, hypoxia-inducible protein 2 and hypoxia induced gene 1 (Stoyanova et al. 2004).

Work on rodent models of *Tsc* has also suggested an effect of *Tsc1* or *Tsc2* associated haploinsufficiency. Heterozygous loss of one *Tsc2* allele has been shown to affect the cognitive abilities of young Eker rats that rarely harbour brain lesions. These animals exhibit enhanced responses to chemically-induced kindling by repeated injection of pentylenetetrazole (Waltereit et al. 2006). Furthermore, in grossly normal $Tsc1^{+/-}$ and $Tsc2^{+/-}$ mouse brains, Uhlmann et al. (2002) noted a 1.5-fold increase in the numbers of astrocytes in the hippocampus. Compound $Tsc1^{+/-}Tsc2^{+/-}$ animals displayed a 2-fold increase in astrocyte number in the hippocampus, suggesting that heterozygosity for both *Tsc* proteins can further promote dysregulation in astrocyte number (Uhlmann et al. 2002). *In vitro,* mouse *Tsc1* haploinsufficient neurons also have increased soma size, decreased spine density and increased spine length and head width (Tavazoie et al. 2005). This abnormal neuronal morphology became more pronounced after loss of the 2nd *Tsc1* allele suggesting that the *Tsc* pathway is sensitive to gene dosage (Tavazoie et al. 2005). Further studies are therefore warranted to determine the effects of *TSC1* and *TSC2* haploinsufficiency and to define the key event(s) in tumour initiation.

5.4.4 Implications for Rapamycin treatment

It has recently been suggested that rapamycin, an mTOR inhibitor, may be an effective drug in treating patients with TSC and other mTOR activation syndromes. Studies have shown that rapamycin treatment of Eker rats resulted in a significant decrease in the size of the *Tsc2*-related renal tumours, accompanied by down-regulation of p-S6 activity (Kenerson et al.

2005). However, rapamycin had no effect on the number of microscopic precursor lesions, suggesting a rapamycin-insensitive pathway during *Tsc2*-associated tumour initiation (Kenerson et al. 2005). Our data may also indicate an mTOR independent pathway during *Tsc1*-associated tumour initiation. Therefore, although rapamycin may help control TSC-associated tumour development, it may not prevent tumour initiation.

Chapter 6: General Discussion

6.1 Targeted mouse strain confirmed to be a valid model for tuberous sclerosis-1 deficiency

In this study, mice bearing a targeted disruption of *Tsc1* were generated by deleting part of exon 6 through to exon 8 with the concurrent insertion of a reporter/selection cassette. The targeting event produced an aberrantly spliced transcript that caused a shift in the reading frame, leading to the introduction of a premature termination codon at the 8th codon of exon 9 of *Tsc1*. Therefore, the targeted mouse strain was confirmed to be a valid model for tuberous sclerosis-1 deficiency.

6.2 *Tsc1*$^{+/-}$ mice exhibit a more severe renal phenotype than existing models

Our new murine model of hamartin deficiency exhibits a more severe renal phenotype than existing models of *Tsc* (Kobayashi *et al.* 2001, Kwiatkowski *et al.* 2002): 80% of mice on a Balb/c background exhibited solid RCCs by 15 to 18 months and in 41%, RCCs were ≥5mm, resulting in grossly deformed kidneys. Some of these carcinomas had a sarcomatoid morphology of spindle cells in whorled patterns and, unlike other *Tsc1*$^{+/-}$ mice, metastasised to the lungs.

The incidence of spontaneous RCC in laboratory strains of mice and rats is very low (<5%) (Kleymenova et al. 2004). Therefore rodent models have been produced to model human familial kidney tumour syndromes. Unfortunately many of these models do not display a kidney lesion

phenotype. *Vhl*$^{+/-}$ mice do not develop spontaneous or chemically induced kidney lesions (Kleymenova et al. 2004). Mice targeted for a mutation in *Wt1* (Wilms's tumour) appear normal and show no tumour development until 10 months of age (Kreidberg et al. 1993). Mice targeted for a mutation in MET that causes hereditary papillary renal carcinoma, do not display a renal lesion phenotype (Liang et al. 1996). Some models do however display a renal lesion phenotype. Rankin et al. (2006) have recently produced a conditional mouse model of *Vhl*. Conditional *Vhl*$^{+/-}$ mice develop renal cysts in 18% of animals when more than 12 months of age, however, they do not develop RCCs. A germline mutation in the Birt Hogg Dube (BHD) gene in a colony of rats (Named the 'Nihon' rat; Okimoto et al. 2004) causes altered renal tubules as early as 3 weeks of age that progress through adenoma to RCC (Kouchi et al. 2006). However, none of these models of kidney lesions display metastasis. Therefore, our *Tsc1*$^{+/-}$ mice will provide a valuable model for studying progression of RCC to metastasis.

6.3 *Tsc* rodent models have a different renal phenotype to humans

It is interesting to note that all the *Tsc1*$^{+/-}$ and *Tsc2*$^{+/-}$ rodent models have a different renal phenotype to humans. In man, angiomyolipomas are the most common renal lesion while in *Tsc* rodent models cysts, CA and RCC are predominant. Although the occurrence of RCC in humans with TSC is unusual, an association is recognised (Henske 2004). The RCCs are typically discovered at a young age and the proportion of sarcomatoid features in TSC renal carcinomas (50%) is far greater than in sporadic RCC (1 –2 %) (Bjornsson *et al.* 1996, Gomez *et al.* 1999). The *Tsc1*$^{+/-}$ mice RCCs

with a sarcomatoid morphology studied here may therefore prove an invaluable model to study this facet of the human disease.

The absence of major brain lesions in our and other mouse models of *Tsc* is surprising considering the brain pathology seen in human patients with *TSC*. Thus a mutation of the same gene can cause phenotypic variation between species. The differences may reflect longevity differences or simply smaller size or cell number. However, it is also possible that the progenitor cells which give rise to human brain lesions have different mechanisms of tuberin/hamartin regulated growth and differentiation compared to mouse brain precursor cells (Cheadle *et al.* 2000a).

6.4 Haploinsufficiency in *Tsc*-associated tumourigenesis

To examine haploinsufficiency in *Tsc*-associated renal lesions, cysts, CAs and RCCs were analysed using a combination of complementary mutation screening strategies and IHC (chapter 5). Interestingly, in 68% of cysts from $Tsc1^{+/-}$ animals we did not identify somatic *Tsc1* mutations implicating haploinsufficiency in there formation. In parallel studies with $Tsc1^{+/-}$ mice on a *Blm*-deficient background (where the frequency of somatic LOH of the wild type *Tsc1* allele is dramatically increased, making the identification of 2^{nd} hits straightforward (chapter 4)) 35% of cysts were haploinsufficient for *Tsc1*. In addition to haploinsufficiency causing cyst formation these data also suggest that in ~33% of $Tsc1^{+/-}$ mouse cysts there was possible undetected silencing of the *Tsc1* wild type allele. Therefore, here we have implicated the possibility that epigenetic or other undetected silencing events of the *Tsc1* wild type allele can occur in a proportion of renal

cysts. Immunohistochemical staining of cysts from a *Tsc1*$^{+/-}$ background indicated that ~37-53% of cysts showed little or no p-S6 and p-mTOR staining. This result is in agreement with molecular analysis of *Tsc1*$^{+/-}$ *Blm*$^{-/-}$ cysts and thus indicates ~35% of cysts are haploinsufficient for *Tsc1*. Therefore indicating that mTOR activation is not necessarily an important step in Tsc-associated renal tumour initiation.

6.5 Haploinsufficiency in other hamartoma syndromes

Recent work on the TSC signal transduction pathway has led to the discovery of links between components of this pathway and genes mutated in other hamartoma syndromes (Fig. 6.1). In the recent review, Inoki *et al.* (2005) classified hamartoma syndromes based on molecular pathogenesis. They proposed two categories; hamartoma syndromes with an established molecular link to the dysregulation of mTOR; including *LKB1*, *PTEN*, *TSC1* and *TSC2*. The second category consisted of hamartoma syndromes that have been implicated with the dysregulation of mTOR or possess clinical similarities to those syndromes in the first category. This category included *PRKAR1A*, *NF1*, *VHL*, *FLCN*, *APC*, *SMAD4* and *BMPR1A* genes (Inoki *et al.* 2005). There is increasing evidence that loss of one allele for the respective gene in these disorders may be necessary for tumour initiation.

6.5.1 Peutz-Jeghers syndrome

Peutz-Jeghers syndrome (PJS) is a dominantly inherited hamartoma syndrome characterised by the development of gastrointestinal hamartomatous polyps (affecting the small bowl, stomach and colon) as well

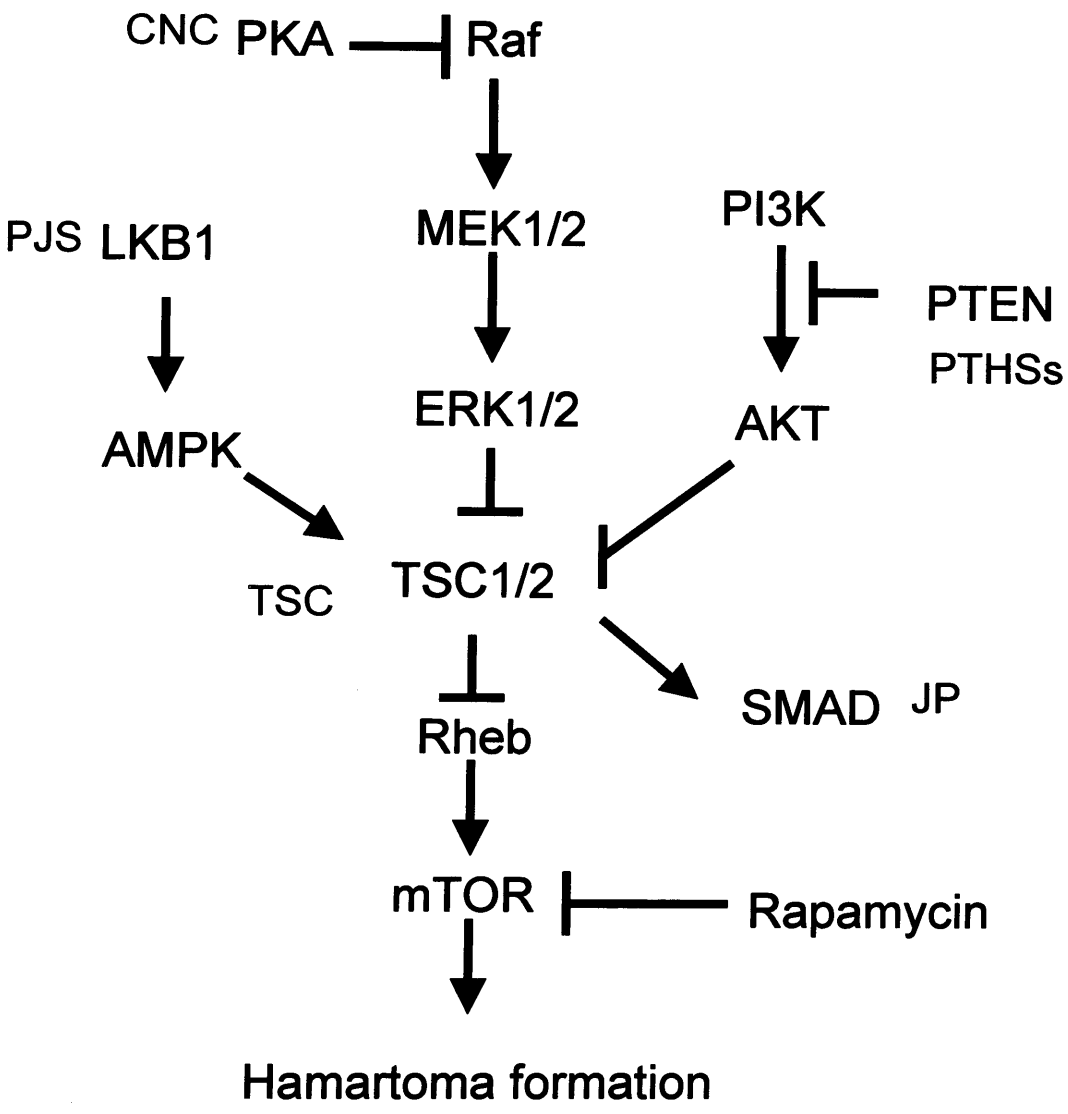

Figure 6.1: Classification of hamartoma syndromes based on molecular pathogenesis (adapted from Inoki *et al.* 2005). Hamartoma syndromes with an established molecular link to the dysregulation of mTOR pathway include PTEN hamartoma syndromes (PTHs), Peutz-Jeghers syndrome (PJS) and Tuberous sclerosis (TSC1/TSC2). Hamartoma syndromes that have been implicated with the dysregulation of mTOR include Juvenile polyposis (JP) and Carney complex (CNC).

as mucocutaneous pigmentation of the lips, buccal mucosa and digits (Peutz 1921, Jeghers *et al.* 1949). PJS patients show a high risk of developing gastrointestinal and non-gastrointestinal cancers at relatively young ages (Giardiello *et al.* 1987, Boardman *et al.* 1998, Giardiello *et al.* 2000). Germline mutations in the *LKB1/STK11* gene have been shown to be the cause of the majority of PJS cases (Hemminki *et al.* 1998, Jenne *et al.* 1998). The *LKB1* tumour suppressor gene encodes a protein kinase that phosphorylates and activates, upon ATP depletion, the AMP-activated protein kinase (AMPK). AMPK is a central sensor of cellular ATP levels and key regulator of cellular energy consumption. Loss of *LKB1* results in down regulation of the TSC complex thus stimulating mTOR activity (Shaw et al. 2004, reviewed in Kwiatkowski and Manning 2005, Hardie 2005). Several studies have shown the vast majority of lesions in PJS patients show loss of the wild type LKB1 allele (Hemminki et al. 1998, Gruber et al. 1998, Resta et al. 1998, Wang et al. 1999, Miyaki et al. 2000, Entius et al. 2001). Gruber et al. (1998) identified LOH of the *LKB1* wild type allele in 70% of tumours. However, others have suggested that biallelic inactivation of *LKB1* may be more rare. Resta et al. (1998) and Entius et al. (2001) found LOH of the LKB1 wild type allele in only 19% and 38% of tumours from PJS patients respectively implicating a role for haploinsufficiency.

Several murine models of *Lkb1* deficiency have been produced (Ylikorkala et al. 2001, Bardeesy et al. 2002, Jishage at al. 2002, Miyoshi et al. 2002). *Lkb1*$^{+/-}$ mice are predisposed to gastrointestinal polyps, which histologically have a striking similarity to human PJS polyps (Miyoshi et al. 2002, Rossi et al. 2002). Miyoshi et al. (2002), Rossi et al. (2002) and

Jishage at al. (2002) have all shown, using a variety of techniques, that loss of only one copy of the *Lkb1* allele is necessary to produce gastrointestinal polyps in *Lkb1*$^{+/-}$ mice.

6.5.2 PTEN hamartoma syndromes

Cowden's disease (CD) is an autosomal dominant disorder characterised by multiple hamartomas including trichilemmomas and mucocutaneous papillomatous papules, as well as a high risk of breast and thyroid cancers (Eng 2000). Bannayan-Riley-Ruvalcaba syndrome (BRRS) is a rare autosomal dominant congenital disorder characterised by macrocephaly, lipomatosis, hemangiomatosis and speckled penis (Gorlin et al. 1992). Proteus syndrome (PS) is a complex disorder characterised by hamartomatous overgrowth of multiple tissues including connective tissue naevi, epidermal naevi and limbs (Biesecker at al. 1999, Zhou et al. 2001). Lhermitte-Duclos disease (LDD), or dysplastic gangliocytoma of the cerebellum is characterised by hamartomatous overgrowth of hypertrophic ganglion cells, resulting in circumscribed enlargement of the cerebellar folia (Nowak and Trost 2002, Zhou et al. 2003). CD, BRRS, PS, Proteus like syndromes (PLS) and LDD, show remarkable clinical overlap (Merks et al. 2003). Although it is controversial whether each disease is a clinically distinct entity, they have been grouped together as PTEN hamartoma syndromes (PTHs) because all are caused by germline mutations in *PTEN* (Marsh et al. 1999, Eng 2003, Inoki et al. 2005).

PTEN encodes a dual-specificity phosphatase that lies upstream of Akt. It reduces intracellular levels of PI3K lipid products thereby inhibiting Akt

activation. Thus in cells lacking *PTEN*, Akt is constitutively active, and there is a corresponding increase in TSC2 phosphorylation and downstream mTOR signalling (Manning *et al.* 2005). Somatic mutations of *PTEN* have been identified in a large fraction of prostate, brain, breast, endometrial, skin and kidney lesions, consequently placing it among the most commonly mutated genes in human cancer (Li et al. 1997, Steck et al. 1997, Risinger 1997, Di Cristofano et al. 1998). However, complete loss of *PTEN* function in early stage tumours occurs only in endometrial and ovarian cancer (Trotman et al. 2003). The vast majority of cancers only show biallelic *PTEN* inactivation as a late event in cancer progression (Byun et al. 2003, Trotman et al. 2003). There has been a number of reports that haploinsufficiency of *PTEN* is sufficient for tumour initiation. Li et al. (2003a) showed that *PTEN* haploinsufficiency results in altered gene expression in subventricular zone precursor cells. Furthermore, CD primary sporadic breast cancers and merkel cell carcinomas have been shown not to have biallelic *PTEN* mutations (Marsh et al. 1999, Van Gele et al. 2001).

Three different groups have produced *Pten* knockout mice (Di Cristofano et al. 1998, Suzuki et al. 1998, Podsypanina et al. 1999). The phenotype of the mice vary. However, features of CS and BRRS have been described. Analysis of hyperplastic-dysplastic changes of the colon mucosa and polyps in the lower gastrointestinal tract in $Pten^{+/-}$ mice has shown that loss of the normal *Pten* allele does not occur (Di Cristofano et al. 1998). Furthermore, $Pten^{+/-}$ mice crossed with $Tsc2^{+/-}$ mice exhibit *Pten* type lesions in compound heterozygous animals that are more severe but still retain heterozygosity at both alleles (Ma et al. 2005, Manning et al. 2005).

6.5.3 Juvenile polyposis

Juvenile polyposis syndrome (JP) is an autosomal dominant disorder, characterised by development of 50-200 hamartomatous polyps distributed throughout the colon (McColl et al. 1964, Chow and Macrae 2005). The cause of some cases of JP has been shown to be germline mutations in *SMAD4* (*DPC4*) (Howe et al. 1998). SMAD4 encodes a cytoplasmic mediator involved in the Transforming growth factors β (TGFβ) signal transduction pathway (Chow and Macrae 2005). Interestingly, molecular and functional association between TGFβ signalling and TSC2 have been described. SMAD4 interacts with its binding partner SMAD3 which interacts with AKT and TSC2 (Birchenall-Roberts et al. 2004). Biallelic somatic *SMAD4* mutations have been identified to a varying degree in JP patients. Wooford-Richens et al. (2000) noted 65% of lesions had LOH of the *SMAD4* wild type allele using microsatellite markers near to the SMAD4 locus. Furthermore, *SMAD4* has been shown to be inactivated specifically during late stages of human colorectal cancer (Takagi et al. 1996, Thiagalingam et al. 1996, Koyama et al. 1999, Miyaki et al. 1999). However, Howe et al. (1998) noted only 9% of gastrointestinal polyps showed LOH of the wild type allele. Therefore it has been suggested that haploid loss of *SMAD4* can initiate hamartoma formation, and diploid loss is may be required for advancement of tumourigenesis. Several independent investigators have addressed this hypothesis using *Smad4* deficient mouse models (Xu et al. 2000, Alberici et al. 2005). In general, mice heterozygous for the *Smad4* allele are predisposed to the development of multiple polyps in the upper

gastrointestinal tract (Sirard et al. 1998, Takaku et al. 1999, Xu et al. 2000, Alberici et al. 2005). Xu et al. (2000) and Alberici et al. (2005) have demonstrated that early gastrointestinal lesions from *Smad4*$^{+/-}$ mice often do not display LOH of the *Smad4* wild type allele, thus supporting a haploinsufficient mechanism of in tumour initiation.

6.5.4 Carney complex

Carney complex (CNC) is an autosomal dominant disorder characterised by myxomas, spotty skin pigmentation and abnormal endocrine activity (Carney 1985). Germline mutations in the PRKARIA gene have been shown to be the cause of approximately 50% of cases (Kirschner at al. 2000a). PRKAR1A encodes the regulatory subunit I-α (RIα) of the cAMP-dependant kinase (PKA) holoenzyme (Tasken et al. 1997). PKA has been shown to target components of the ERK-MAPK signalling system. Specifically, mutated PRKAR1A leads to reversal of PKA-mediated inhibition of MAPK signalling (Robinson-White et al. 2003, Robinson-White et al. 2006). TSC2 has been shown to be a phosphorylation target of ERK signalling and this phosphorylation results in the suppression of its tumour suppressor functions (Ma et al. 2005). LOH of the PRKAR1A wild type allele has been found in a variety of tumours from patients with CNC (Kirschner at al. 2000b, Stergiopoulos and Stratakis 2003). However, analysis of cardiac and eyelid myxomas and primary pigmented nodular adrenocortical tumours from patients with CNC showed no somatic mutations of the PRKAR1A wild type allele (Casey et al. 2000, Groussin et al. 2002, Bertherat et al. 2003, Tsilou et al. 2004).

Prkar1a$^{+/-}$ mice have been produced to address the question of haploinsufficiency in lesion formation (Amieux et al. 2002, Griffin et al. 2004). The *Prkar1a*$^{+/-}$ mice develop features reminiscent of CNC. Splenic hemangiosarcomas and soft tissue sarcomas did not display LOH of the *Prkar1a* wild type allele or altered PKA activity and they retained expression of wild type RIα protein (Veugelers et al. 2004). Again, haploinsufficiency is therefore implicated in tumour initiation.

6.5.5 Somatic inactivation of the wild type allele is an important factor in the later stages of tumourigenesis

In addition to the haploinsufficiency seen in early lesions of hamartoma syndromes, a common theme observed is that more advanced lesions display biallelic inactivation of their corresponding TSG allele. Analysis of advanced hepatocellular carcinomas in *Lkb1*$^{+/-}$ mice has revealed biallelic inactivation of the *Lkb1* gene (Nakau et al. 2002). Xu et al. (2000) demonstrated in *Smad4*$^{+/-}$ mice, that only 20% of gastrointestinal lesions less than 0.4mm and 63% of lesions more than 0.4mm displayed LOH of the *Smad4* allele. In agreement, Alberici et al. (2005) showed that LOH of the *Smad4* allele was detected in 40% of lesions from *Smad4*$^{+/-}$ mice up to 15 months, which increased to 64% in tumours from mice over 18 months. In humans, Entius et al. (2001) found LOH of the *LKB1* wild type allele in only 38% of polyps from PJS patients but in contrast, LOH of the *LKB1* wild type allele was found in 100% carcinomas. Furthermore, homozygous inactivation of PTEN is generally associated with only advanced cancer and metastasis (Di Cristofano and Pandolfi 2000, Trotman et al. 2003).

Here, we have identified somatic *Tsc1* mutations and mTOR activation in more than 80% of CAs and RCCs from *Tsc1*$^{+/-}$ mice. Therefore, 2nd hits at the *Tsc1* locus are found in the vast majority of more advanced tumours. This suggests that although haploinsufficiency may be an important step in the initiation of *Tsc*-associated renal tumourigenesis, biallelic inactivation of *Tsc1* is an important factor in the latter stages. Together, these results suggest a possible common mechanism of tumour initiation in hamartoma syndromes, whereby 1-hit initiates tumourigenesis, while a second hit promotes the progression to more advanced lesions.

6.6 *Blm*$^{m3/m3}$ mice and mapping loci involved in tumour progression

Microarray-based comparative genomic hybridization (aCGH) provides a means to quantitatively measure DNA copy-number aberrations and to map them directly onto genomic sequence (Snijders et al. 2001). Briefly, aCGH involves co-hybridisation of both labelled tumour DNA (with Cy3 green) and normal genomic DNA (with Cy5 red) to an array made up of oligos probes or clones. A laser scanner reads spot intensities on the hybridised array. The relative intensities of Cy3:Cy5 for each spot and thus the ratios of normal to tumour DNA can be computed and plotted for visual analysis (Fig. 6.2). While aCGH is not useful for detection of small intragenic mutations, is extremely well suited to high-throughput, whole genome detection of chromosomal gains and losses at high resolution (Weber 2002). Normally, a diverse range of mutations and epigenetic silencing, are implicated in the somatic inactivation of the wild type allele of TSGs. This diversity of somatic alterations makes genetic mapping of loci involved in

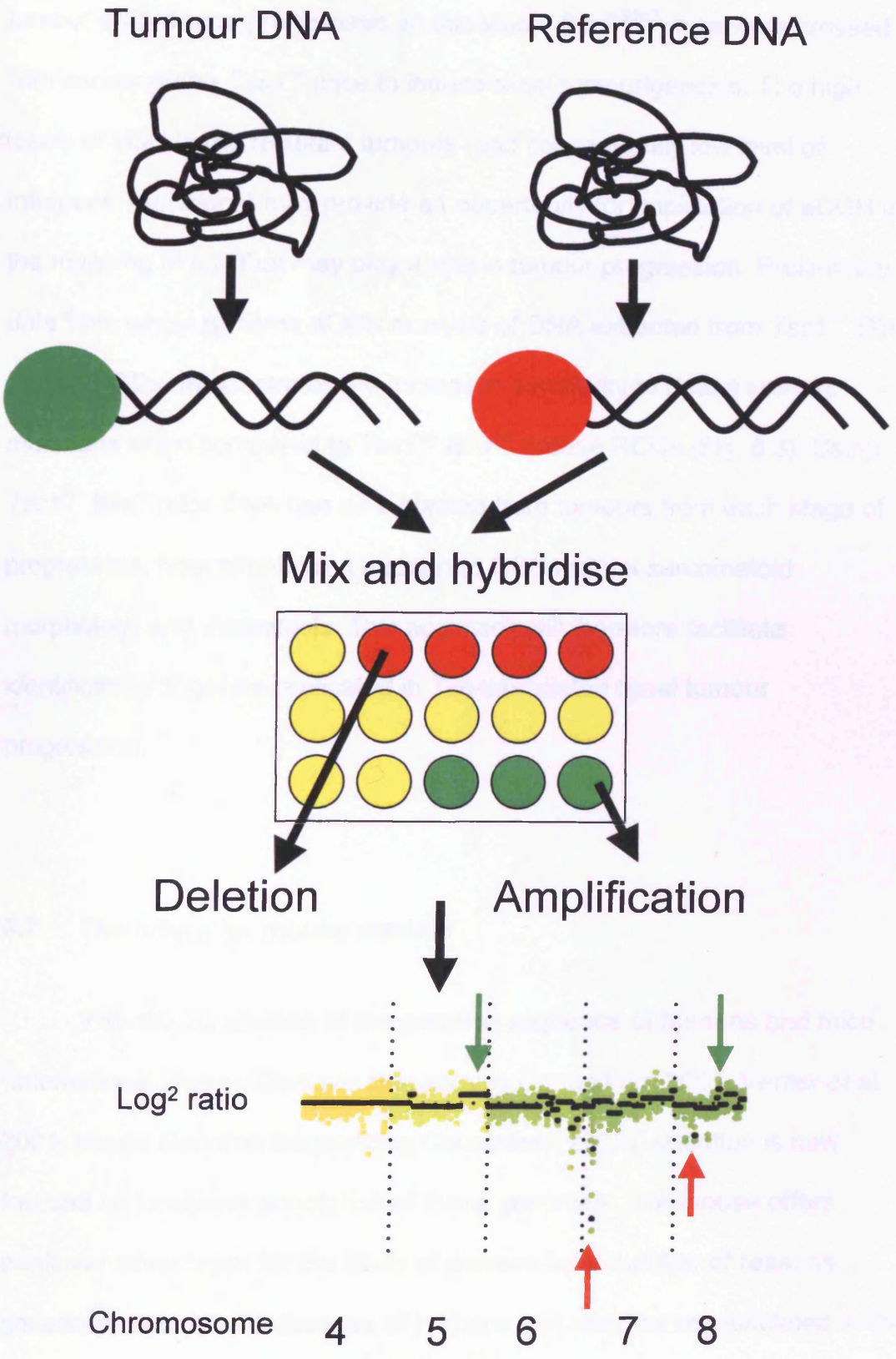

Figure 6.2: The process of array based comparative genomic hybridisation (aCGH). Firstly, both labelled tumour DNA (with Cy3 green) and normal genomic DNA (with Cy5 red) are co-hybridised to an array. A laser scanner reads spot intensities on the hybridised array. The relative intensities of Cy3:Cy5 for each spot and thus the ratios of normal to tumour DNA can be computed (red for deletion, green for amplification) and plotted for visual analysis (red arrows deleted areas of chromosomes, green duplicated areas of chromosome).

tumour progression problematic. In this study, *Blm*$^{m3/m3}$ mice were crossed with cancer prone *Tsc1*$^{+/-}$ mice to induce renal tumourigenesis. The high levels of LOH in the resultant tumours (and consequently low level of intragenic mutations) may provide an oppertunity for application of aCGH in the mapping of loci that may play a role in tumour progression. Preliminary data from whole genome aCGH analysis of DNA extracted from *Tsc1*$^{+/-}$ *Blm*$^{-/-}$ mouse RCCs demonstrates the increased sensitivity to detect somatic mutations when compared to *Tsc1*$^{+/-}$ *Blm*$^{+/+}$ mouse RCCs (Fig. 6.3). Using *Tsc1*$^{+/-}$ *Blm*$^{-/-}$ mice DNA can be extracted from tumours from each stage of progression, from simple cyst through to RCCs with a sarcomatoid morphology and metastasis. This approach will therefore facilitate identification of genes implicated in *Tsc*-associated renal tumour progression.

6.7 The future for mouse models

With the completion of the genome sequence of humans and mice (International Human Genome Sequencing Consortium 2001, Venter et al. 2001, Mouse Genome Sequencing Consortium 2002), attention is now focused on functional annotation of these genomes. The mouse offers particular advantages for the study of disease for a number of reasons; genetically determined diseases of humans can often be recapitulated in the mouse since 99% of mouse genes have human homologs and these can be easily manipulated with the use of targeted mutagenesis and ES cell technologies. However, to date published knockouts exist for only about 10%

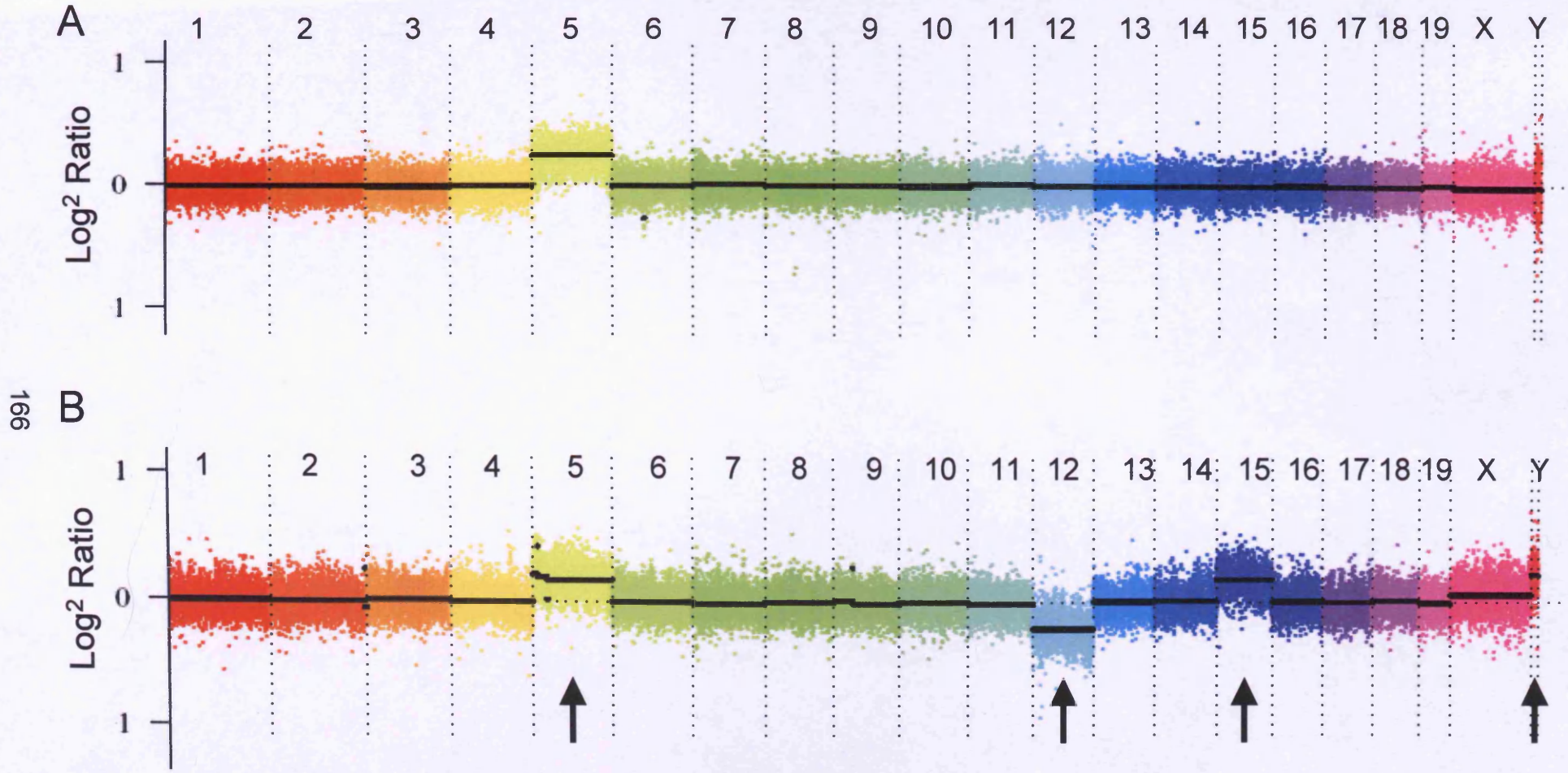

Figure 6.3: Preliminary data for whole genome aCGH analysis of DNA extracted from (A) a *Tsc1*$^{+/-}$ mouse RCC, and (B) a *Tsc1*$^{+/-}$ *Blm*$^{-/-}$ mouse RCC. DNA from the *Tsc1*$^{+/-}$ mouse RCC shows increased copy number of only chromosome 5, whereas DNA from the *Tsc1*$^{+/-}$ *Blm*$^{-/-}$ mouse RCC shows increased copy number of chromosomes 5, 15 and Y, and loss of chromosome 12 (arrows), therefore demonstrating the increased sensitivity to detect somatic mutations by aCGH analysis on a *Blm*-deficient background.

of mouse genes (The Comprehensive Knockout Mouse Project Consortium 2004). Large-scale mouse mutagenesis programs are currently being initiated (The Comprehensive Knockout Mouse Project Consortium 2004, The European Mouse Mutagenesis Consortium 2004) using gene targeting, gene trapping and RNA interference methods. The aim is to phenotype large numbers of mouse mutants with standardised screens and place these resources into the public domain (The Eumorphia Consortium 2005). These genome-wide knockout mouse projects could provide targeting and trapping constructs and vectors, ES cell lines, live mice, frozen embryos or sperm, tissue samples and phenotypic data (The Comprehensive Knockout Mouse Project Consortium 2004) and will help to relies the potential of the genome projects and their translation to benefit human health.

Publications resulting from this work

Wilson C, Idziaszczyk S, Parry L, Guy C, Griffiths DF, Lazda E, Bayne RA, Smith AJ, Sampson JR, Cheadle JP. (2005) A mouse model of tuberous sclerosis 1 showing background specific early post-natal mortality and metastatic renal cell carcinoma. *Hum Mol Genet.* 14(13): 1839-50.

Wilson C, Idziaszczyk S, Colley J, Humphreys V, Guy C, Maynard J, Sampson JR, Cheadle JP. (2005) Induction of renal tumorigenesis with elevated levels of somatic loss of heterozygosity in Tsc1+/- mice on a Blm-deficient background. *Cancer Res.* 65(22): 10179-82.

Wilson C, Bonnet C, Guy C, Idziaszczyk S, Colley J, Humphreys V, Maynard J, Sampson JR, Cheadle JP. (2006) *Tsc1*-haploinsufficiency without mTOR activation is sufficient for renal cyst formation in *Tsc1*$^{+/-}$ mice. *Cancer Res.* In press.

References

Aicher LD, Campbell JS, Yeung RS. (2001) Tuberin phosphorylation regulates its interaction with hamartin. Two proteins involved in tuberous sclerosis.
J Biol Chem. 276(24): 21017-21.

Albuquerque C, Breukel C, van der Luijt R, Fidalgo P, Lage P, Slors FJ, Leitao CN, Fodde R, Smits R. (2002) The 'just-right' signaling model: APC somatic mutations are selected based on a specific level of activation of the beta-catenin signaling cascade. *Hum Mol Genet.* 11(13): 1549-60.

Alberici P, Jagmohan-Changur S, De Pater E, Van Der Valk M, Smits R, Hohenstein P, Fodde R. (2005) Smad4 haploinsufficiency in mouse models for intestinal cancer. *Oncogene.* 25(13): 1841-51.

Armitage P, Doll R (2004) The age distribution of cancer and a multi-stage theory of carcinogenesis. *Int J Epidemiol.* 33(6): 1174-9.

Al-Saleem T, Wessner LL, Scheithauer BW, Patterson K, Roach ES, Dreyer SJ, Fujikawa K, Bjornsson J, Bernstein J, Henske EP. (1998) Malignant tumors of the kidney, brain, and soft tissues in children and young adults with the tuberous sclerosis complex. *Cancer.* 83(10): 2208-16.

Amieux PS, Howe DG, Knickerbocker H, Lee DC, Su T, Laszlo GS, Idzerda RL, McKnight GS. (2002) Increased basal cAMP-dependent protein kinase activity inhibits the formation of mesoderm-derived structures in the developing mouse embryo. *J Biol Chem.* 277(30): 27294-304.

Astrinidis A, Senapedis W, Coleman TR, Henske EP. (2003) Cell cycle-regulated phosphorylation of hamartin, the product of the tuberous sclerosis complex 1 gene, by cyclin-dependent kinase 1/cyclin B. *J Biol Chem.* 278(51): 51372-9.

Astrinidis A, Henske EP. (2005) Tuberous sclerosis complex: linking growth and energy signaling pathways with human disease. *Oncogene.* 24(50): 7475-81.

Au KS, Merrell J, Buckler A, Blanton SH, Northrup H. (1996) Report of a critical recombination further narrowing the TSC1 region. *J Med Genet* 33: 559-61.

Au KS, Williams AT, Gambello MJ, Northrup H. (2004) Molecular genetic basis of tuberous sclerosis complex: from bench to bedside. *J Child Neurol.* 19(9): 699-709.

Ayers KM, Jones SR. (1978) The cardiovascular system. In: *Pathology of laboratory animals Vol. 1.* Bernishke FM, Garner, Jones TC. Springer-Verlag, New York, Heidekberg, Berlin. 1-69.

Bardeesy N, Sinha M, Hezel AF, Signoretti S, Hathaway NA, Sharpless NE, Loda M, Carrasco DR, DePinho RA. (2002) Loss of the Lkb1 tumour suppressor provokes intestinal polyposis but resistance to transformation. *Nature*. 419(6903): 162-7.

Bass JL, Breningstall GN, Swaiman KF. (1985) Echocardiographic incidence of cardiac rhabdomyoma in tuberous sclerosis. *Am J Cardiol.* 55: 1379-1382.

Benvenuto G, Li S, Brown SJ, Braverman R, Vass WC, Cheadle JP, Halley DJ, Sampson JR, Wienecke R, DeClue JE. (2000) The tuberous sclerosis-1 (TSC1) gene product hamartin suppresses cell growth and augments the expression of the TSC2 product tuberin by inhibiting its ubiquitination. *Oncogene.* 19(54): 6306-16.

Berg H. (1913) Vererbung der tuberosen skerose durch zwei bzw. Drei Generationon. *Z. Ges. Neurol. Psychiatri.* 19:528-539.

Bernstein J. (1993) Renal cystic disease in the tuberous sclerosis complex. *Pediatr Nephrol.* 7(4): 490-5.

Bertherat J, Groussin L, Sandrini F, Matyakhina L, Bei T, Stergiopoulos S, Papageorgiou T, Bourdeau I, Kirschner LS, Vincent-Dejean C, Perlemoine K, Gicquel C, Bertagna X, Stratakis CA. (2003) Molecular and functional analysis of PRKAR1A and its locus (17q22-24) in sporadic adrenocortical

tumors: 17q losses, somatic mutations, and protein kinase A expression and activity. *Cancer Res.* 63(17): 5308-19.

Biesecker LG, Happle R, Mulliken JB, Weksberg R, Graham JM Jr, Viljoen DL, Cohen MM Jr. (1999) Proteus syndrome: diagnostic criteria, differential diagnosis, and patient evaluation. *Am J Med Genet.* 84(5): 389-95.

Birchenall-Roberts MC, Fu T, Bang OS, Dambach M, Resau JH, Sadowski CL, Bertolette DC, Lee HJ, Kim SJ, Ruscetti FW. (2004) Tuberous sclerosis complex 2 gene product interacts with human SMAD proteins. A molecular link of two tumor suppressor pathways. *J Biol Chem.* 279(24): 25605-13.

Bjornsson J, Short MP, Kwiatkowski DJ, Henske EP. (1996) Tuberous sclerosis-associated renal cell carcinoma. Clinical, pathological, and genetic features. *Am J Pathol.* 149(4): 1201-8.

Bjornsson J, Henske EP, Bernstein J. (1999) Renal manifestations In: Gomez, MR, Sampson, JR and Whittemore VH (1999) *The Tuberous sclerosis complex.* Oxford University press, Oxford, UK. 181-193.

Bloom D. (1954) Congenital telangiectatic erythema resembling lupus erythematosus in dwarfs; probably a syndrome entity. *AMA Am J Dis Child.* 88(6): 754-8.

Boehler A, Speich R, Russi EW, Weder W. (1996) Lung transplantation for lymphangioleiomyomatosis. *N Engl J Med.* 335(17): 1275-80.

Boardman LA, Thibodeau SN, Schaid DJ, Lindor NM, McDonnell SK, Burgart LJ, Ahlquist DA, Podratz KC, Pittelkow M, Hartmann LC. (1998) Increased risk for cancer in patients with the Peutz-Jeghers syndrome. *Ann Intern Med.* 128(11): 896-9.

Boulter C, Mulroy S, Webb S, Fleming S, Brindle K, Sandford R. (2001) Cardiovascular, skeletal, and renal defects in mice with a targeted disruption of the *Pkd1* gene. *Proc Natl Acad Sci USA.* 98: 12174-12179.

Bourneville DM. (1880) Sclerose tubereuse des circonvolutions cerebrales: idiotie et epilepsie hemiplegique. *Arch Neurol* (Paris) 1: 81-91.

Brugarolas J, Lei K, Hurley RL, Manning BD, Reiling JH, Hafen E, Witters LA, Ellisen LW, Kaelin WG Jr. (2004) Regulation of mTOR function in response to hypoxia by REDD1 and the TSC1/TSC2 tumor suppressor complex. *Genes Dev.* 18(23): 2893-904.

Byun DS, Cho K, Ryu BK, Lee MG, Park JI, Chae KS, Kim HJ, Chi SG. (2003) Frequent monoallelic deletion of PTEN and its reciprocal associatioin with PIK3CA amplification in gastric carcinoma. *Int J Cancer.* 104(3): 318-27.

Cancer research UK (http://www.cancerresearchuk.org/).

Carlton WW, Engelhardt JA. (1991) Atreial thrombosis: rat, mouse and hamster. In: *Cardiovascular and musculosketetal systems, Monographs on pathology of laboratory animals*. Jones TC, Mohr U, Hunt RD. Springer-Verlag, New York, Heidekberg, Berlin. 37-41.

Casey M, Vaughan CJ, He J, Hatcher CJ, Winter JM, Weremowicz S, Montgomery K, Kucherlapati R, Morton CC, Basson CT. (2000) Mutations in the protein kinase A R1alpha regulatory subunit cause familial cardiac myxomas and Carney complex. *J Clin Invest.* 106(5): R31-8.

Cavenee WK, Dryja TP, Phillips RA, Benedict WF, Godbout R, Gallie BL, Murphree AL, Strong LC, White RL. (1983) Expression of recessive alleles by chromosomal mechanisms in retinoblastoma. *Nature.* 305(5937): 779-84.

Cheadle JP, Reeve MP, Sampson JR, Kwiatkowski DJ. (2000a) Molecular genetic advances in tuberous sclerosis. Hum Genet. 107(2), 97-114.

Cheadle JP, Dobbie L, Idziaszczyk S, Hodges AK, Smith AJ, Sampson JR, Young J. (2000b) Genomic organization and comparative analysis of the mouse tuberous sclerosis 1 (*Tsc1*) locus. *Mamm Genome.* 11: 135-138.

Cheadle JP, Krawczak M, Thomas MW, Hodges AK, Al-Tassan N, Fleming N, Sampson JR. (2002) Different combinations of biallelic APC mutation

confer different growth advantages in colorectal tumours. *Cancer Res.* 62(2): 363-6.

Chen Y, Yee D, Dains K, Chatterjee A, Cavalcoli J, Schneider E, Om J, Woychik RP, Magnuson T. (2000) Genotype-based screen for ENU-induced mutations in mouse embryonic stem cells. *Nat Genet.* 24(3): 314-7.

Cheok CF, Bachrati CZ, Chan KL, Ralf C, Wu L, Hickson I. (2005) Roles of the Bloom's syndrome helicase in the maintenance of genome stability. *Biochem Soc Trans.* 33(6): 1456-9.

Chester N, Kuo F, Kozak C, O'Hara CD, Leder P. (1998) Stage-specific apoptosis, developmental delay, and embryonic lethality in mice homozygous for a targeted disruption in the murine Bloom's syndrome gene. *Genes Dev.* 12(21): 3382-93.

Chow E, Macrae F. (2005) A review of juvenile polyposis syndrome. J *Gastroenterol Hepatol.* 20(11): 1634-40.

The Comprehensive Knockout Mouse Project Consortium. (2004) The Knockout Mouse Project. *Nature Genetics.* 36(9): 921-924.

Connor JM, Pirrit LA, Yates JR, Fryer AE, Ferguson-Smith MA. (1987) Linkage of the tuberous sclerosis locus to a DNA polymorphism detected by v-abl. *J Med Genet.* 24(9): 544-6.

Cook JA, Oliver K, Mueller RF, Sampson JA. (1996) Cross sectional study of renal involvement in tuberous sclerosis. *J Med Genet.* 33(6): 480-4.

Cristofano AD, Pesce B, Cordon-Cardo C, Pandolfi PP. (1998) *Pten* is essential for embryonic development and tumour suppression. *Nature Genetics.* 19: 348-355.

Curatolo P, Cusmai R, Cortesi F, Chiron C, Jambaque I, Dulac O. (1991) Neuropsychiatric aspects of tuberous sclerosis. *Ann N Y Acad Sci.* 615: 8-16.

Curatolo P. (2003) Tuberous Sclerosis Complex From Basic Science to Clinical Phenotypes *Ed.* by Paolo Curatolo. Mac Keith press, London, UK.

Dan HC, Sun M, Yang L, Feldman RI, Sui XM, Ou CC, Nellist M, Yeung RS, Halley DJ, Nicosia SV, Pledger WJ, Cheng JQ. (2002) Phosphatidylinositol 3-kinase/Akt pathway regulates tuberous sclerosis tumor suppressor complex by phosphorylation of tuberin. *J Biol Chem.* 277(38): 35364-70.

Dabora SL, Jozwiak S, Franz DN, Roberts PS, Nieto A, Chung J, Choy YS, Reeve MP, Thiele E, Egelhoff JC, Kasprzyk-Obara J, Domanska-Pakiela D, Kwiatkowski DJ. (2001) Mutational analysis in a cohort of 224 tuberous sclerosis patients indicates increased severity of TSC2, compared with TSC1, disease in multiple organs. *Am J Hum Genet.* 68(1): 64-80.

Dawson J. (1954) Pulmonary tuberous sclerosis and its relation to other forms of a disease. *Q. J. Med.* 23: 113-145.

Di Cristofano A, Pesce B, Cordon-Cardo C, Pandolfi PP. (1998) *Pten* is essential for embryonic development and tumour suppression. *Nat. Genet.* 19: 348-355.

Di Cristofano A, Pandolfi PP. (2000) The multiple roles of PTEN in tumor suppression. *Cell.* 100(4): 387-90.

El-Hashemite N, Walker V, Kwiatkowski DJ. (2005) Estrogen enhances whereas tamoxifen retards development of Tsc mouse liver hemangioma: a tumor related to renal angiomyolipoma and pulmonary lymphangioleiomyomatosis. *Cancer Res.* 65(6): 2474-81.

Eng C. (2000) Will the real Cowden syndrome please stand up: revised diagnostic criteria. *J Med Genet.* 37(11): 828-30.

Eng C. (2003) PTEN: one gene, many syndromes. *Hum Mutat.* 22(3): 183-98.

Entius MM, Keller JJ, Westerman AM, van Rees BP, van Velthuysen ML, de Goeij AF, Wilson JH, Giardiello FM, Offerhaus GJ. (2001) Molecular genetic

alterations in hamartomatous polyps and carcinomas of patients with Peutz-Jeghers syndrome. *J Clin Pathol.* 54(2): 126-31.

Eker R (1954) Acta path et microbiol *Scand.* 34: 554.

Eker R, Mossige J. (1961) A dominant gene for renal adenomas in the rat. *Nature.* 189: 858-859.

Eker R, Mossige J, Johannessen JV, Aars H. (1981) Hereditary renal adenomas and adenocarcinomas in rats. *Diagn Histopathol.* 4(1): 99-110.

The European Polycystic Kidney Disease Consortium. (1994) The polycystic kidney disease 1 gene encodes a 14 kb transcript and lies within a duplicated region on chromosome 16. *Cell.* 78(4): 725.

The European Chromosome 16 Tuberous Sclerosis Consortium. (1993) Identification and characterization of the tuberous sclerosis gene on chromosome 16. *Cell.* 75(7): 1305-15.

The European Mouse Mutagenesis Consortium. (2004) The European dimension for the mouse genome mutagenesis program. *Nature Genetics.* 36(9): 925-927.

The Eumorphia Consortium. (2005) EMPReSS: standardized phenotype screens for functional annotation of the mouse genome. *Nature Genetics.* 37(11): 1155.

Evans MJ, Kaufman MH. (1981) Establishment in culture of pluripotential cells from mouse embryos. *Nature.* 292(5819): 154-6.

Everitt, JI, Goldsworthy TL, Wolf DC, Walker CL. (1992) Hereditary renal cell carcinoma in the Eker rat: a rodent familial cancer syndrome. *J. Urol.* 148: 1932-1936.

Ewalt DH, Sheffield E, Sparagana SP, Delgado MR, Roach ES. (1998) Renal lesion growth in children with tuberous sclerosis complex. *J Urol.* 160(1): 141-5.

Fearon ER, Vogelstein B. (1990) A genetic model for colorectal tumorigenesis. *Cell.* 61(5): 759-67.

Fearon ER. Vogelstein B. (2000) Tumor Suppressor Gene Defects in Human Cancer In: Bast RC, Kufe DW, Pollock RE, Weichselbaum RR, Holland JF, Frei E, Gansler TS. (2000) *Cancer Medicine e.5.* B.C. Decker Inc. Hamilton, Ontario, Canada.

Fenoglio JJ Jr, MCAllister HA Jr, Ferrans VJ. (1976) Cardiac rhabdomyoma: a clinicopathologic and electron microscopic study. *Am J Cardiol.* 38(2): 241-51.

Fero ML, Randel E, Gurley KE, Roberts JM, Kemp CJ. (1998) The murine gene p27Kip1 is haplo-insufficient for tumour suppression. *Nature.* 396(6707): 177-80.

Flannagan N, Watson R, O'Connor WJ. (1995) Developmental enamel defects in tuberopus sclerosis- a genetic marker. *Br. J. Dermatol.* 133: 51.

Fodde R. Smits. (2002) Cancer biology: A matter of dosage. *Science.* 298(5594): 761-3.

Franz DN, Leonard J, Tudor C, Chuck G, Care M, Sethuraman G, Dinopoulos A, Thomas G, Crone KR. (2006) Rapamycin causes regression of astrocytomas in tuberous sclerosis complex. *Ann Neurol.* 59(3): 490-8.

Frith CH, Highman B, Burger G, Sheldon WD. (1983) Spontaneous lesions in virgin and retired breeder BALB/c and C57BL/6 mice. *Lab Anim Sci.* 33(3): 273-86.

Fryer AE, Chalmers A, Connor JM, Fraser I, Povey S, Yates AD, Yates JR, Osborne JP. (1987) Evidence that the gene for tuberous sclerosis is on chromosome 9. *Lancet.* 1(8534): 659-61.

Fukuda T, Kobayashi T, Momose S, Yasui H, Hino O. (2000) Distribution of Tsc1 protein detected by immunohistochemistry in various normal rat tissues and the renal carcinomas of Eker rat: detection of limited colocalization with Tsc1 and Tsc2 gene products in vivo. *Lab Invest.* 80(9): 1347-59.

Gao X, Pan D. (2001) TSC1 and TSC2 tumor suppressors antagonize insulin signaling in cell growth. *Genes Dev.* 15(11): 1383-92.

Gao X, Zhang Y, Arrazola P, Hino O, Kobayashi T, Yeung RS, Ru B, Pan D. (2002) Tsc tumour suppressor proteins antagonize amino-acid-TOR signalling. *Nat Cell Biol.* (9): 699-704.

German J. (1993) Blooms syndrome: a mendelian prototype of somatic mutational disease. *Medicine (Baltimore)* 72(6): 393-406.

German J, Roe AM, Leppert MF, Ellis N A. (1994) Bloom syndrome: an analysis of consanguineous families assigns the locus mutated to chromosome band 15q26.1. *Proc. Nat. Acad. Sci.* 91: 6669-6673.

Giardiello FM, Welsh SB, Hamilton SR, Offerhaus GJ, Gittelsohn AM, Booker SV, Krush AJ, Yardley JH, Luk GD. (1987) Increased risk of cancer in the Peutz-Jeghers syndrome. *N Engl J Med.* 316(24): 1511-4.

Giardiello FM, Brensinger JD, Tersmette AC, Goodman SN, Petersen GM, Booker SV, Cruz-Correa M, Offerhaus JA. (2000) Very high risk of cancer in familial Peutz-Jeghers syndrome. *Gastroenterology*. 119(6): 1447-53.

Gillberg IC, Gillberg C, Ahlsen G. (1994) Autistic behaviour and attention deficits in tuberous sclerosis: a population-based study. *Dev Med Child Neurol*. 36(1): 50-6.

Gomez MR. (1979) Tuberous sclerosis. New York: Raven Press.

Gomez MR. (1988) Critera for diagnosis. In: Gomez MR. (1988) *Tuberous sclerosis. 2nd edition.* New York: Raven Press 9-19.

Gomez MR, Sampson JR. Whittemore VH. (1999) The Tuberous sclerosis complex. Oxford University press, Oxford, UK.

Goodman M, Lamm SH, Engel A, Shepherd CW, Houser OW, Gomez MR. (1997) Cortical tuber count: a biomarker indicating neurologic severity of tuberous sclerosis complex. *J Child Neurol*. 12(2): 85-90.

Gordon JW, Scangos GA, Plotkin DJ, Barbosa JA, Ruddle FH. (1980) Genetic transformation of mouse embryos by microinjection of purified DNA. *Proc Natl Acad Sci USA*. 77(12): 7380-4.

Gorlin RJ, Cohen MM Jr, Condon LM, Burke BA. (1992) Bannayan-Riley-Ruvalcaba syndrome. *Am J Med Genet.* 44(3): 307-14.

Goss KH, Risinger MA, Kordich JJ, Sanz MM, Straughen JE, Slovek LE, Capobianco AJ, German J, Boivin GP, Groden J. (2002) Enhanced tumor formation in mice heterozygous for Blm mutation. *Science.* 297(5589): 2051-3.

Griffin KJ, Kirschner LS, Matyakhina L, Stergiopoulos S, Robinson-White A, Weinberg F, Meoli E, Bornstein SR, Stratakis CA. (2004) A mouse model for Carney complex. *Endocr Res.* 30(4): 903-11.

Groussin L, Jullian E, Perlemoine K, Louvel A, Leheup B, Luton JP, Bertagna X, Bertherat J. (2002) Mutations of the PRKAR1A gene in Cushing's syndrome due to sporadic primary pigmented nodular adrenocortical disease. *J Clin Endocrinol Metab.* 87(9): 4324-9.

Gruber SB, Entius MM, Petersen GM, Laken SJ, Longo PA, Boyer R, Levin AM, Mujumdar UJ, Trent JM, Kinzler KW, Vogelstein B, Hamilton SR, Polymeropoulos MH, Offerhaus GJ, Giardiello FM. (1998) Pathogenesis of adenocarcinoma in Peutz-Jeghers syndrome. *Cancer Res.* 58(23): 5267-70.

Gruber SB, Ellis NA, Scott KK, *et al.* BLM heterozygosity and the risk of colorectal cancer. Science 2002;297:2013.

Guertin DA, Sabatini DM. (2005) An expanding role for mTOR in cancer. *Trends Mol Med.* 11(8): 353-61.

Guo G, Wang W, Bradley A. (2004) Mismatch repair genes identified using genetic screens in Blm-deficient embryonic stem cells. *Nature.* 429(6994): 891-5.

Gutmann DH, Zhang Y, Hasbani MJ, Goldberg MP, Plank TL, Petri Henske E. (2000) Expression of the tuberous sclerosis complex gene products, hamartin and tuberin, in central nervous system tissues. *Acta Neuropathol (Berl).* 99(3): 223-30.

Gunther M, Penrose LS. (1935) The genetics of epiloia. *J. Genet.* 31: 413-430.

Haddad LA, Smith N, Bowser M, Niida Y, Murthy V, Gonzalez-Agosti C, Ramesh V. (2002) The TSC1 tumor suppressor hamartin interacts with neurofilament-L and possibly functions as a novel integrator of the neuronal cytoskeleton. *J Biol Chem.* 277(46): 44180-6.

Hahn WC, Counter CM, Lundberg AS, Beijersbergen RL, Brooks MW, Weinberg RA. (1999) Creation of human tumour cells with defined genetic elements. *Nature.* 400(6743): 464-8.

Haines JL, Short MP, Kwiatkowski DJ, Jewell A, Andermann E, Bejjani B, Yang CH, Gusella JF, Amos JA. (1991) Localization of one gene for tuberous sclerosis within 9q32-9q34, and further evidence for heterogeneity. *Am J Hum Genet.* 49(4): 764-72.

Han S, Santos TM, Puga A, Roy J, Thiele EA, McCollin M, Stemmer-Rachamimov A, Ramesh V. (2004) Phosphorylation of tuberin as a novel mechanism for somatic inactivation of the tuberous sclerosis complex proteins in brain lesions. *Cancer Res.* 64(3): 812-6.

Hardie DG. (2005) New roles for the LKB1-->AMPK pathway. *Curr Opin Cell Biol.* 17(2): 167-73.

Harrington LS, Findlay GM, Gray A, Tolkacheva T, Wigfield S, Rebholz H, Barnett J, Leslie NR, Cheng S, Shepherd PR, Gout I, Downes CP, Lamb RF. (2004) The TSC1-2 tumor suppressor controls insulin-PI3K signaling via regulation of IRS proteins. *J Cell Biol.* 166(2): 213-23.

Heitman J, Movva NR, Hall MN. (1991) Targets for cell cycle arrest by the immunosuppressant rapamycin in yeast. *Science.* 253(5022): 905-9.

Hemminki A, Markie D, Tomlinson I, Avizienyte E, Roth S, Loukola A, Bignell G, Warren W, Aminoff M, Hoglund P, Jarvinen H, Kristo P, Pelin K, Ridanpaa M, Salovaara R, Toro T, Bodmer W, Olschwang S, Olsen AS, Stratton MR, de la Chapelle A, Aaltonen LA. (1998) A serine/threonine kinase gene defective in Peutz-Jeghers syndrome. *Nature.* 391(6663): 184-7.

Henske EP, Scheithauer BW, Short MP, Wollmann R, Nahmias J, Hornigold N, van Slegtenhorst M, Welsh CT, Kwiatkowski DJ. (1996) Allelic loss is frequent in tuberous sclerosis kidney lesions but rare in brain lesions. *Am J Hum Genet.* 59(2): 400-6.

Henske EP. (2003) Metastasis of benign tumor cells in tuberous sclerosis complex. Genes Chromosomes *Cancer.* 38(4): 376-81.

Henske EP. (2004) The genetic basis of kidney cancer: why is tuberous sclerosis complex often overlooked? *Curr Mol Med.* 4(8): 825-31.

Hickson ID. (2003) RecQ helicases: caretakers of the genome. *Nat Rev Cancer.* 3(3): 169-78.

Hino O, Mitani H, Nishizawa M, Katsuyama H, Kobayashi E, Hirayama Y. (1993a) A novel renal cell carcinoma susceptibility gene maps on chromosome 10 in the Eker rat. *Jpn J Cancer Res.* 84(11): 1106-9.

Hino O, Klein-Szanto AJ, Freed JJ, Testa JR, Brown DQ, Vilensky M, Yeung RS, Tartof KD, Knudson AG. (1993b) Spontaneous and radiation-induced renal tumors in the Eker rat model of dominantly inherited cancer. *Proc Natl Acad Sci USA.* 90(1): 327-31.

Hino O, Kobayashi T, Tsuchiya H, Kikuchi Y, Kobayashi E, Mitani H, Hirayama Y. (1994) The predisposing gene of the Eker rat inherited cancer syndrome is tightly linked to the tuberous sclerosis (TSC2) gene. *Biochem Biophys Res Commun.* 203(2): 1302-8.

Hino O, Okimoto K, Kouchi M, Sakurai J. (2001) A novel renal carcinoma predisposing gene of the Nihon rat maps on chromosome 10. *Jpn J Cancer Res.* 92(11): 1147-9.

Hino O, Kobayashi T, Momose S, Kikuchi Y, Adachi H, Okimoto K. (2003) Renal carcinogenesis: genotype, phenotype and dramatype. *Cancer Sci.* 94(2): 142-7.

van der Hoeve J. (1920) Eye symptons in tuberous sclerosis of the brain. *Trans Ophthalmol Soc UK.* 20: 329-34.

Hodges AK, Li S, Maynard J, Parry L, Braverman R, Cheadle JP, DeClue JE, Sampson JR. (2001) Pathological mutations in TSC1 and TSC2 disrupt the interaction between hamartin and tuberin. *Hum Mol Genet.* 10(25): 2899-905.

Hornigold N, van Slegtenhorst M, Nahmias J, Ekong R, Rousseaux S, Hermans C, Halley D, Povey S, Wolfe J. (1997) A 1.7-megabase sequence-ready cosmid contig covering the TSC1 candidate region in 9q34.*Genomics.* 41(3): 385-9.

Hosoya M, Naito H, Nihei K. (1999) Neurological prognosis correlated with variations over time in the number of subependymal nodules in tuberous sclerosis. *Brain Dev.* 21(8): 544-7.

Howe JR, Roth S, Ringold JC, Summers RW, Jarvinen HJ, Sistonen P, Tomlinson IP, Houlston RS, Bevan S, Mitros FA, Stone EM, Aaltonen LA. (1998) Mutations in the SMAD4/DPC4 gene in juvenile polyposis. *Science.* 280(5366): 1086-8.

Hrabe de Angelis M, Balling R. (1998) Large scale ENU screens in the mouse: genetics meets genomics. *Mutat Res.* 400(1-2): 25-32.

Ito N, Rubin GM. (1999) Gigas, a Drosophila homolog of tuberous sclerosis gene product-2, regulates the cell cycle. *Cell.* 96(4): 529-39.

Inoki K, Li Y, Xu T, Guan KL. (2003a) Rheb GTPase is a direct target of TSC2 GAP activity and regulates mTOR signaling. *Genes Dev.* 17(15): 1829-34.

Inoki K, Zhu T, Guan KL. (2003b) TSC2 mediates cellular energy response to control cell growth and survival. *Cell.* 115(5): 577-90.

Inoki K, Corradetti MN, Guan KL. (2005) Dysregulation of the TSC-mTOR pathway in human disease. *Nat Genet.* 37(1): 19-24.

International Human Genome Sequencing Consortium. (2001) Initial sequencing and analysis of the human genome. *Nature*. 409(6822): 860-921.

Janssen LA, Sandkuyl LA, Merkens EC, Maat-Kievit JA, Sampson JR, Fleury P, Hennekam RC, Grosveld GC, Lindhout D, Halley DJ. (1990) Genetic heterogeneity in tuberous sclerosis. *Genomics*. 8(2): 237-42.

Janssen B, Sampson J, van der Est M, Deelen W, Verhoef S, Daniels I, Hesseling A, Brook-Carter P, Nellist M, Lindhout D, et al. (1994) Refined localization of TSC1 by combined analysis of 9q34 and 16p13 data in 14 tuberous sclerosis families. *Hum Genet*. 94(4):437-40.

Jeghers H, McKusick VA, Katz KH. (1949) Generalized intestinal polyposis and melanin spots of the oral mucosa, lips and digits; a syndrome of diagnostic significance, *N Engl J Med* 241: 993–1005, 1031–36.

Jenne DE, Reimann H, Nezu J, Friedel W, Loff S, Jeschke R, Muller O, Back W, Zimmer M. (1998) Peutz-Jeghers syndrome is caused by mutations in a novel serine threonine kinase. *Nat Genet*. 18(1): 38-43.

Jishage K, Nezu J, Kawase Y, Iwata T, Watanabe M, Miyoshi A, Ose A, Habu K, Kake T, Kamada N, Ueda O, Kinoshita M, Jenne DE, Shimane M, Suzuki H. (2002) Role of Lkb1, the causative gene of Peutz-Jegher's syndrome, in embryogenesis and polyposis. *Proc Natl Acad Sci USA*. 99(13): 8903-8.

Jones AC, Daniells CE, Snell RG, Tachataki M, Idziaszczyk SA, Krawczak M, Sampson JR, Cheadle JP. (1997) Molecular genetic and phenotypic analysis reveals differences between TSC1 and TSC2 associated familial and sporadic tuberous sclerosis. *Hum Mol Genet.* 6(12): 2155-61.

Jones AC, Shyamsundar MM, Thomas MW, Maynard J, Idziaszczyk S, Tomkins S, Sampson JR, Cheadle JP. (1999) Comprehensive mutation analysis of TSC1 and TSC2-and phenotypic correlations in 150 families with tuberous sclerosis. *Am J Hum Genet.* 64(5): 1305-15.

Johnson MW, Kerfoot C, Bushnell T, Li M, Vinters HV. (2001) Hamartin and tuberin expression in human tissues. *Mod Pathol.* 14(3): 202-10.

Jozwiak S, Pedich M, Rajszys P, Michalowicz R. (1992) Incidence of hepatic hamartomas in tuberous sclerosis. *Arch Dis Child.* 67(11): 1363-5.

Jozwiak S, Kawalec W, Dluzewska J, Daszkowska J, Mirkowicz-Malek M, Michalowicz R. (1994) Cardiac tumours in tuberous sclerosis: their incidence and course. *Eur J Pediatr.* 153(3): 155-7.

Jozwiak J, Jozwiak S, Grzela T, Lazarczyk M. (2005) Positive and negative regulation of TSC2 activity and its effects on downstream effectors of the mTOR pathway. *Neuromolecular Med.* 7(4): 287-96.

Kamada Y, Sekito T, Ohsumi Y. (2004) Autophagy in yeast: a TOR-mediated response to nutrient starvation. *Curr Top Microbiol Immunol.* 279: 73-84.

Karbowniczek M, Astrinidis A, Balsara BR, Testa JR, Lium JH, Colby TV, McCormack FX, Henske EP. (2003) Recurrent lymphangiomyomatosis after transplantation: genetic analyses reveal a metastatic mechanism. *Am J Respir Crit Care Med.* 167(7): 976-82.

Kandt RS, Pericak-Vance MA, Hung WY, Gardner RJ, Nellist M, Phillips K, Warner K, Speer MC, Crossen PE, Laing NG, et al. (1989) Absence of linkage of ABO blood group locus to familial tuberous sclerosis. *Exp Neurol.* 104(3): 223-8.

Kandt RS, Haines JL, Smith M, Northrup H, Gardner RJ, Short MP, Dumars K, Roach ES, Steingold S, Wall S, et al. (1992) Linkage of an important gene locus for tuberous sclerosis to a chromosome 16 marker for polycystic kidney disease. *Nat Genet.* 2(1): 37-41.

Kenerson H, Dundon TA, Yeung RS. (2005) Effects of rapamycin in the Eker rat model of tuberous sclerosis complex. *Pediatr Res.* 57(1): 67-75.

Kirschner LS, Sandrini F, Monbo J, Lin JP, Carney JA, Stratakis CA. (2000a) Genetic heterogeneity and spectrum of mutations of the PRKAR1A gene in patients with the carney complex. *Hum Mol Genet.* 9(20): 3037-46.

Kirschner LS, Carney JA, Pack SD, Taymans SE, Giatzakis C, Cho YS, Cho-Chung YS, Stratakis CA. (2000b) Mutations of the gene encoding the protein kinase A type I-alpha regulatory subunit in patients with the Carney complex. *Nat Genet.* 26(1): 89-92.

Kirpicznik J.(1910) Ein fall von Tuberoser Sklerose und gleichzeitigen multiplen Nierengeschwulsten. *Virchows Arch F Path Anat.* 202: 358.

Kleymenova E, Everitt JI, Pluta L, Portis M, Gnarra JR, Walker CL. (2004) Susceptibility to vascular neoplasms but no increased susceptibility to renal carcinogenesis in Vhl knockout mice. *Carcinogenesis.* 25(3): 309-15.

Klysik J. (2002) Mice and humans: chromosome engineering and its application to functional genomics. *Acta Biochim Pol.* 49(3): 553-69.

Knudson AG. Jr. (1971) Mutation and cancer: statistical study of retinoblastoma. *Proc Natl Acad Sci USA.* 68: 820-823.

Knudson (1996) Hereditary cancer: two hits revisited. *J Cancer Res Clin Oncol.*122(3): 135-40.

Kobayashi T, Hirayama Y, Kobayashi E, Kubo Y, Hino O. (1995) A germline insertion in the tuberous sclerosis (Tsc2) gene gives rise to the Eker rat model of dominantly inherited cancer. *Nat Genet.* 9(1): 70-4.

Kobayashi T, Urakami S, Cheadle JP, Aspinwall R, Harris P, Sampson JR, Hino O. (1997) Identification of a leader exon and a core promoter for the rat tuberous sclerosis 2 (Tsc2) gene and structural comparison with the human homolog. *Mamm Genome.* 8(8): 554-8.

Kobayashi T, Minowa O, Kuno J, Mitani H, Hino O, Noda T. (1999) Renal carcinogenesis, hepatic hemangiomatosis, and embryonic lethality caused by a germ-line Tsc2 mutation in mice. *Cancer Res.* 59(6): 1206-11.

Kobayashi T, Minowa O, Sugitani Y, Takai S, Mitani H, Kobayashi E, Noda T, Hino OA. (2001) A germ-line Tsc1 mutation causes tumor development and embryonic lethality that are similar, but not identical to, those caused by Tsc2 mutation in mice. *Proc Natl Acad Sci USA.* 98(15): 8762-7.

Kouchi M, Okimoto K, Matsumoto I, Tanaka K, Yasuba M, Hino O. (2006) Natural history of the Nihon (Bhd gene mutant) rat, a novel model for human Birt-Hogg-Dube syndrome. *Virchows Arch.*;448(4): 463-71.

Koyama M, Ito M, Nagai H, Emi M, Moriyama Y. (1999) Inactivation of both alleles of the DPC4/SMAD4 gene in advanced colorectal cancers: identification of seven novel somatic mutations in tumors from Japanese patients. *Mutat Res.* 406(2-4): 71-7.

Kreidberg JA, Sariola H, Loring JM, Maeda M, Pelletier J, Housman D, Jaenisch R. (1993) WT-1 is required for early kidney development. *Cell.* 74(4): 679-91.

Kubo Y, Kikuchi Y, Mitani H, Kobayashi E, Kobayashi T, Hino O. (1995) Allelic loss at the tuberous sclerosis (Tsc2) gene locus in spontaneous uterine leiomyosarcomas and pituitary adenomas in the Eker rat model. *Jpn J Cancer Res.* 86(9): 828-32.

Kuma A, Hatano M, Matsui M, Yamamoto A, Nakaya H, Yoshimori T, Ohsumi Y, Tokuhisa T, Mizushima N. (2004) The role of autophagy during the early neonatal starvation period. *Nature.* 432(7020): 1032-6.

Kumar RA, Chan KL, Wong AH, Little KQ, Rajcan-Separovic E, Abrahams BS, Simpson EM. (2004) Unexpected embryonic stem (ES) cell mutations represent a concern in gene targeting: lessons from "fierce" mice. *Genesis* 38: 51-57.

Kuraguchi M, Yang K, Wong E, Avdievich E, Fan K, Kolodner RD, Lipkin M, Brown AM, Kucherlapati R, Edelmann W. (2001) The distinct spectra of tumor-associated Apc mutations in mismatch repair-deficient Apc1638N mice define the roles of MSH3 and MSH6 in DNA repair and intestinal tumorigenesis. *Cancer Res.* 61(21): 7934-42.

Kwiatkowski DJ, Short MP. (1994) Tuberous sclerosis. *Arch Dermatol.* 130(3): 348-54.

Kwiatkowski DJ, Zhang H, Bandura JL, Heiberger KM, Glogauer M, el-Hashemite N, Onda H. (2002) A mouse model of TSC1 reveals sex-dependent lethality from liver hemangiomas, and up-regulation of p70S6 kinase activity in Tsc1 null cells. *Hum Mol Genet.* 11(5): 525-34.

Kwiatkowski DJ. (2005a) TSC1, TSC2, TSC3? or mosaicism? *Euro J Hum Genet.* 13: 695-696.

Kwiatkowski DJ, Manning BD. (2005b) Tuberous sclerosis: a GAP at the crossroads of multiple signaling pathways. *Hum Mol Genet.* 14(2): R251-8.

Lamb RF, Roy C, Diefenbach TJ, Vinters HV, Johnson MW, Jay DG, Hall A. (2000) The TSC1 tumour suppressor hamartin regulates cell adhesion through ERM proteins and the GTPase Rho. *Nat Cell Biol.* 2(5): 281-7.

Lamlum H, Ilyas M, Rowan A, Clark S, Johnson V, Bell J, Frayling I, Efstathiou J, Pack K, Payne S, Roylance R, Gorman P, Sheer D, Neale K, Phillips R, Talbot I, Bodmer W, Tomlinson I. (1999) The type of somatic mutation at APC in familial adenomatous polyposis is determined by the site of the germline mutation: a new facet to Knudson's 'two-hit' hypothesis. *Nat Med.* 5(9): 1071-5.

Lee L, Sudentas P, Donohue B, Asrican K, Worku A, Walker V, Sun Y, Schmidt K, Albert MS, El-Hashemite N, Lader AS, Onda H, Zhang H, Kwiatkowski DJ, Dabora SL. (2005) Efficacy of a rapamycin analog (CCI-779) and IFN-gamma in tuberous sclerosis mouse models.*Genes Chromosomes Cancer.* 42(3): 213-27.

Lee-Jones L, Aligianis I, Davies PA, Puga A, Farndon PA, Stemmer-Rachamimov A, Ramesh V, Sampson JR. (2004) Sacrococcygeal chordomas in patients with tuberous sclerosis complex show somatic loss of TSC1 or TSC2. *Genes Chromosomes Cancer.* 41(1): 80-5.

Lewandoski M. (2001) Conditional control of gene expression in the mouse. *Nat Rev Genet.* 2(10): 743-55.

Li J, Yen C, Liaw D, Podsypanina K, Bose S, Wang SI, Puc J, Miliaresis C, Rodgers L, McCombie R, Bigner SH, Giovanella BC, Ittmann M, Tycko B, Hibshoosh H, Wigler MH, Parsons R. (1997) PTEN, a putative protein tyrosine phosphatase gene mutated in human brain, breast, and prostate cancer. *Science.* 275(5308): 1943-7.

Li L, He F, Litofsky NS, Recht LD, Ross AH. (2003a) Profiling of genes expressed by PTEN haploinsufficient neural precursor cells. *Mol Cell Neurosci.* 24(4): 1051-61.

Li Y, Inoki K, Vacratsis P, Guan KL. (2003b) The p38 and MK2 kinase cascade phosphorylates tuberin, the tuberous sclerosis 2 gene product, and enhances its interaction with 14-3-3. *J Biol Chem.* 278(16): 13663-71.

Liang TJ, Reid AE, Xavier R, Cardiff RD, Wang TC. (1996) Transgenic expression of tpr-met oncogene leads to development of mammary hyperplasia and tumors. *J Clin Invest.* 97(12): 2872-7.

Luo G, Santoro IM, McDaniel LD, Nishijima I, Mills M, Youssoufian H, Vogel H, Schultz RA, Bradley A. (2000) Cancer predisposition caused by elevated mitotic recombination in Bloom mice. *Nat Genet.* 26(4): 424-9.

Lou D, Griffith N, Noonan DJ. (2001) The tuberous sclerosis 2 gene product can localize to nuclei in a phosphorylation-dependent manner. *Mol Cell Biol Res Commun.* 4(6): 374-80.

Ma L, Chen Z, Erdjument-Bromage H, Tempst P, Pandolfi PP. (2005) Phosphorylation and functional inactivation of TSC2 by Erk implications for tuberous sclerosis and cancer pathogenesis. *Cell.* 121(2): 179-93.

Ma L, Teruya-Feldstein J, Behrendt N, Chen Z, Noda T, Hino O, Cordon-Cardo C, Pandolfi PP. (2005) Genetic analysis of Pten and Tsc2 functional interactions in the mouse reveals asymmetrical haploinsufficiency in tumor suppression. *Genes Dev.* 19(15): 1779-86.

Mair DD, Edwards WD, Seward JB. (1999) Cardiac manifestations. In Gomez MR, Sampson JR, Whittemore VH. *The Tuberous sclerosis complex.* Oxford University press, Oxford, UK. pp 194-206.

Mak BC, Takemaru K, Kenerson HL, Moon RT, Yeung RS. (2003) The tuberin-hamartin complex negatively regulates beta-catenin signaling activity. *J Biol Chem.* 278(8): 5947-51.

Mak BC, Kenerson HL, Aicher LD, Barnes EA, Yeung RS. (2005) Aberrant beta-catenin signaling in tuberous sclerosis. *Am J Pathol.* 167(1): 107-16.

Mankouri HW, Hickson ID. (2004) Understanding the roles of RecQ helicases in the maintenance of genome integrity and suppression of tumorigenesis.*Biochem Soc Trans.* 32(6): 957-8.

Manning BD. (2004) Balancing Akt with S6K: implications for both metabolic diseases and tumorigenesis. *J Cell Biol.* 167(3): 399-403.

Manning BD, Logsdon MN, Lipovsky AI, Abbott D, Kwiatkowski DJ, Cantley LC. (2005) Feedback inhibition of Akt signaling limits the growth of tumors lacking Tsc2.*Genes Dev.* 19(15): 1773-8.

Mansour SL, Thomas KR, Capecchi MR. (1988) Disruption of the proto-oncogene int-2 in mouse embryo-derived stem cells: a general strategy for targeting mutations to non-selectable genes. *Nature* 336: 348-352.

Marsh DJ, Dahia PL, Caron S, Kum JB, Frayling IM, Tomlinson IP, Hughes KS, Eeles RA, Hodgson SV, Murday VA, Houlston R, Eng C. (1998) Germline PTEN mutations in Cowden syndrome-like families. *J Med Genet.* 35(11): 881-5.

Marsh DJ, Kum JB, Lunetta KL, Bennett MJ, Gorlin RJ, Ahmed SF, Bodurtha J, Crowe C, Curtis MA, Dasouki M, Dunn T, Feit H, Geraghty MT, Graham JM Jr, Hodgson SV, Hunter A, Korf BR, Manchester D, Miesfeldt S, Murday VA, Nathanson KL, Parisi M, Pober B, Romano C, Eng C, et al. (1999) PTEN mutation spectrum and genotype-phenotype correlations in Bannayan-Riley-Ruvalcaba syndrome suggest a single entity with Cowden syndrome. *Hum Mol Genet.* 8(8): 1461-72.

Martin DE, Hall MN. (2005) The expanding TOR signaling network. *Curr Opin Cell Biol.* 17(2): 158-66.

Matsumoto S, Bandyopadhyay A, Kwiatkowski DJ, Maitra U, Matsumoto T. (2002) Role of the Tsc1-Tsc2 complex in signaling and transport across the cell membrane in the fission yeast Schizosaccharomyces pombe. *Genetics.* 161(3): 1053-63.

McColl IBH, Veale Am, Morson BC. (1964) Juvenile Polyposis Coli. *Proc R Soc Med.* 57: 896-7.

McDaniel LD, Chester N, Watson M, Borowsky AD, Leder P, Schultz RA. Chromosome instability and tumor predisposition inversely correlate with BLM protein levels. DNA Repair 2003;2:1387-404.

Meikle L, McMullen JR, Sherwood MC, Lader AS, Walker V, Chan JA, Kwiatkowski DJ. (2005) A mouse model of cardiac rhabdomyoma generated by loss of Tsc1 in ventricular myocytes. *Hum Mol Genet.* 14(3): 429-35.

Merks JH, de Vries LS, Zhou XP, Nikkels P, Barth PG, Eng C, Hennekam RC. (2003) PTEN hamartoma tumour syndrome: variability of an entity. *J Med Genet.* 40(10): e111.

Miyaki M, Iijima T, Konishi M, Sakai K, Ishii A, Yasuno M, Hishima T, Koike M, Shitara N, Iwama T, Utsunomiya J, Kuroki T, Mori T. (1999) Higher frequency of Smad4 gene mutation in human colorectal cancer with distant metastasis.
Oncogene. 18(20): 3098-103.

Miyaki M, Iijima T, Hosono K, Ishii R, Yasuno M, Mori T, Toi M, Hishima T, Shitara N, Tamura K, Utsunomiya J, Kobayashi N, Kuroki T, Iwama T. (2000) Somatic mutations of LKB1 and beta-catenin genes in gastrointestinal polyps from patients with Peutz-Jeghers syndrome. *Cancer Res.* 2000 60(22): 6311-3.

Miyoshi H, Nakau M, Ishikawa TO, Seldin MF, Oshima M, Taketo MM. (2002) Gastrointestinal hamartomatous polyposis in *Lkb1* heterozygous knockout mice. *Cancer Res.* 62: 2261-6.

Mizuguchi M, Ikeda K, Takashima S. (2000a) Simultaneous loss of hamartin and tuberin from the cerebrum, kidney and heart with tuberous sclerosis. *Acta Neuropathol (Berl).* 99(5): 503-10.

Mizuguchi M, Takashima S, Yamanouchi H, Nakazato Y, Mitani H, Hino O. (2000b) Novel cerebral lesions in the Eker rat model of tuberous sclerosis: cortical tuber and anaplastic ganglioglioma. *J. Neuropathol. Exp. Neurol.* 59: 188-196.

Moolten SE. (1942) Hamartial nature of the tuberous sclerosis complex and its bearing on the tumour problem: report of one case with tumour anomaly of the kidney and adenoma sebaceum. *Arch Intern Med* 69: 589-623.

Mouse Genome Sequencing Consortium. (2002) Initial sequencing and comparative analysis of the mouse genome. *Nature.* 420(6915): 520-62.

Nakau M, Miyoshi H, Seldin MF, Imamura M, Oshima M, Taketo MM. (2002) Hepatocellular carcinoma caused by loss of heterozygosity in *Lkb1* gene knockout mice. *Cancer Res.* 62: 4549-53.

Nehls M, Kyewski B, Messerle M, Waldschutz R, Schuddekopf K, Smith AJH, Boehm T. (1996) Two genetically separable steps in the differentiation of thymic epithelium. *Science* 272: 886-889.

Nellist M, Brook-Carter PT, Connor JM, Kwiatkowski DJ, Johnson P, Sampson JR. (1993) Identification of markers flanking the tuberous sclerosis locus on chromosome 9 (TSC1). *J Med Genet.* 30(3): 224-7.

Nellist M, van Slegtenhorst MA, Goedbloed M, van den Ouweland AM, Halley DJ, van der Sluijs P. (1999) Characterization of the cytosolic tuberin-hamartin complex. Tuberin is a cytosolic chaperone for hamartin. *J Biol Chem.* 274(50): 35647-52.

Nellist M, Verhaaf B, Goedbloed MA, Reuser AJ, van den Ouweland AM, Halley DJ. (2001) TSC2 missense mutations inhibit tuberin phosphorylation and prevent formation of the tuberin-hamartin complex. *Hum Mol Genet.* 10(25): 2889-98.

Nellist M, Burgers PC, van den Ouweland AM, Halley DJ, Luider TM. (2005a) Phosphorylation and binding partner analysis of the TSC1-TSC2 complex. Biochem *Biophys Res Commun.* 333(3): 818-26.

Nellist M, Sancak O, Goedbloed MA, Rohe C, van Netten D, Mayer K, Tucker-Williams A, van den Ouweland AM, Halley DJ. (2005b) Distinct

effects of single amino-acid changes to tuberin on the function of the tuberin-hamartin complex. *Eur J Hum Genet.* 13(1): 59-68.

Nevin NC, Pearce WG (1968) Diagnostic and genetical aspects of tuberous sclerosis. *J Med Genet.* 5(4): 273-80.

Niida Y, Lawrence-Smith N, Banwell A, Hammer E, Lewis J, Beauchamp RL, Sims K, Ramesh V, Ozelius L. (1999) Analysis of both TSC1 and TSC2 for germline mutations in 126 unrelated patients with tuberous sclerosis. *Hum Mutat.* 14(5): 412-22.

Niida Y, Stemmer-Rachamimov AO, Logrip M, Tapon D, Perez R, Kwiatkowski DJ, Sims K, MacCollin M, Louis DN, Ramesh V. (2001) Survey of somatic mutations in tuberous sclerosis complex (TSC) hamartomas suggests different genetic mechanisms for pathogenesis of TSC lesions. *Am J Hum Genet.* 69(3): 493-503.

Noonan DJ, Lou D, Griffith N, Vanaman TC. (2002) A calmodulin binding site in the tuberous sclerosis 2 gene product is essential for regulation of transcription events and is altered by mutations linked to tuberous sclerosis and lymphangioleiomyomatosis. *Arch Biochem Biophys.* 398(1): 132-40.

Northrup H, Beaudet AL, O'Brien WE, Herman GE, Lewis RA, Pollack MS. (1987) Linkage of tuberous sclerosis to ABO blood group. *Lancet.* 2(8562): 804-5.

Northrup H, Kwiatkowski DJ, Roach ES, Dobyns WB, Lewis RA, Herman GE, Rodriguez E Jr, Daiger SP, Blanton SH. (1992) Evidence for genetic heterogeneity in tuberous sclerosis: one locus on chromosome 9 and at least one locus elsewhere. *Am J Hum Genet.* 51(4): 709-20.

Nowak DA, Trost HA. (2002) Lhermitte-Duclos disease (dysplastic cerebellar gangliocytoma): a malformation, hamartoma or neoplasm? *Acta Neurol Scand.* 105(3): 137-45.

Okimoto K, Sakurai J, Kobayashi T, Mitani H, Hirayama Y, Nickerson ML, Warren MB, Zbar B, Schmidt LS, Hino O. (2004) A germ-line insertion in the Birt-Hogg-Dube (BHD) gene gives rise to the Nihon rat model of inherited renal cancer. *Proc Natl Acad Sci USA.* 101(7): 2023-7.

Onda H, Lueck A, Marks PW, Warren HB, Kwiatkowski DJ. (1999) Tsc2(+/-) mice develop tumors in multiple sites that express gelsolin and are influenced by genetic background. *J Clin Invest.* 104(6): 687-95.

Patel PH, Thapar N, Guo L, Martinez M, Maris J, Gau CL, Lengyel JA, Tamanoi F. (2003) Drosophila Rheb GTPase is required for cell cycle progression and cell growth. *J Cell Sci.* 116(17): 3601-10.

Paulson GW and Lyle CB. (1966) Tuberous sclerosis. *Dev. Med. Child Neurol.* 8: 571-586.

Peutz JLA. (1921) Over een zeer merkwaardige, gecombineerde familiaire polyposis van de slijmliezen van den tractus intestinalis met die van de neuskeelholte en gepaard met eigenaardige pigmentaties van huid-en slijmvliezen, *Ned Maandschr v Gen* 10: 134–146.

Pitiot G. Waksman G. Bragado-Nilsson E. Jobert S. Cornelis F. Mallet J. (1994) Linkage analysis place TSC1 gene distal to D9s10. *Ann. Hum. Genet.* 58: 232-233.

Palmiter RD, Brinster RL. (1986) Germ-line transformation of mice. *Annu Rev Genet.* 20: 465-99.

Plank TL, Yeung RS, Henske EP. (1998) Hamartin, the product of the tuberous sclerosis 1 (TSC1) gene, interacts with tuberin and appears to be localized to cytoplasmic vesicles. *Cancer Res.* 58(21): 4766-70.

Podsypanina K, Ellenson LH, Nemes A, Gu J, Tamura M, Yamada KM, Cordon-Cardo C, Catoretti G, Fisher PE, Parsons R. (1999) Mutation of Pten/Mmac1 in mice causes neoplasia in multiple organ systems. *Proc Natl Acad Sci USA.* 96(4): 1563-8.

Potter CJ, Huang H, Xu T. (2001) Drosophila Tsc1 functions with Tsc2 to antagonize insulin signaling in regulating cell growth, cell proliferation, and organ size. *Cell.* 105(3): 357-68.

Povey S, Burley MW, Fryer AE, Osborne J, Al-Gazali LI, Mueller R. (1988) Genetic recombination between tuberous sclerosis and oncogene v-abl. *Lancet.* 2(8605): 279-80.

Povey S, Burley MW, Attwood J, Benham F, Hunt D, Jeremiah SJ, Franklin D, Gillett G, Malas S, Robson EB, et al. (1994) Two loci for tuberous sclerosis: one on 9q34 and one on 16p13. *Ann Hum Genet.* 58 (2): 107-27.

Quon, Berns. (2001) Haplo-insufficiency? Let me count the ways. *Genes Dev.* 5(22): 2917-21.

Rankin EB, Tomaszewski JE, Haase VH. (2006) Renal cyst development in mice with conditional inactivation of the von Hippel-Lindau tumor suppressor. *Cancer Res.* 66(5): 2576-83.

Rassool FV, North PS, Mufti GJ, Hickson ID. (2003) Constitutive DNA damage is linked to DNA replication abnormalities in Bloom's syndrome cells. *Oncogene.* 22(54): 8749-57.

Rayer PFO (1835) *Traite theorique e practique des maladies de la peau*, 2nd edn. JB bailliere, Paris.

Renan MJ. (1993) How many mutations are required for tumorigenesis? Implications from human cancer data. *Mol Carcinog.* 7(3): 139-46.

Resta N, Simone C, Mareni C, Montera M, Gentile M, Susca F, Gristina R, Pozzi S, Bertario L, Bufo P, Carlomagno N, Ingrosso M, Rossini FP, Tenconi R, Guanti G. (1998) STK11 mutations in Peutz-Jeghers syndrome and sporadic colon cancer. *Cancer Res.* 58(21): 4799-801.

Risinger JI, Hayes AK, Berchuck A, Barrett JC. (1997) PTEN/MMAC1 mutations in endometrial cancers. *Cancer Res.* 57(21): 4736-8.

Roach ES, Williams DP, Laster DW. (1987) Magnetic resonance imaging in tuberous sclerosis. *Arch Neurol.* 44(3): 301-3.

Roach ES, Gomez MR, Northrup H. (1998) Tuberous sclerosis complex consensus conference: revised clinical diagnostic criteria. *J Child Neurol.* 13(12): 624-8.

Robinson-White A, Hundley TR, Shiferaw M, Bertherat J, Sandrini F, Stratakis CA. (2003) Protein kinase-A activity in PRKAR1A-mutant cells, and regulation of mitogen-activated protein kinases ERK1/2. *Hum Mol Genet.* 12(13): 1475-84.

Robinson-White A, Meoli E, Stergiopoulos S, Horvath A, Boikos S, Bossis I, Stratakis CA. (2006) PRKAR1A Mutations and protein kinase A interactions with other signaling pathways in the adrenal cortex. *J Clin Endocrinol Metab.* 91(6): 2380-8.

Ross AT and Dickerson WW. (1943) Tuberous Sclerosis. *Arch Neurol Psychiatry.* 50: 233-257.

Rossi DJ, Ylikorkala A, Korsisaari N, Salovaara R, Luukko K, Launonen V, Henkemeyer M, Ristimaki A, Aaltonen LA, Makela TP. (2002) Induction of cyclooxygenase-2 in a mouse model of Peutz-Jeghers polyposis. *Proc Natl Acad Sci. USA.* 99: 12327-12332.

Roux PP, Ballif BA, Anjum R, Gygi SP, Blenis J. (2004) Tumor-promoting phorbol esters and activated Ras inactivate the tuberous sclerosis tumor suppressor complex via p90 ribosomal S6 kinase. *Proc Natl Acad Sci USA.* 101(37): 13489-94.

Sampson JR, Yates JR, Pirrit LA, Fleury P, Winship I, Beighton P, Connor JM. (1989) Evidence for genetic heterogeneity in tuberous sclerosis. *J Med Genet.* 26(8): 511-6.

Sampson JR, Janssen LA, Sandkuijl LA. (1992) Linkage investigation of three putative tuberous sclerosis determining loci on chromosomes 9q, 11q, and 12q. The Tuberous Sclerosis Collaborative Group. *J Med Genet.* 29(12): 861-6.

Sampson JR, Maheshwar MM, Aspinwall R, Thompson P, Cheadle JP, Ravine D, Roy S, Haan E, Bernstein J, Harris PC. (1997) Renal cystic

disease in tuberous sclerosis: role of the polycystic kidney disease 1 gene. *Am J Hum Genet.* 61(4): 843-51.

Sancak O, Nellist M, Goedbloed M, Elfferich P, Wouters C, Maat-Kievit A, Zonnenberg B, Verhoef S, Halley D, van den Ouweland A. (2005) Mutational analysis of the TSC1 and TSC2 genes in a diagnostic setting: genotype--phenotype correlations and comparison of diagnostic DNA techniques in Tuberous Sclerosis Complex. *Eur J Hum Genet.* 13(6): 731-41.

Santarosa, Ashworth. (2004) Haploinsufficiency for tumour suppressor genes: when you don't need to go all the way. *Biochim Biophys Acta.* 1654(2): 105-22.

Sarbassov DD, Guertin DA, Ali SM, Sabatini DM. (2005) Phosphorylation and regulation of Akt/PKB by the rictor-mTOR complex. *Science.* 307(5712): 1098-101.

Saucedo LJ, Gao X, Chiarelli DA, Li L, Pan D, Edgar BA. (2003) Rheb promotes cell growth as a component of the insulin/TOR signalling network. *Nat Cell Biol.* 5(6): 566-71.

Scheithauer BW. (1992) The neuropathology of tuberous sclerosis. *J Dermatol.* 19(11): 897-903.

Sehgal SN, Baker H, Vezina C. (1975) Rapamycin (AY-22,989), a new antifungal antibiotic. II. Fermentation, isolation and characterization. *J Antibiot (Tokyo).* 28(10): 727-32.

Shepherd CW. Beard CM. Gomez MR. Kurland JT. Whisnant JP. (1991) Tuberous sclerosis complex in Olmsted County, Minnesota, 1950- 1989. *Arch. Neurol.* 48: 400-401.

Shaw RJ, Bardeesy N, Manning BD, Lopez L, Kosmatka M, DePinho RA, Cantley LC. (2004) The LKB1 tumor suppressor negatively regulates mTOR signaling. *Cancer Cell.* 6(1): 91-9.

Shepherd CW, Houser OW, Gomez MR. (1995) MR findings in tuberous sclerosis complex and correlation with seizure development and mental impairment. *AJNR Am J Neuroradiol.* 16(1): 149-55.

Sieber O, Segditsas S, Knudsen A, Zhang J, Luz J, Rowan A, Spain S, Thirlwell C, Howarth K, Jaeger E, Robinson J, Volikos E, Silver A, Kelly G, Aretz S, Frayling I, Hutter P, Dunlop M, Guenther T, Neale K, Phillips R, Heinimann K, Tomlinson I. (2006) Disease severity and genetic pathways in attenuated familial adenomatous polyposis vary greatly, but depend on the site of the germline mutation. *Gut.* Feb 4. (Epub. ahead of print)

Sirard C, de la Pompa JL, Elia A, Itie A, Mirtsos C, Cheung A, Hahn S, Wakeham A, Schwartz L, Kern SE, Rossant J, Mak TW. (1998) The tumor

suppressor gene Smad4/Dpc4 is required for gastrulation and later for anterior development of the mouse embryo. *Genes Dev.* 12(1): 107-19.

van Slegtenhorst M, Janssen B, Nellist M, Ramlakhan S, Hermans C, Hesseling A, van den Ouweland A, Kwiatkowski D, Eussen B, Sampson J, et al. (1995) Cosmid contigs from the tuberous sclerosis candidate region on chromosome 9q34. *Eur J Hum Genet.* 3(2): 78-86.

van Slegtenhorst M, de Hoogt R, Hermans C, Nellist M, Janssen B, Verhoef S, Lindhout D, van den Ouweland A, Halley D, Young J, Burley M, Jeremiah S, Woodward K, Nahmias J, Fox M, Ekong R, Osborne J, Wolfe J, Povey S, Snell RG, Cheadle JP, Jones AC, Tachataki M, Ravine D, Sampson JR, Reeve MP, Richardson P, Wilmer F, Munro C, Hawkins TL, Sepp T, Ali JB, Ward S, Green AJ, Yates JR, Kwiatkowska J, Henske EP, Short MP, Haines JH, Jozwiak S, Kwiatkowski DJ. (1997) Identification of the tuberous sclerosis gene TSC1 on chromosome 9q34. *Science.* 277(5327): 805-8.

van Slegtenhorst M, Nellist M, Nagelkerken B, Cheadle J, Snell R, van den Ouweland A, Reuser A, Sampson J, Halley D, van der Sluijs P. Interaction between hamartin and tuberin, the TSC1 and TSC2 gene products.
Plank TL, Yeung RS, Henske EP. (1998) Hamartin, the product of the tuberous sclerosis 1 (TSC1) gene, interacts with tuberin and appears to be localized to cytoplasmic vesicles. *Cancer Res.* 58(21): 4766-70.

van Slegtenhorst M, Verhoef S, Tempelaars A, Bakker L, Wang Q, Wessels M, Bakker R, Nellist M, Lindhout D, Halley D, van den Ouweland A. (1999) Mutational spectrum of the TSC1 gene in a cohort of 225 tuberous sclerosis complex patients: no evidence for genotype-phenotype correlation. *J Med Genet.* 36(4): 285-9.

van Slegtenhorst M, Carr E, Stoyanova R, Kruger WD, Henske EP. (2004) Tsc1+ and tsc2+ regulate arginine uptake and metabolism in Schizosaccharomyces pombe. *J Biol Chem.* 279(13): 12706-13.

Smalley SL, Tanguay PE, Smith M, (1992) Gutierrez GAutism and tuberous sclerosis. *J Autism Dev Disord.* 22(3): 339-55.

Smith HC, Watson GH, Patel RG, Super M. (1989) Cardiac rhabdomyomata in tuberous sclerosis: their course and diagnostic value. *Arch Dis Child.* 64(2): 196-200.

Smith AJH, De Sousa MA, Kwabi-Addo B, Heppell-Parton A, Impey H, Rabbitts P. (1995) A site-directed chromosomal translocation induced in embryonic stem cells by Cre-loxP recombination. *Nat Genet.* 9: 376-385.

Smits R, Hofland N, Edelmann W, Geugien M, Jagmohan-Changur S, Albuquerque C, Breukel C, Kucherlapati R, Kielman MF, Fodde R. (2000) Somatic Apc mutations are selected upon their capacity to inactivate the

beta-catenin downregulating activity. *Genes Chromosomes Cancer.* 29(3): 229-39.

Snijders AM, Nowak N, Segraves R, Blackwood S, Brown N, Conroy J, Hamilton G, Hindle AK, Huey B, Kimura K, Law S, Myambo K, Palmer J, Ylstra B, Yue JP, Gray JW, Jain AN, Pinkel D, Albertson DG. (2001) Assembly of microarrays for genome-wide measurement of DNA copy number. *Nat Genet.* 29(3): 263-4.

Stapleton FB, Johnson D, Kaplan GW, Griswold W. (1980) The cystic renal lesion in tuberous sclerosis. *J Pediatr.* 97(4): 574-9.

Steck PA, Pershouse MA, Jasser SA, Yung WK, Lin H, Ligon AH, Langford LA, Baumgard ML, Hattier T, Davis T, Frye C, Hu R, Swedlund B, Teng DH, Tavtigian SV. (1997) Identification of a candidate tumour suppressor gene, MMAC1, at chromosome 10q23.3 that is mutated in multiple advanced cancers. *Nat Genet.* 15(4): 356-62.

Stergiopoulos SG, Stratakis CA. (2003) Human tumors associated with Carney complex and germline PRKAR1A mutations: a protein kinase A disease! *FEBS Lett.* 546(1): 59-64.

Stillwell TJ, Gomez MR, Kelalis PP. (1987) Renal lesions in tuberous sclerosis. *J Urol.* 138(3): 477-81.

Stocker H, Radimerski T, Schindelholz B, Wittwer F, Belawat P, Daram P, Breuer S, Thomas G, Hafen E. (2003) Rheb is an essential regulator of S6K in controlling cell growth in Drosophila. *Nat Cell Biol.* 5(6): 559-65.

Stoyanova R, Clapper ML, Bellacosa A, Henske EP, Testa JR, Ross EA, Yeung AT, Nicolas E, Tsichlis N, Li YS *et al.* (2004) Altered gene expression in phenotypically normal renal cells from carriers of tumor suppressor gene mutations. *Cancer Biol Ther.* 3(12): 1313-21.

Strachan T, Read AP. (1996) *Human Molecular Genetics Second Edition.* John Wiley and sons Inc. New York, USA.

Suzuki A, de la Pompa JL, Stambolic V, Elia AJ, Sasaki T, del Barco Barrantes I, Ho A, Wakeham A, Itie A, Khoo W, Fukumoto M, Mak TW. (1998) High cancer susceptibility and embryonic lethality associated with mutation of the PTEN tumor suppressor gene in mice. *Curr Biol.* 8(21): 1169-78.

Takagi Y, Kohmura H, Futamura M, Kida H, Tanemura H, Shimokawa K, Saji S. (1996) Somatic alterations of the DPC4 gene in human colorectal cancers in vivo. *Gastroenterology.* 111(5): 1369-72.

Takaku K, Miyoshi H, Matsunaga A, Oshima M, Sasaki N, Taketo MM. (1999) Gastric and duodenal polyps in Smad4 (Dpc4) knockout mice. *Cancer Res.* 59(24): 6113-7.

Tapon N, Ito N, Dickson BJ, Treisman JE, Hariharan IK. (2001) The Drosophila tuberous sclerosis complex gene homologs restrict cell growth and cell proliferation. *Cell.* 105(3): 345-55.

Tasken K, Skalhegg BS, Tasken KA, Solberg R, Knutsen HK, Levy FO, Sandberg M, Orstavik S, Larsen T, Johansen AK, Vang T, Schrader HP, Reinton NT, Torgersen KM, Hansson V, Jahnsen T. (1997) Structure, function, and regulation of human cAMP-dependent protein kinases. *Adv Second Messenger Phosphoprotein Res.* 31:191-204.

Tavazoie SF, Alvarez VA, Ridenour DA, Kwiatkowski DJ, Sabatini BL. (2005) Regulation of neuronal morphology and function by the tumor suppressors *Tsc1* and *Tsc2*. *Nat Neurosci.* **8**: 1727-1734.

Taylor JR, Ryu J, Colby TV, Raffin TA. (1990) Lymphangioleiomyomatosis. Clinical course in 32 patients. *N Engl J Med.* 323(18): 1254-60.

Tee AR, Manning BD, Roux PP, Cantley LC, Blenis J. (2003) Tuberous sclerosis complex gene products, Tuberin and Hamartin, control mTOR signaling by acting as a GTPase-activating protein complex toward Rheb. *Curr Biol.* 13(15): 1259-68.

Thiagalingam S, Lengauer C, Leach FS, Schutte M, Hahn SA, Overhauser J, Willson JK, Markowitz S, Hamilton SR, Kern SE, Kinzler KW, Vogelstein B.

(1996) Evaluation of candidate tumour suppressor genes on chromosome 18 in colorectal cancers. *Nat Genet.* 13(3): 343-6.

Torres VE, Bjornsson J, King BF, Kumar R, Zincke H, Edell ES, Wilson TO, Hattery RR, Gomez MR. (1995) Extrapulmonary lymphangioleiomyomatosis and lymphangiomatous cysts in tuberous sclerosis complex. *Mayo Clin Proc.* 70(7): 641-8.

Trotman LC, Niki M, Dotan ZA, Koutcher JA, Di Cristofano A, Xiao A, Khoo AS, Roy-Burman P, Greenberg NM, Van Dyke T, Cordon-Cardo C, Pandolfi PP. (2003) Pten dose dictates cancer progression in the prostate. *PLoS Biol.* 1(3): E59.

Tsilou ET, Chan CC, Sandrini F, Rubin BI, Shen de F, Carney JA, Kaiser-Kupfer M, Stratakis CA. (2004) Eyelid myxoma in Carney complex without PRKAR1A allelic loss. *Am J Med Genet.* 130(4): 395-7.

Uhlmann EJ, Wong M, Baldwin RL, Bajenaru ML, Onda H, Kwiatkowski DJ, Yamada K, Gutmann DH. (2002) Astrocyte-specific TSC1 conditional knockout mice exhibit abnormal neuronal organization and seizures. *Ann Neurol.* 52(3): 285-96.

Uzzo RG, Libby DM, Vaughan ED Jr, Levey SH. (1994) Coexisting lymphangioleiomyomatosis and bilateral angiomyolipomas in a patient with tuberous sclerosis. *J Urol.* 151(6): 1612-5.

Van Gele M, Leonard JH, Van Roy N, Cook AL, De Paepe A, Speleman F. (2001) Frequent allelic loss at 10q23 but low incidence of PTEN mutations in Merkel cell carcinoma. *Int J Cancer.* 92(3):409-13.

Venkatachalam S, Shi YP, Jones SN, Vogel H, Bradley A, Pinkel D, Donehower LA. (1998) Retention of wild-type p53 in tumors from p53 heterozygous mice: reduction of p53 dosage can promote cancer formation. *EMBO J.* 17(16): 4657-67.

Venter JC, Adams MD, Myers EW. et al. (2001) The sequence of the human genome. *Science.* 291(5507): 1304-51.

Veugelers M, Wilkes D, Burton K, McDermott DA, Song Y, Goldstein MM, La Perle K, Vaughan CJ, O'Hagan A, Bennett KR, Meyer BJ, Legius E, Karttunen M, Norio R, Kaariainen H, Lavyne M, Neau JP, Richter G, Kirali K, Farnsworth A, Stapleton K, Morelli P, Takanashi Y, Bamforth JS, Eitelberger F, Noszian I, Manfroi W, Powers J, Mochizuki Y, Imai T, Ko GT, Driscoll DA, Goldmuntz E, Edelberg JM, Collins A, Eccles D, Irvine AD, McKnight GS, Basson CT. (2004) Comparative PRKAR1A genotype-phenotype analyses in humans with Carney complex and prkar1a haploinsufficient mice. *Proc Natl Acad Sci USA.* 101(39): 14222-7.

Vogelstein B, Kinzler. (2004) Cancer genes and the pathways they control. *Nature Medicine.* 10: 789-799.

Vogt H. (1908) Zur pathologie und pathologischen Anatomie der verschiedenen Idiotieform. *Monatsschr Psychiatr Neurol* 24: 106-50.

Waltereit R, Welzl H, Dichgans J, Lipp HP, Schmidt WJ, Weller M. (2006) Enhanced episodic-like memory and kindling epilepsy in a rat model of tuberous sclerosis. *J Neurochem.* 96: 407-413.

Wang ZJ, Ellis I, Zauber P, Iwama T, Marchese C, Talbot I, Xue WH, Yan ZY, Tomlinson I. (1999) Allelic imbalance at the LKB1 (STK11) locus in tumours from patients with Peutz-Jeghers' syndrome provides evidence for a hamartoma-(adenoma)-carcinoma sequence. *J Pathol.* 188(1): 9-13.

Weber BL. (2002) Cancer genomics. *Cancer Cell* 1(1): 37-47.

Wiederholt WC, Gomez MR, Kurland LT. (1985) Incidence and prevalence of tuberous sclerosis in Rocester, Minnesota, 1950 through 1882. *Neurology.* 35:600-603

Weiner DM, Ewalt DH, Roach ES, Hensle TW. (1998) The tuberous sclerosis complex: a comprehensive review. *J Am Coll Surg.* 187(5): 548-61.

Wienecke R, Konig A, DeClue JE. (1995) Identification of tuberin, the tuberous sclerosis-2 product. Tuberin possesses specific Rap1GAP activity. *J Biol Chem.* 270(27): 16409-14.

Wienecke R, Maize JC Jr, Shoarinejad F, Vass WC, Reed J, Bonifacino JS, Resau JH, de Gunzburg J, Yeung RS, DeClue JE. (1996) Co-localization of the TSC2 product tuberin with its target Rap1 in the Golgi apparatus. *Oncogene*. 13(5): 913-23.

Wilkie AO, Lamb J, Harris PC, Finney RD, Higgs DR. (1990) A truncated human chromosome 16 associated with alpha thalassaemia is stabilized by addition of telomeric repeat (TTAGGG)n. *Nature*. 346(6287): 868-71.

Wolf DC, Whiteley HE, Everitt JI. (1995) Preneoplastic and neoplastic lesions of rat hereditary renal cell tumors express markers of proximal and distal nephron. *Veterinary Pathology*. 32(4): 379-386.

Woodford-Richens K, Williamson J, Bevan S, Young J, Leggett B, Frayling I, Thway Y, Hodgson S, Kim JC, Iwama T, Novelli M, Sheer D, Poulsom R, Wright N, Houlston R, Tomlinson I. (2000) Allelic loss at SMAD4 in polyps from juvenile polyposis patients and use of fluorescence in situ hybridization to demonstrate clonal origin of the epithelium. *Cancer Res*. 60(9): 2477-82.

Wu L, Hickson ID. (2003) The Bloom's syndrome helicase suppresses crossing over during homologous recombination. *Nature*. 426(6968): 870-4.

Xiao GH, Shoarinejad F, Jin F, Golemis EA, Yeung RS. (1997) The tuberous sclerosis 2 gene product, tuberin, functions as a Rab5 GTPase activating protein (GAP) in modulating endocytosis. *J Biol Chem.* 272(10): 6097-100.

Xu L, Sterner C, Maheshwar MM, Wilson PJ, Nellist M, Short PM, Haines JL, Sampson JR, Ramesh V. (1995) Alternative splicing of the tuberous sclerosis 2 (TSC2) gene in human and mouse tissues. *Genomics.* 27(3): 475-80.

Xu X, Brodie SG, Yang X, Im YH, Parks WT, Chen L, Zhou YX, Weinstein M, Kim SJ, Deng CX. (2000) Haploid loss of the tumor suppressor *Smad4/Dpc4* initiates gastric polyposis and cancer in mice. *Oncogene.* 19: 1868-74.

Yeung RS, Buetow KH, Testa JR, Knudson AG Jr. (1993) Susceptibility to renal carcinoma in the Eker rat involves a tumor suppressor gene on chromosome 10. *Proc Natl Acad Sci USA.* 90(17): 8038-42.

Yeung RS, Xiao GH, Jin F, Lee WC, Testa JR, Knudson AG. (1994) Predisposition to renal carcinoma in the Eker rat is determined by germ-line mutation of the tuberous sclerosis 2 (TSC2) gene. *Proc Natl Acad Sci USA.* 91(24): 11413-6.

Yeung RS, Katsetos CD, Klein-Szanto A. (1997) Subependymal astrocytic hamartomas in the Eker rat model of tuberous sclerosis. *Am J Pathol.* 151(5): 1477-86.

Ylikorkala A, Rossi DJ, Korsisaari N, Luukko K, Alitalo K, Henkemeyer M, Makela TP. (2001) Vascular abnormalities and deregulation of VEGF in Lkb1-deficient mice. *Science*. 293(5533): 1323-6.

York B, Lou D, Panettieri RA Jr, Krymskaya VP, Vanaman TC, Noonan DJ. (2005) Cross-talk between tuberin, calmodulin, and estrogen signaling pathways. *FASEB J.* 19(9): 1202-4.

Yu Y, Bradley A. (2001) Engineering chromosomal rearrangements in mice. *Nat Rev Genet.* 2(10): 780-90.

Yusa K, Horie K, Kondoh G, Kouno M, Maeda Y, Kinoshita T, Takeda J. (2004) Genome-wide phenotype analysis in ES cells by regulated disruption of Bloom's syndrome gene.
Nature. 429(6994): 896-9.

Zaremba J. (1968) Tuberous sclerosis: a clinical and genetical investigation. *J Ment. Defic. Res.* 12: 63-80.

Zhang H, Cicchetti G, Onda H, Koon HB, Asrican K, Bajraszewski N, Vazquez F, Carpenter CL, Kwiatkowski DJ. (2003) Loss of Tsc1/Tsc2 activates mTOR and disrupts PI3K-Akt signaling through downregulation of PDGFR. *J Clin Invest.* 112(8): 1223-33.

Zhou CY, Wu KY, Leversha MA, Furlong RA, Ferguson-Smith MA, Affara NA. (1995) Physical analysis of the tuberous sclerosis region in 9q34. *Genomics*. 25(1): 304-8.

Zhou X, Hampel H, Thiele H, Gorlin RJ, Hennekam RC, Parisi M, Winter RM, Eng C. (2001) Association of germline mutation in the PTEN tumour suppressor gene and Proteus and Proteus-like syndromes. *Lancet*. 358(9277): 210-1.

Zhou XP, Marsh DJ, Morrison CD, Chaudhury AR, Maxwell M, Reifenberger G, Eng C. (2003) Germline inactivation of PTEN and dysregulation of the phosphoinositol-3-kinase/Akt pathway cause human Lhermitte-Duclos disease in adults. *Am J Hum Genet*. 73(5): 1191-8.

Zhou CZ, Qiu GQ, Zhang F, He L, Peng ZH. Loss of heterozygosity on chromosome 1 in sporadic colorectal carcinoma. World J Gastroenterol 2004;10:1431-5.